

PETROGENESIS
OF THE
GOOSE COVE COPPER DEPOSIT
NORTHWESTERN NEWFOUNDLAND

by

JENNIFER L.E. BATES

Submitted in partial fulfillment of the requirements
for a Bachelor of Science (Honours) Degree at
Dalhousie University, Halifax, Nova Scotia, May, 1983



DALHOUSIE UNIVERSITY

Department of Geology

Halifax, N.S. Canada B3H 3J5

Telephone (902) 424-2358 Telex: 019-21863

DALHOUSIE UNIVERSITY, DEPARTMENT OF GEOLOGY

B.Sc. HONOURS THESIS

Author: JENNIFER L.E. BATES

Title: PETROGENESIS OF THE GOOSE COVE COPPER DEPOSIT,
NORTHWESTERN NEWFOUNDLAND

Permission is herewith granted to the Department of Geology, Dalhousie University to circulate and have copied for non-commercial purposes, at its discretion, the above title at the request of individuals or institutions. The quotation of data or conclusions in this thesis within 5 years of the date of completion is prohibited without permission of the Department of Geology, Dalhousie University, or the author.

The author reserves other publication rights, and neither the thesis nor extensive extracts from it may be printed or otherwise reproduced without the authors written permission.

Date: *April 19, 1985.*

COPYRIGHT

Distribution License

DalSpace requires agreement to this non-exclusive distribution license before your item can appear on DalSpace.

NON-EXCLUSIVE DISTRIBUTION LICENSE

You (the author(s) or copyright owner) grant to Dalhousie University the non-exclusive right to reproduce and distribute your submission worldwide in any medium.

You agree that Dalhousie University may, without changing the content, reformat the submission for the purpose of preservation.

You also agree that Dalhousie University may keep more than one copy of this submission for purposes of security, back-up and preservation.

You agree that the submission is your original work, and that you have the right to grant the rights contained in this license. You also agree that your submission does not, to the best of your knowledge, infringe upon anyone's copyright.

If the submission contains material for which you do not hold copyright, you agree that you have obtained the unrestricted permission of the copyright owner to grant Dalhousie University the rights required by this license, and that such third-party owned material is clearly identified and acknowledged within the text or content of the submission.

If the submission is based upon work that has been sponsored or supported by an agency or organization other than Dalhousie University, you assert that you have fulfilled any right of review or other obligations required by such contract or agreement.

Dalhousie University will clearly identify your name(s) as the author(s) or owner(s) of the submission, and will not make any alteration to the content of the files that you have submitted.

If you have questions regarding this license please contact the repository manager at dalspace@dal.ca.

Grant the distribution license by signing and dating below.

Name of signatory

Date

TABLE OF CONTENTS

Acknowledgements	i
Abstract	ii
Introduction	1
Field Relations	8
(a) regional geology and tectonic setting	8
(b) the thesis area	15
(c) ore- host rock relationship	25
Petrography	30
(a) host rocks	30
(b) ore	35
Geochemistry	37
Mineral Chemistry	43
(a) microprobe analyses of sulphides and oxides	43
(b) sphalerite geobarometry	46
Petrogenesis	51
Conclusions	55
Appendix I	57
Appendix II	68
Appendix III	76
Appendix IV	79
References	80

Acknowledgements

Sincere thanks is offered to Dr. R.A. Jamieson for the financial aid that made field work possible, for the guidance which was appreciated throughout the course of the study and the opportunity to investigate an aspect of geology that is of particular interest to me. The help of R. MacKay with the microprobe analyses and S.Parikh with the chemical analyses was essential. I would like to gratefully acknowledge M. Justino for accompanying me in the field, coping with the word processor and drafting the 'last-minute' figures. Much of the thesis was expertly typed by J. Spicer.

Abstract

The Goose Cove copper deposit lies within the Goose Cove Schist of the St. Anthony Complex, northwestern Newfoundland. The initial theory of ore emplacement was epigenetic replacement of the greenschist host rocks (Stephenson, 1937). Field relations, petrography and geochemistry investigated in the course of this thesis indicate an opposing model of formation.

The ore consisting of pyrite, chalcopyrite, pyrrhotite and sphalerite is generally confined to the porphyroclastic metavolcanics and related to the main foliation (Sm).

The porphyroclastic metavolcanics are depleted of Cu, Ni and Zn with respect to their protoliths (the undeformed porphyritic pillow lavas of the Ireland Point Volcanics) suggesting a mobilization of the ore-forming elements in the pillow lavas and resulting reconcentration either prior to or synchronous with the Fm folding event.

Although the exact paleoenvironment of the primary pillow lavas cannot be defined, it is likely that the volcanics formed in a tectonically unstable oceanic setting (i.e.: mid-ocean ridge, ocean island or ocean floor). Syngenetic mineralization of the basaltic lavas may have occurred.

The fragmented texture of the ore, the equivalent percentages of chalcopyrite, pyrite, and pyrrhotite and consistent Cu:Zn ratios over unity designate the ore body as a deformed "Cyprus-type" massive sulphide deposit.

CHAPTER 1

INTRODUCTION

The Goose Cove copper deposit lies within the Hare Bay Allochthon of northwestern Newfoundland (Fig.1-1). The host rocks are intensely deformed metavolcanics and metasediments of the St. Anthony Complex, which represents the ophiolitic slice of the transported rock assemblage. The initial theory of ore emplacement (Cooper,1937;Stephenson,1937) was hydrothermal replacement of the host rocks by mineralized solutions generated from a deep-seated magma. Since 1937, there has been no critical study of the deposit. Considering the theories developed on the formation of massive sulphide deposits since that time, the need to test the hydrothermal model is obvious. The association of mineralized mafic volcanics with ophiolite emplacement is analogous to the Cyprus type model of massive sulphide deposits. Consequently, the application of this model to the Goose Cove deposit, which illustrates similiar characteristics, is appropriate. The purpose of the thesis is to test the two theories of ore emplacement and to develop an appropriate model that incorporates the paleoenvironment and petrogenesis of the Goose Cove massive sulphide deposit.

Location and Access

St. Anthony is situated on the northeastern coast of the Great Northern Peninsula of Newfoundland. The town is accessible by

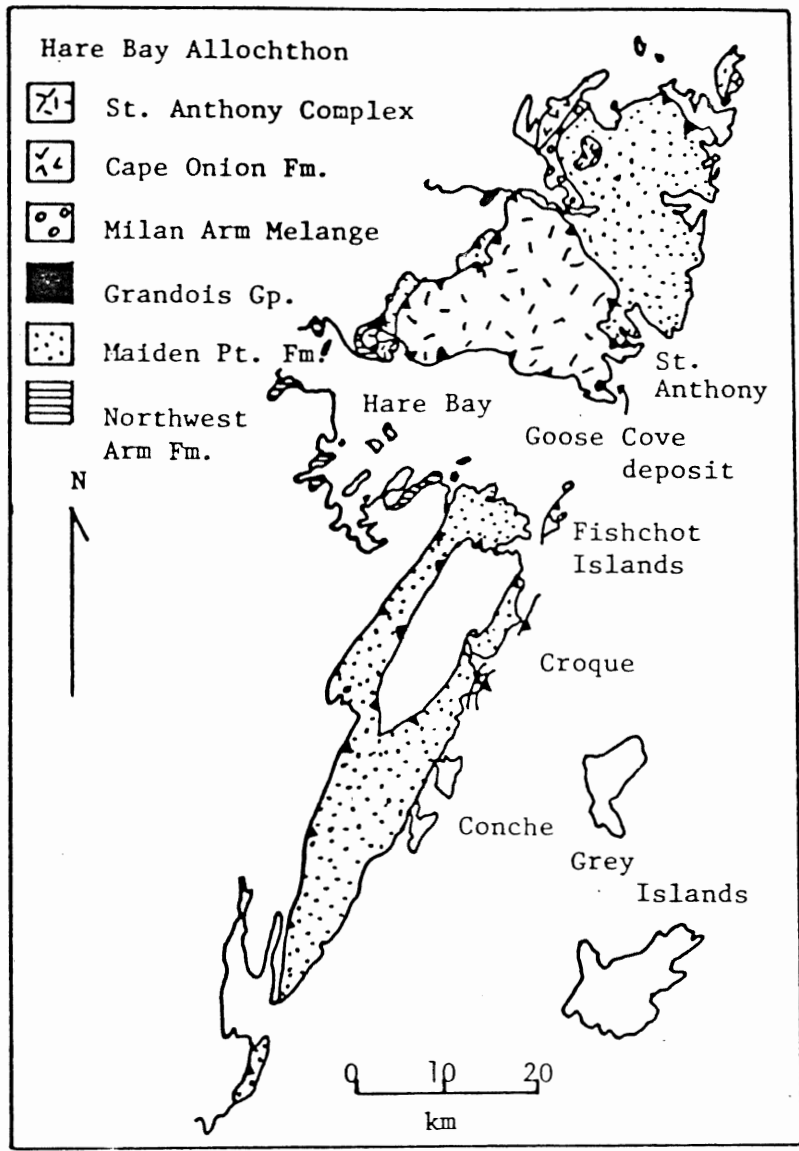


Fig. 1.1 Geology of the Hare Bay Allochthon and location of Goose Cove deposit. (after Jamieson, 1979)

paved road, land-based aircraft and Canadian National coastal services. The thesis area is located east of the village of Goose Cove, which is approximately twelve kilometers south of St. Anthony. Land access is by the Goose Cove Road which connects Goose Cove to St. Anthony. Goose Cove is connected with other coastal communities north of Hare Bay by secondary gravel roads. A small path leads to the copper deposit which is approximately 600 meters east of the village.

The mineralized area is found, along the northeastern shore of Hare Bay, in a topographic depression between Goose Cove and Three Mountain Harbour, locally known as, Little Back Cove (Fig 1.2). Three Mountain Summit, rising to a height of 180 meters, borders the deposit on the north with the highland of Goose Cape, approximately 100 meters above sea level, forming the southern boundary. Abandoned mine workings are confined to an arc-shaped area that begins west of Three Mountain Harbour and extends to the north and then east toward Norcat Point.

History of the Mine

In May, 1908, the Goose Cove copper deposit was opened under the management of Mr. Brenton Symons of London (Cooper, 1937; Stephenson, 1937). Over the next several years, \$40,000 was spent opening shafts, erecting buildings and constructing a tramway from the shafts to the shore of Big Back

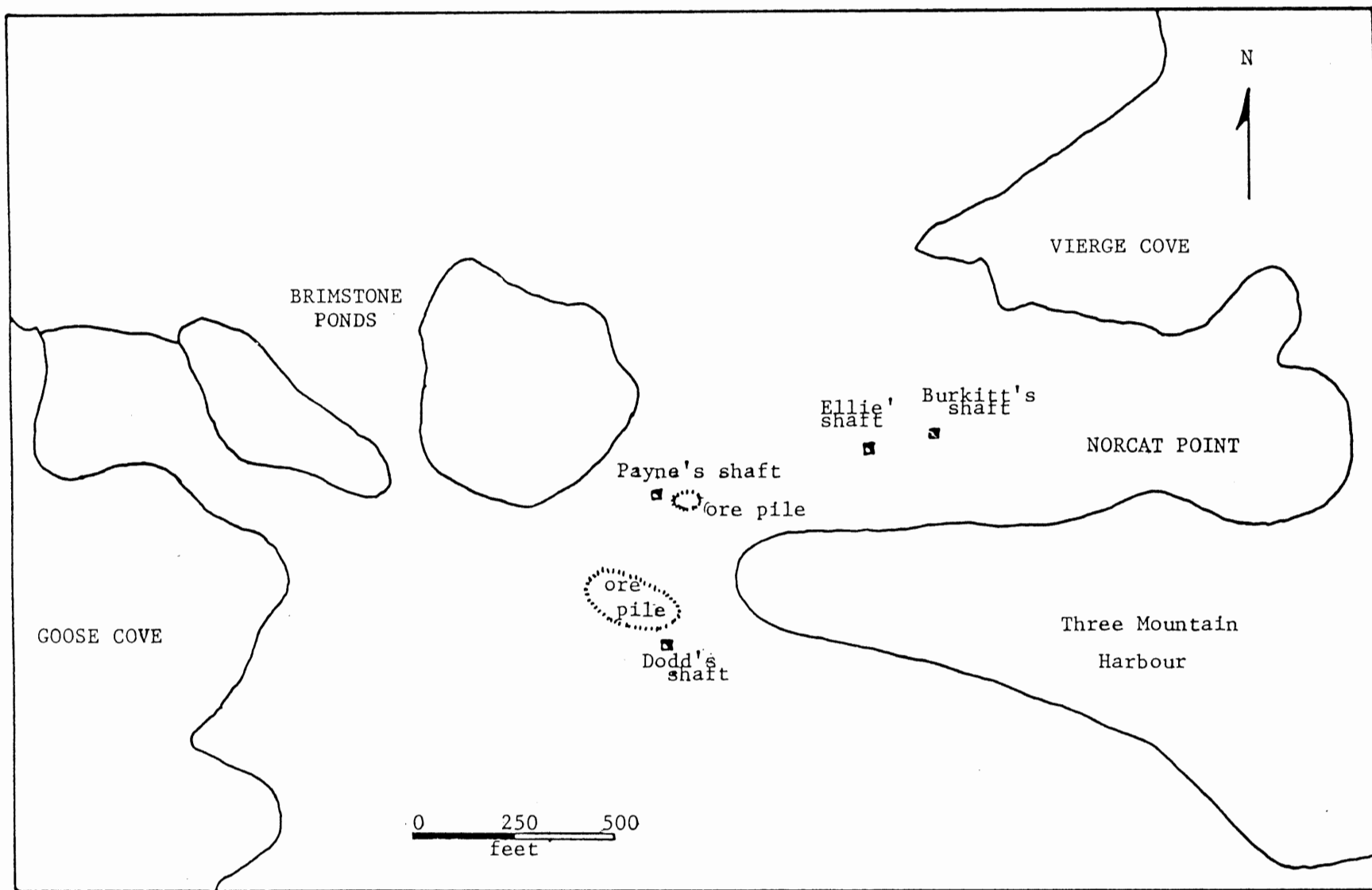


Figure 1.2 Map of the thesis area showing the location of the shafts and ore piles (modified after Douglas et al, 1937).

Cove. Mined and dressed ore, totalling 1800 tons, was never shipped and, to this date, remains in piles about the shafts. None of the buildings stand today and aside from the ore piles only a few pieces of machinery attest to the existence of the workings.

Four shafts were sunk and several prospect holes were dug in mineralized outcrops. Dodd's Shaft, the deepest of the four, extended about 40 meters along the slope of the ore body (Cooper, 1937). Variation in the thickness of the ore was great over short distances and the records of operation state that Dodd's Shaft was abandoned due to the reduction in the width of the ore to as little as 5-10 centimeters. At that time the ore was estimated to contain 2-12% copper with traces of gold and zinc. Since the mine operators believed only a small percent of the total ore contained high copper concentrations, and the thickness and extent of the ore body were variable and unpredictable, the operation of the deposit was deemed unprofitable.

Previous Work

A study by Stephenson (1937) concluded that the copper ore was formed by hydrothermal replacement of the schist. He suggested that solutions migrated upward along foliation planes and concentrated in the "drag" folds. Thrust faults within the area were designated as additional channels for movement of the

solutions. However, a source for the mineralized solutions was a problem since igneous bodies, expected to provide such solutions, were not found in the immediate vicinity. Consequently, it was proposed that a deep-seated magma undergoing differentiation produced the ore forming solutions (Cooper, 1937). This theory is questionable as it does not provide evidence of a concealed magma, it does not explain the occurrence of mineralized zones not associated with drag folds and not confined to the mine area and it is not compatible with the belief that the deposit lies within an oceanic allochthon (Williams, 1975; Jamieson, 1979).

Aside from the brief report on the geology of the Goose Cove mine by Kirk Stephenson in 1937 and subsequent summaries of the results (Cooper, 1937; Douglaset al., 1940), which provide no detailed mineralogical, structural or geochemical information, studies of the Goose Cove deposit are virtually non-existent. Regional studies of the Hare Bay Allochthon (Williamset al., 1973; Williams, 1975; Talkington, 1978; Lynas, 1980) discuss the origin of the host rocks with respect to tectonic models but do not make specific reference to the Goose Cove deposit. A study of the St. Anthony Complex by Jamieson (1979, 1980 and 1981) is the only detailed account of the local geology. A recent unpublished report by Bailey (1982), which concentrates on petrographic work and microprobe analysis, is the one existing study of the ores. Although limited in scope, the results of Bailey's study provoke a

number of questions regarding Stephenson's theory of ore emplacement.

Purpose and Scope

Models of the origin of massive sulphide deposits have been greatly modified since the report by Stephenson (1937). The Cyprus-type model, which is considered to represent the formation of a cupriferous pyrite ore body by syngenetic mineralization of mafic volcanics in a tectonically-active ocean environment (Grenneet al., 1979; Mitchell and Garson, 1981), has become a standard with which to compare investigated deposits. Since the Goose Cove deposit is a copper-dominated massive sulphide deposit associated with an ophiolite it may be studied with respect to the Cyprus-type model. However, there are two aspects that must be considered when applying the Cyprus model. First, the host rocks are highly deformed and the question posed is whether the Goose Cove deposit represents a deformed Cyprus-type massive sulphide deposit. Second, the host rocks are not pillow lavas within an ophiolite suite as designated in the Cyprus-type deposit but are marginal marine lavas that adhered to the lower surface of the ophiolite suite during obduction (Jamieson, 1981).

To test the validity of the epigenetic and syngenetic theories of ore genesis, field relations, petrography and geochemistry of

the ore and host rocks were examined. Structural, mineralogical and textural studies are expected to indicate whether the ore emplacement was pre- or post-deformational. Geochemistry of the host rocks is expected to delineate a trend in metal concentrations, which is characteristic of one of the models of ore formation. A centralized mechanism of ore emplacement (i.e.: epigenetic replacement) may be characterized by decreasing metal concentration from the area of replacement. The syngenetic model is dependent upon a host rock lithologic unit which may contain anomalous element concentrations. With respect to the syngenetic model, it is important to consider the effect of deformation on stratabound ore. The host rocks of the Goose Cove deposit have undergone several folding events and therefore it is important to incorporate the structure when interpreting the geochemical results.

Microprobe analysis of the sulphides and oxides in the ores and host rocks was undertaken to reveal any trends in the mineral chemistry, which may be explained with respect to the equilibration history of the ore minerals. If variation exists, it is important to determine whether it can be attributed to separate emplacement events.

Sphalerite geobarometry was applied to the deposit in an attempt to determine the pressure existing at the time of the latest equilibration. This analysis is useful when defining the

paleoenvironment of the ore deposit.

In summary, field relationships, petrography and geochemistry were integrated to define the ore-host rock relationship and to develop an acceptable model for the origin of the Goose Cove massive sulphide deposit.

CHAPTER 2 FIELD RELATIONS

(a) Regional Geology

The regional geology and tectonic setting of the allochthonous rocks of western Newfoundland are crucial to the determination of the paleoenvironment and structural history of the host rocks of the Goose Cove massive sulphide deposit. This chapter will briefly outline the geology of western Newfoundland, with reference to the host rocks of the Goose Cove deposit. In addition, the tectonic setting and its significance to the interpretation of the origin of the deposit will be considered.

The geology of western Newfoundland is represented by a Precambrian basement overlain by autochthonous and allochthonous suites of rocks (Fig.2.1). The autochthonous rock assemblages include late Precambrian plateau basalts and coarse clastic rocks and Lower Cambrian to Middle Ordovician shallow water marine sediments. The allochthonous rock suite is composed of late Precambrian to Cambrian deep water clastic sediments and Lower Ordovician igneous and metamorphic rocks, which include ophiolite suites.

The Hare Bay Allochthon is composed of six distinct rock groups, each of which is an individual thrust sheet. The allochthonous sheets were emplaced during the Lower-Middle Ordovician Taconian Orogeny. The dip of the Hare Bay Allochthon, measured by

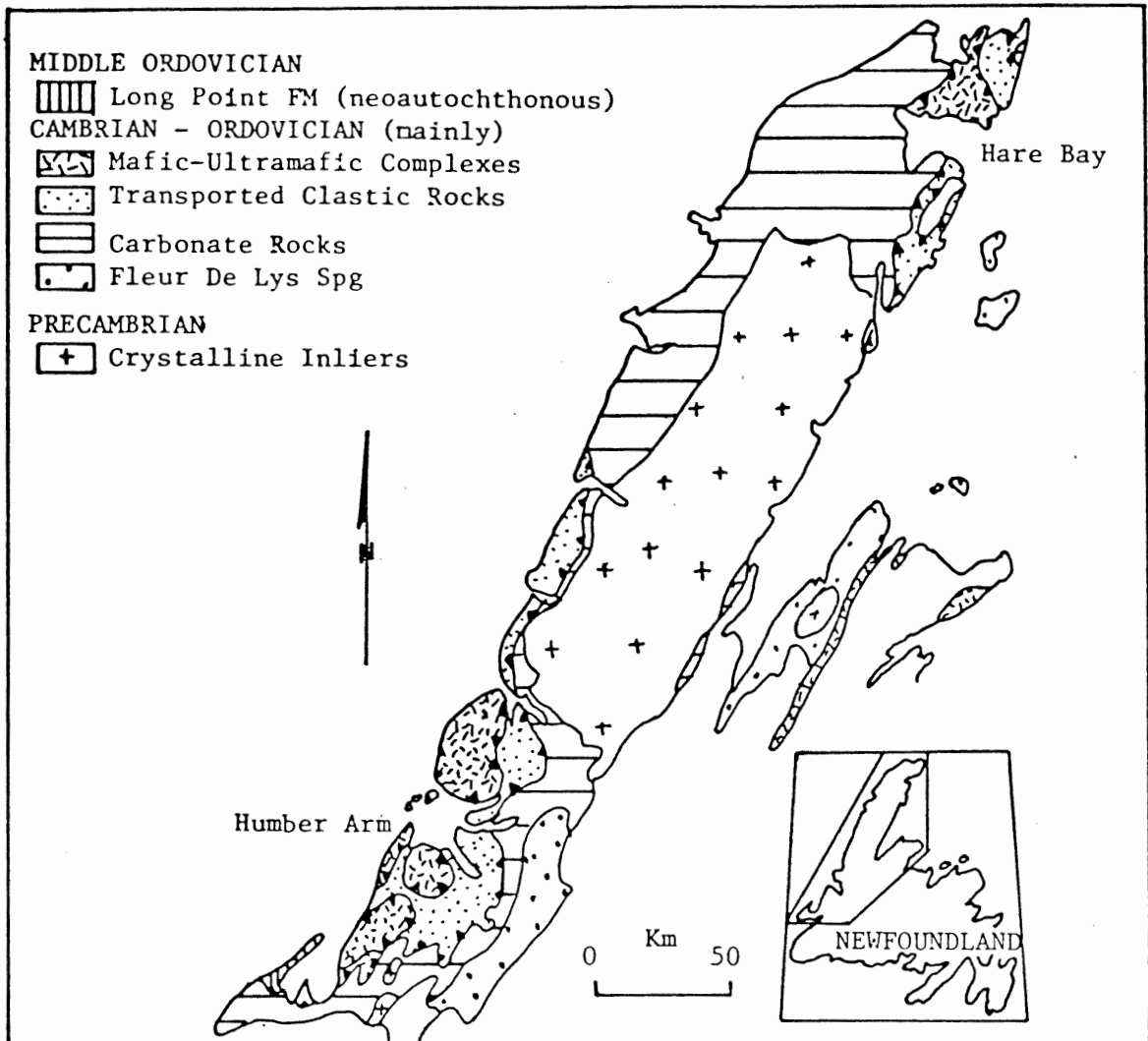


Fig. 2.1 Regional geology of the Great Northern Peninsula of Western Newfoundland illustrating the location of the Hare Bay Allochthon (after Williams, 1975).

geophysical means, averages one degree (Haworth, 1978). The present vertical sequence corresponds to a former west to east arrangement of the individual units with the stratigraphically highest unit originating from the most eastward position. More specifically, the lowest structural slice consists of sedimentary rocks deposited in a marginal continental or marine environment and the highest slice is an ophiolite representing the ocean crust and mantle. The inclusion of sedimentary, volcanic and plutonic blocks of more easterly located rock assemblages within the structurally lowest melange attests to the hypothesis that movement along the lowest surface was the last to occur (Williams, 1971).

Occupying the highest structural position within the transported sequence, the St. Anthony Complex is the ophiolitic segment of the allochthon. The complex consists of the ultramafic remnant of an ophiolite and the underlying, 450-500 meter thick, metamorphic aureole. The dynamothermal aureole is interpreted as a composite sequence formed by the accretion of material to the base of the ophiolite during displacement from the oceanic lithosphere and emplacement upon a continental margin (Jamieson, 1980).

Williams (1975) divided the St. Anthony Complex into four formations whereby the Ireland Point Volcanics, the Goose Cove Schist and the Green Ridge Amphibolite represent the aureole of increasing metamorphic grade and structural intensity upward to the White Hills Peridotite. Jamieson (1980) considered the section

of metagabbro underlying the peridotite as a fifth unit and defined it as the Long Ridge Metagabbro. The type section for the complex is found along the north shore of Hare Bay. Gradational contacts exist between all the adjacent formations. Metamorphic and structural characteristics are the basis for definition of the rocks.

Evidence of pre-emplacment deformation of the St. Anthony slice includes the contrast with less complex and structurally lower allochthonous and autochthonous rocks, the presence of metamorphic high grade amphibolites above lower grade melange and the inclusion of schistose volcanic blocks in the melange. The Hare Bay thrust fault, which marks the base of the St. Anthony Complex, truncates all the units and therefore post-dates pre- and syn-emplacment metamorphism. Altogether, a series of metamorphic and deformational events leads to the existence of a complicated structural pattern within the complex.

The Ireland Point Volcanics consist of undeformed alkaline to transitional pillow basalts and agglomerates (Jamieson, 1977). Northwest of Goose Cove, the volcanics grade progressively into the Goose Cove Schist with a corresponding increase in the intensity of deformation and metamorphic grade. The Goose Cove Schist is composed of greenschist and epidote-amphibolite facies metabasites and metasediments (Jamieson, 1979). The transition into Green Ridge Amphibolite is interrupted by a metasomatized,

syn-metamorphic mylonite zone believed to have formed after the metamorphic sequence was established but before metamorphism and deformation had ended (Jamieson and Strong, 1981). The Long Ridge Metagabbro underlying the White Hills Peridotite contains relict textures supporting an igneous origin although it has been metamorphosed to the amphibolite grade. By analogy with the the Bay of Islands Complex of the Humber Arm Allochthon, the White Hills Peridotite is generally interpreted as an ultramafic remnant of an ophiolite suite (Talkington and Jamieson, 1980).

Goose Cove Schist

The Goose Cove Schist structurally underlies, and in map pattern concentrically surrounds, the White Hills Peridotite. The estimate of the structural thickness ranges from 80 to 180 meters (Williams, 1973; Williams and Smyth, 1975). Williams (1975) described the sequence as polydeformed and metamorphosed green tuff and agglomerate and mafic pillow lavas with thin units of greywacke, black pyritic shale and limestone. Jamieson (1979) has subdivided the formation on the basis of metamorphic grade into greenschist and epidote-amphibolite facies metabasites and metasediments. The greenschists grade upward into the epidote-amphibolite in accordance with the reverse metamorphism characteristic of the aureole.

According to Jamieson (1979), the metabasites can be divided

into massive, spotted and banded greenschists and epidote-amphibolites. The massive greenschists are coarse-grained, weakly foliated, pre-tectonic dykes and sills within the Goose Cove Schist, distinguished by relict diabasic texture. The spotted greenschists are characterized by relict plagioclase phenocrysts (now porphyroclasts) generally altered to epidote, calcite, albite and muscovite in a fine-grained matrix of hornblende and chlorite. The porphyroclasts are presumed to be deformed equivalents of the phenocrysts in porphyritic pillow lavas of the Ireland Point Volcanics. The banded greenschists are characterized by thin, pale green bands of epidote, plagioclase and calcite in a fine-grained, dark-green matrix of amphibole, chlorite and epidote. These rocks resemble intensely deformed spotted greenschists and are essentially mylonitic in character. The banded greenschists grade into the epidote-amphibolites, which are characterized by bands, lenses or isolated grains of epidote in a matrix of hornblende, quartz, sphene and plagioclase.

The metasediments range from psammites to pelites depending upon the relative proportions of quartz and feldspar to mica and chlorite. Compositional banding is defined by alternating quartz-rich and mica-rich bands. Within higher-grade metasediments, biotite and garnet form at the expense of chlorite. Rare marbles, calcium-rich tuffaceous horizons and fine-grained, laminated metacherts have been observed within the Goose Cove Schist.

A complex structural pattern resulting from a series of deformational events is characteristic of the formation. The first schistosity (S1) represents metamorphic banding which is defined by the alignment of platy minerals (Jamieson, 1979). In turn, S1 is folded about recumbent, isoclinal second-phase folds (F2). On the regional scale, the shallow-dipping axial surfaces (S2) tend to parallel the first schistosity and the base of the peridotite (Williams, 1975). Post F2 folding produces a dominant west to north-west trending foliation (S3) that deforms earlier structures. The F2 generation of folding is prominent in the mine area and therefore will be important to consider when studying the ore-host rock relationship. Thrust faulting, related to F2 folding, and late normal faulting are common within the area.

Tectonic Setting

Numerous studies (Dewey and Bird, 1971; Williams, 1971;

Williams and Stevens, 1974; Stronge et al, 1974; Haworth, 1978) strongly support the theory that the allochthonous rocks of western Newfoundland are formed at an ancient continental margin. The rock assemblages are the result of rifting and evolution of a stable continental margin, subduction, ocean closing and ophiolite obduction leading to the final destruction of the continental margin (Williams, 1975). While the location, dip and number of the subduction zones are still subject to dispute, geophysical (Haworth, 1978) and geochemical and metallogenic evidence (Stronge et al, 1974) from more recent studies indicates an east-dipping subduction zone.

Williams (1975) has stated that the Dunnage Melange of the Central Mobile Belt of central Newfoundland represents the North American subduction zone and therefore marks the eastern limit of the source terrain for the transported rocks. Seismic profiling has defined a magnetic anomaly off northern Newfoundland approximately 15 to 35 kilometers east of Hare Bay. The anomaly has been interpreted as thrust sheets of ultramafic rocks and is believed to represent the roots of the Hare Bay Allochthon (Haworth, 1978). Thus, the allochthonous sequences originated from an area between the continental margin and an off-shore trench. The ophiolites are derived from an ocean basin adjacent to the continental margin (Fig. 2.2). However, the distance of the pre-tectonic setting of the protoliths of the St. Anthony Complex

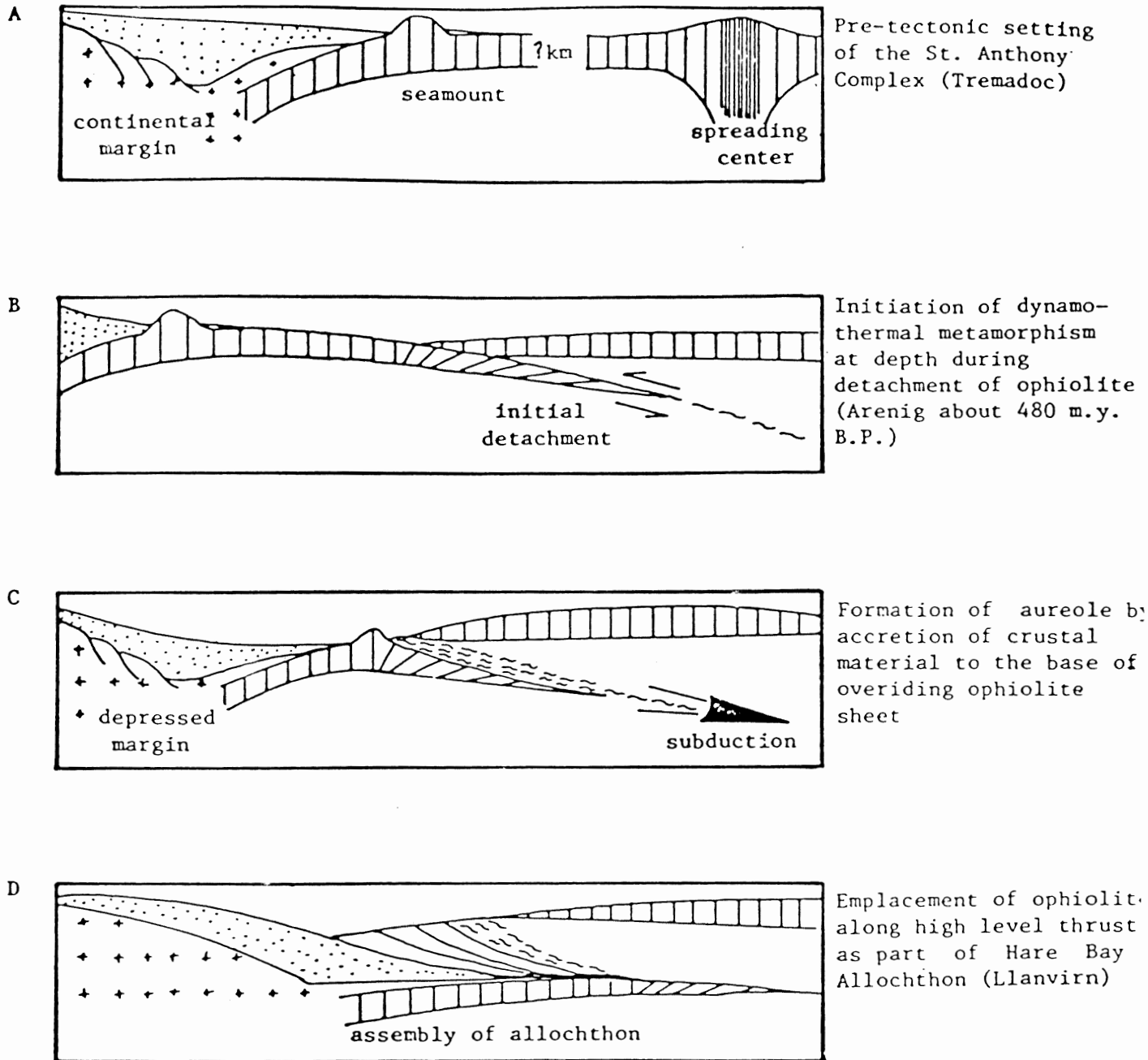


Fig. 2.2 Model for the formation of the St. Anthony Complex. (a) Pre-tectonic setting of the protoliths of the St. Anthony Complex (b) Formation of the St. Anthony Complex by Metamorphism beneath an overriding ophiolite sheet (c) Emplacement of the already formed St. Anthony Complex along high level thrust faults (after Jamieson, 1980).

from the spreading center to the east has not been determined and therefore the exact oceanic paleoenvironment is not known (i.e.: flank of the mid-ocean ridge, ocean island, ocean floor). Since massive sulphide deposits (including Cyprus-type) can be generated in oceanic environments, with the essential requirements for the formation of hydrothermal deposits (ie: permeable basaltic source rock, hot sea water and high heat flow related to a convection system) (Pearce and Gale, 1977; Mitchell and Garson, 1981) the model of syngenetic ore deposition can be applied to the Goose Cove deposit.

(b) The Thesis Area

The thesis area was mapped over a total of six days in late May and early September, 1982. In May, bad weather and snow cover along much of the shoreline and in topographic lows reduced the potential for detailed geological and structural analysis. Plate I is the map produced as a result of the field work.

Lithologic Variation

Jamieson (1979) divides the Goose Cove Schist into greenschist facies metasediments, banded metavolcanics and spotted metavolcanics and epidote-amphibolite facies metabasic rocks. The banded metavolcanics are a higher-grade equivalent of the Ireland Point Volcanics.

metavolcanics. The protolith of the spotted greenschists is presumed to be the porphyritic pillow lavas at Stark's Bight, on the north shore of Hare Bay. The white spots are considered to represent relict plagioclase phenocrysts that have been deformed and replaced by epidote, calcite and albite. More intensely-formed spotted greenschists may have originally been laminated schist with feldspar porphyroblasts. The gradational contact between the undeformed Ireland Point Volcanics and spotted greenschists of the Goose Cove Schist has been observed and is accepted by this author as evidence that the spotted greenschists are deformed porphyritic pillow lavas. Jamieson (1979) notes the presence of predominantly psammitic with minor pelitic metasediments east of Goose Cove. However, specifics about the rocks are not given.

As a result of field work, four distinct lithologic units can be defined within the thesis area - fine-grained greenschists metasediments, calc-silicate schists and coarse-grained greenschists. The fine-grained greenschists may be subdivided, on the basis of textural and structural features, into massive, porphyroclastic, banded or mylonitic greenschists. The metasediments include (garnetiferous) semi-pelitic and (siliceous) psammitic units. A discussion of the genetic origin of the lithologic units will follow the description of the individual rock types.

The massive greenschists are predominant in the outcrops along

the Goose Cove Road, west of Vierge Cove and intercalated with porphyroclastic greenschists at Norcat Point. Green-grey to dark grey, dense and often fissile, very fine-grained, moderately to well-foliated, homogeneous schists typify the unit. Rare plagioclase stringers (0.5-1.0 mm. long) parallel the foliation and serve to mark the folding pattern. The rocks are intensely deformed into isoclinal folds (amplitude 3 cm.-1 m.). A section along the road exposes a fold with thrust faulting (photos 2.1 and 2.2). Epidote stringers parallel and cross-cut the foliation and are particularly prominent along the shore of Vierge Cove. Since a protolith of the massive greenschist was not observed in the field, a genetic interpretation was not possible.

The porphyroclastic greenschists are spatially the most abundant lithologic unit within the thesis area. The unit dominates the shore of Three Mountain Harbour, the peninsula leading to Norcat Point and the mineralized area about Dodd's Shaft. Cream to light green, circular to elongated porphyroclasts (1.0 mm. to 1.5 cm. long) define a prominent foliation and lineation within a dark, greenish-grey matrix which resembles the colour and texture of the massive greenschists. It is not unusual in areas of shearing (ie: Dodd's Shaft) to find weakly and strongly-deformed augen coexisting in a hand sample (photo 2.3). The gradation from oval phenocrysts to stretched augen and eventually thin lenses within the transition zone from volcanics



PHOTO 2.1: Section along the Goose Cove Road exposing a Fm fold.



PHOTO 2.2: Thrust faulting associated with the Fm fold in photo 2.1.

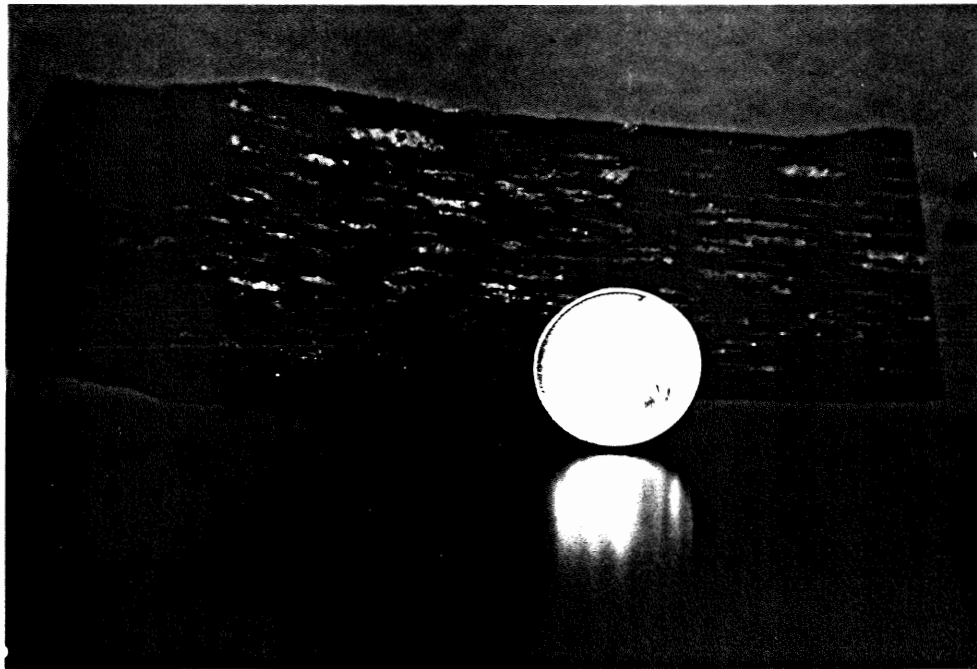


PHOTO 2.3: Porphyroclastic metvolcanics with oval to elongated porphyroclasts.



PHOTO 2.4: Porphyroclastic metvolcanics at Norcat Point showing the transition of augens(center) to lenses and bands(margins) within the unit.

to greenschist along Hare Bay attests to the origin of the porphyroclasts and relict plagioclase phenocrysts (Jamieson, 1979) and justifies the definition of the unit as porphyroclastic metavolcanics. At Norcat Point porphyroclastic greenschist, interbedded with banded greenschist, shows the change from augen to lenses or bands with increasing distance from the center of the unit which probably corresponds to progressive deformation (photo 2.4).

The banded (mylonitic) greenschists concentrate in two linear areas extending east-west along the south shores of Three Mountain Harbour and Vierge Cove. The unit consists of very fine-grained, well-foliated, fissile schists characterized by alternating white to light green and dark, green-grey layers (photo 2.5). The light-coloured bands which define the foliation can be traced for meters but are also locally interrupted by deformed augen structures (2-4 mm. long) which are similar to the forms in the porphyroclastic greenschists. The very fine grain size, the presence of porphyroclasts, the segregation of the rock components and the continuity of the banding defines the unit as a mylonite. Since mylonite is indicative of intense ductile deformation (Tullis, 1982) these areas correspond to zones of high strain.

In the field, there are two distinct divisions of metasediments based upon mineralogy and texture - garnetiferous semi-pelites and siliceous psammites. The classification is very general and



PHOTO 2.5: Kink folds in the banded metavolcanics.

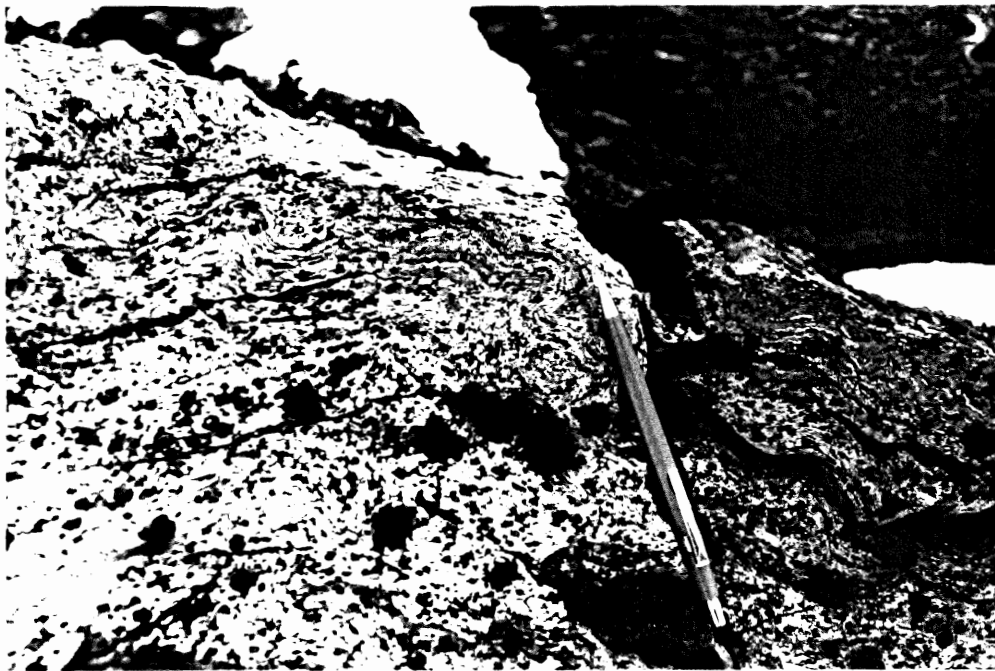


PHOTO 2.6: Crenulations in the semi-pelite on the north-west shore of Goose Cove.

is based upon the quartz/muscovite ratio whereby high values and low values are indicative of psammite and pelite, respectively. The garnetiferous semi-pelites are grey-brown, fine to medium-grained, dense, well-foliated, garnet-mica-bearing schists located on the south shore of Three Mountain Harbour. Round to oval garnets (0.5-1.0 mm. long) are visible in low percentages (< 5%). The foliation is defined by the alignment of micaceous minerals.

West of the Goose Cove Road, the semi-pelites are buff to light grey, very fine-grained, well-foliated schists (photo 2.6). Buff, very fissile bands (2-5 mm. thick) alternate with light green-grey, dense bands (1.5-3.0 cm. thick). Tight, upright continuous (10-20 cm.) crenulations (amplitude approximately 1 cm.) with parasitic crenulations define a lineation (photo 2.7).

The metasediments on the northwest shore of Vierge Cove may be subdivided into two types. East of the major north-south trending fault, the mylonitic siliceous metasediments are light to medium-grey, very fine-grained, well-foliated schists. Alternating 1 to 3 mm., light grey, silica-rich and 1 to 5 mm. medium-grey, silica-poor bands define the foliation (photo 2.8). Augen (1-2 mm. diameter) follow tight crenulations (approximately 1 cm. amplitude) oriented parallel to the foliation. Thin (1-2 mm. thick) lenses and veinlets (1-2 cm. long) of quartz parallel the foliation. West of the fault, the psammites are medium greenish grey, fine-grained, moderately-foliated schists. The foliation is

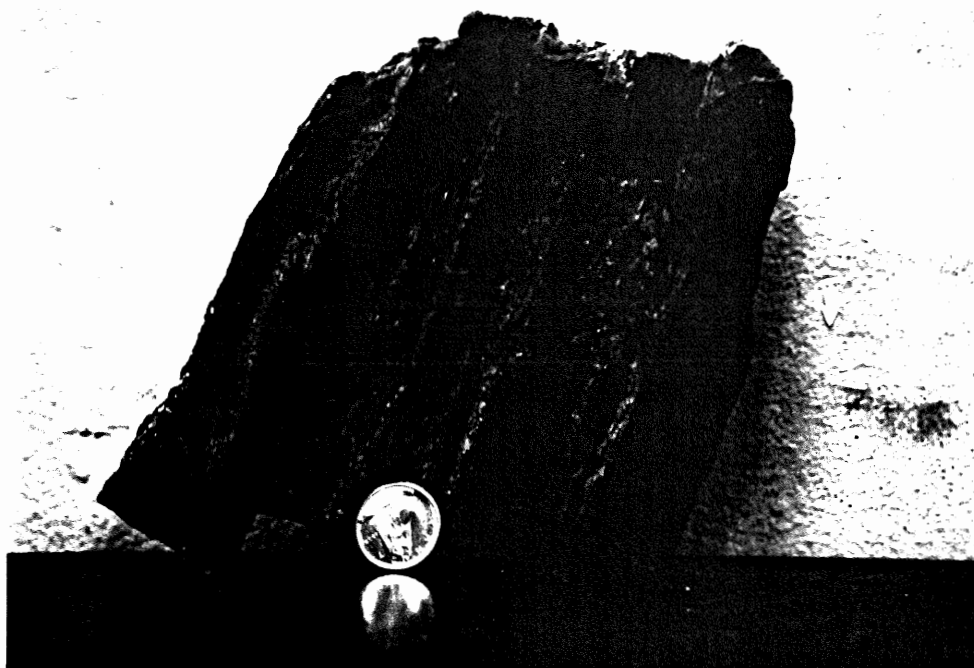


PHOTO 2.7: Crenulations marking the lineations in the semi-pelite.



PHOTO 2.8: Siliceous psammite from the west of Vierge Cove.

defined by alternating silica and muscovite-rich layers. Crenulations have a locally variable orientation. Quartz occurs as lenses (1-2 mm. thick) that had been deformed into open Z-shapes. These quartz lenses may be the wispy, deformed quartz aggregates within the semi-pelites on Fischot Island, south of Goose Cove, as described by Jamieson (1979).

The coarse-grained greenschists, intercalated with banded metavolcanics and calc-silicate schists on the shore of Vierge Cove, exhibit a local variation in texture but a consistent mineralogy. The rocks are coarse-grained, green-grey, well-foliated to mylonitic schists. Alternating light green-grey and dark green-black layers (1-3 mm. thick) define the foliation. The layers vary from crenulated and highly contorted to very regular, continuous and mylonitic in accordance with progressive deformation. Dark green-black equant minerals (1 mm. diameter) present as augen in a finer-grained matrix follow the foliation of the schist. Calcite veinlets (1-2 mm. thick; 1-10 cm. long) cross-cut the foliation. The unit may be a metamorphosed intrusive sill or dyke or a coarse-grained lava flow. The former is preferred by this author.

The calc-silicate schists are restricted to the south shore of Vierge Cove. The schists are medium greenish-grey, fine-grained, dense, well-foliated rocks (photo 2.10). Intercalated light green-grey and predominant (60-90%) dark

green-black layers (0.5-4.0 cm. thick) are continuous and define the foliation (photo 2.9). Fine fractures (3-5 mm. thick) parallel but most often cross cut the foliation and are filled with epidote. Micaceous minerals, feldspar and other siliceous minerals, mafics and calcium-bearing minerals are the major constituents. The origin of the calc-silicate schist is uncertain but the initial rock type may have been a calcium-rich, fine-grained metasediment. The calc-silicate schist was probably mapped by Jamieson (1979) as metasediments.

Weathering products are present in all lithologic units and they include chlorite, sericite and iron oxides.

Structure

A complete structural analysis is beyond the scope of this thesis but the following discussion serves to demonstrate the intensity of deformation and the complexity of the structure within the thesis area. The main foliation (S_m) trends east-west and the folding events will be interpreted with respect to this dominant structure.

Two specific areas were studied in detail in an attempt to more clearly define the history of deformation. A pale yellow-green band intercalated with the greenschist facies metavolcanics on the south shore of Three Mountain Harbour provided a good marker horizon for structural interpretation. The second locality was the



PHOTO 2.9: Isoclinally folded calc-silicate schist on the south shore of Vierge Cove.



PHOTO 2.10: Shallow, westward plunging Fm fold at Norcat Point.

main ore body at Dodd's Shaft, where a critical look at the ore-host rock relationship should aid in the delineation of the structural controls of the ore. The results are depicted in plan and cross-sectional views and appear on Plate I. In addition, two geological profiles including these two areas accompany the map.

The marker band is folded into asymmetric Fm folds which dip shallowly to the west (photo 10). Within 10 to 15 meters along a northward traverse, tight, east-west trending folds (Fm) grade into isoclinal folds with steep dipping limbs and eventually into a shear zone of vertically orientated foliation surfaces (photos 2.11 and 2.12). This structural transition is coincident with a lithologic change from porphyroclastic to banded mylonitic greenschist. Parasitic folds within the Fm folds are common. In the hinges of the Fm folds (inset #3 of marker bed data on Plate I), the foliation is highly contorted. This suggests the existence of previous folding events. In the area of less-intense deformation to the south, tight to isoclinal Fm-1 folds are orientated at an angle to the Sm foliation. The Fm-1 steeply-dipping fold axes have a variable orientation in response to the Fm folding event (Fig. 2.3a). The banding and elongation of the porphyroclasts in the greenschists is considered to be a metamorphic fabric, Sm-2, which is folded by the Fm-1 folding event. At this point, it is not possible to confirm whether Sm-2 is the result of the first folding event or there are additional



PHOTO 2.11: Marker band intercalated with meta-volcanics illustrates the trend of the Fm folds and Sm foliation (looking west).



PHOTO 2.12: The vertically oriented foliation (Sm), 15 meters to the north of photo 2.11 (looking west).

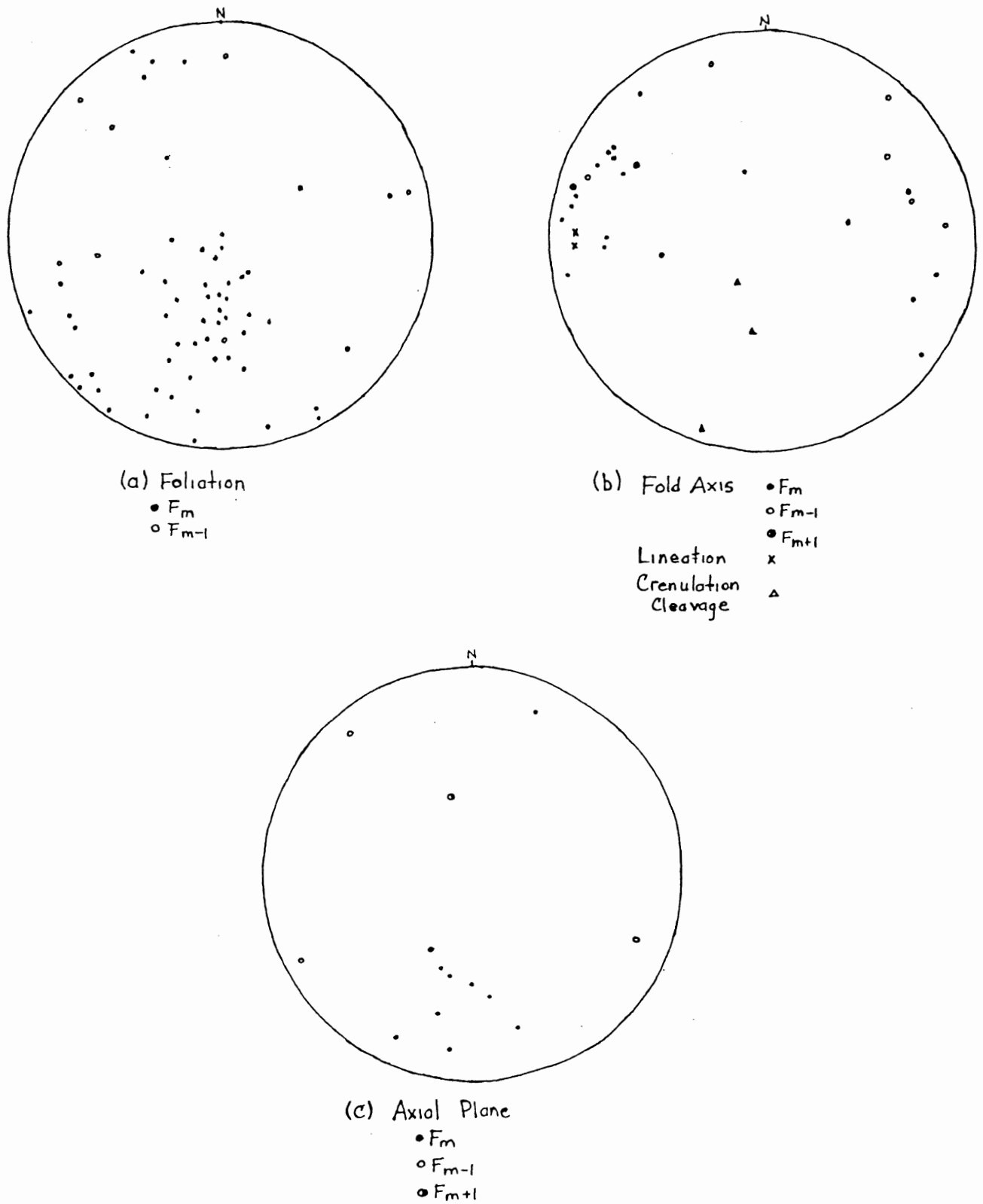
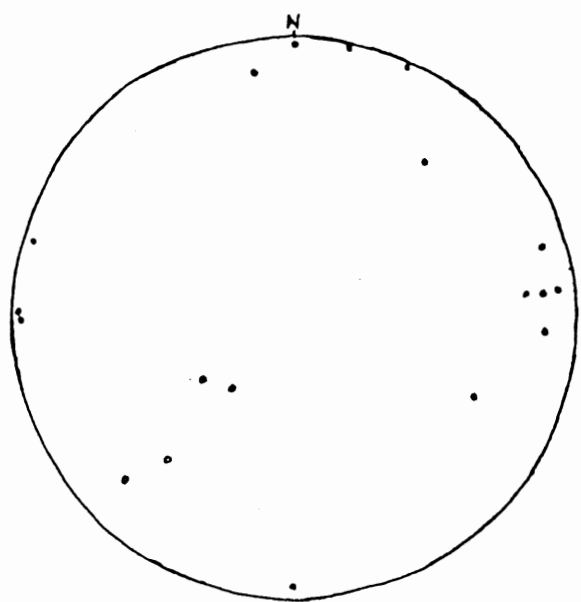
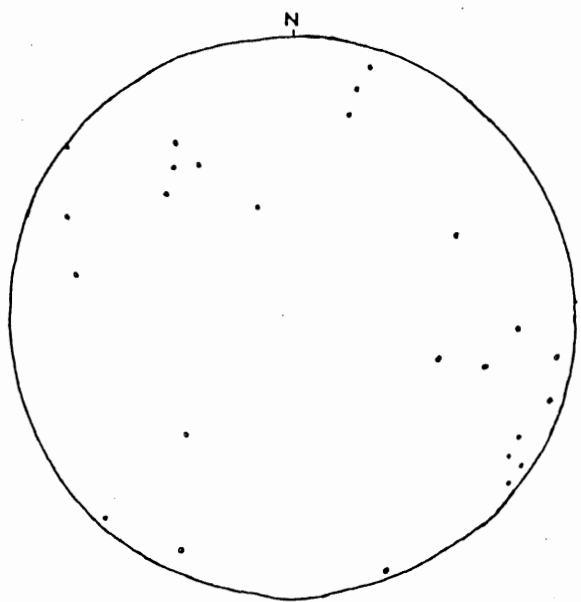


Figure 2.3: Stereonets of (a)foliation (b)fold axes (c)axial planes.



(d) Faults
• Normal
◦ Thrust



(e) Joints

Figure 2.4: Stereonets of (d) faults and (e) joints.

stages of folding prior to Fm-2. Considering the extreme intensity of deformation in the area, it is probable that there were previous deformational events.

The ore body at Dodd's Shaft is confined to the hinges of an asymmetric Fm fold, that plunges shallowly to the west. The ore follows the Sm foliation that dips to the north. The foliation (Sm) of the porphyroclastic metavolcanics immediately above the ore body, is highly contorted and variable (photo 2.13). The banding (Sm-2) considered to be metamorphic layering (as exists with the marker band), is folded into rare, tight Fm-1 folds oblique to Sm.

Figure 2.3(a) is a compilation of the poles to all foliations including Sm, pre-Sm and post-Sm. There are several aspects that should be noted.

(1) The Sm poles tend to cluster in the southwest corner and are indicative of a foliation trending north of west and dipping variably to the north (photo 2.14). This pattern is characteristic of asymmetric folds with inclined axial planes. In this case, the axial planes dip to the north-northeast (photo 2.15).

(2) The deviation of Sm from a westerly to northerly trend, although possibly a result of statistical variation, may indicate a regular deforming of Sm by a post-Fm event.

(3) The pre-Sm foliations display no consistent structural pattern. This may be related to insufficient data or to the

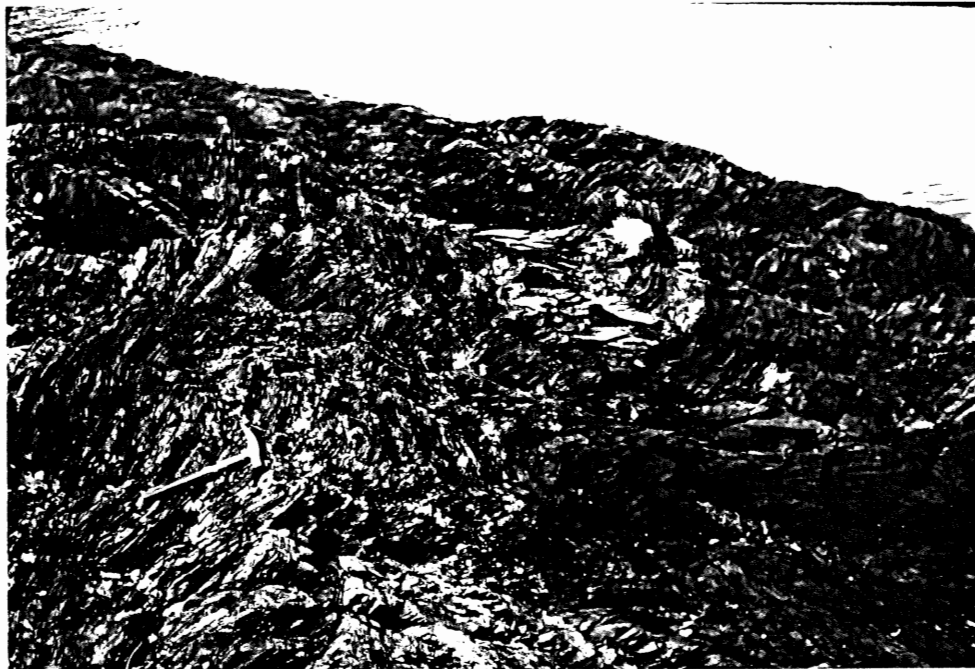


PHOTO 2.13: Extreme intensity and contortion of the foliation (Sm) near Dodd's Shaft.



PHOTO 2.14: The northward dipping Sm foliation on the north shore of Three Mountain Harbour.



PHOTO 2.15: Tight asymmetric Fm folds on the north shore of Three Mountain Harbour.

complexity of folding.

(4) The S_m foliations at the mine exhibit a strike and dip variation that is indicative of highly-contorted foliation surfaces.

There are a number of features that attest to the possibility of a post-Fm deformational event:

(1) variation of the Fm fold axis from an east-dipping axis along the shores of Three Mountain Harbour to a west-dipping axis along the Goose Cove Road

(2) the rotation of S_m from east-west to north-south at the base of Three Mountain Summit which may be related to the development of two oblique trending shear zones (Jamieson, pers. comm.)

(3) crenulation cleavage (Fig. 2.1c) that cross-cuts S_m

(4) the presence of shear zones in the metavolcanics and metasediments on the shores of Three Mountain Harbour and Vierge Cove.

The shearing has resulted in the formation of mylonite that strikes east-west and dips vertically. It is difficult to determine whether this deformational event is a separate stage of deformation. The mylonite which is coincident with areas of high strain, may have a spacial rather than temporal explanation or may have developed parallel to linear weaknesses in S_m . The distortion of the Fm fold axes and foliation indicates a complicated arrangement of deformational forces related to the Fm+1 event.

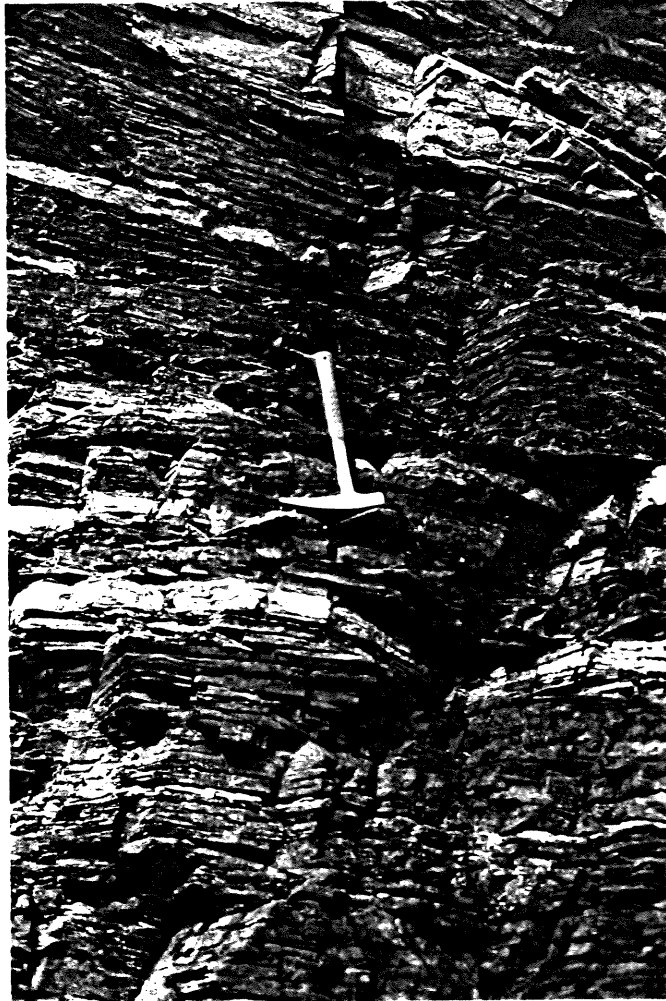


PHOTO 2.16: Intercalated porphyroclastic (light) and banded (dark) meta-volcanics at Norcat Point.

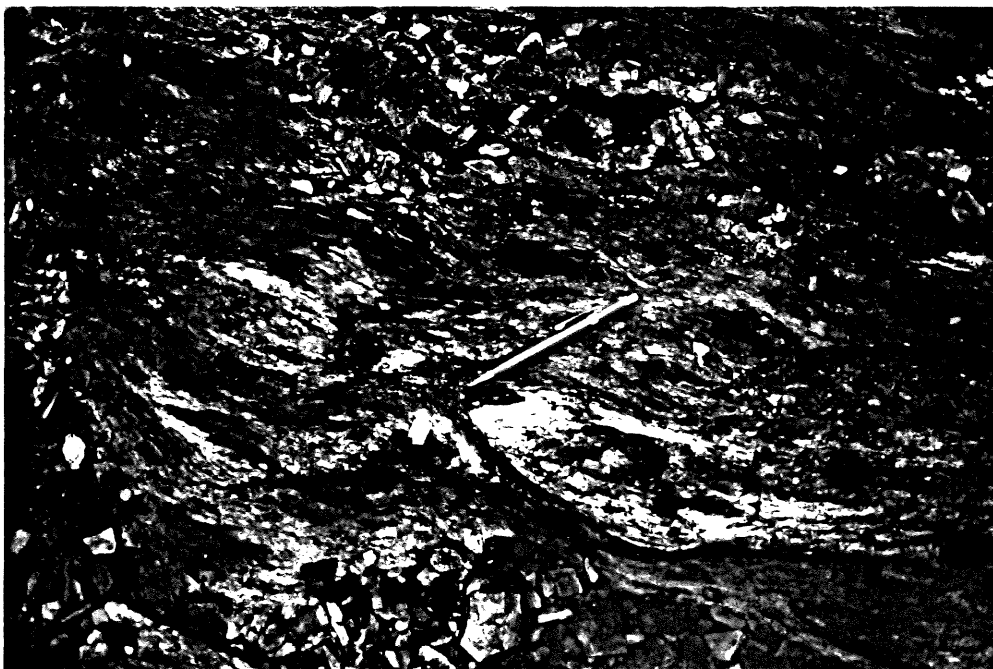


PHOTO 2.17: Mineralized boudinage in the post-Fm shear zone on the west shore of Three Mountain Harbour.

Late stage deformation includes faulting (Fig. 2.4d) and jointing (Fig. 2.4e) and fracture filling. The major faults trend north-south, dip vertically and are generally confined to the eastern portion of the thesis area. Sinistral movement, as determined by the bending of the foliation at the fault, is probably not extreme. Minor faults trend east-west and north of west, dip near the vertical and generally do not extend beyond 100 meters along the surface. Jointing is common and the major trending directions are northeast-southwest and approximately 60 and 90 degrees to this direction. The dips are generally steep but vary between 35 and 90 degrees. The orientation of these two planar features suggests a conjugate system of faults and joints. Fractures that parallel and cross-cut the main foliation are filled with quartz, epidote and calcite. A prominent 10 cm. thick quartz vein cross-cuts the main foliation and can be traced for 5 meters at the base of Three Mountain Summit. Quartz veins (1-3 cm. thick) are most prominent in regions of faulting. Epidote and calcite veinlets (< 1 cm. thick; < 2 m. long) cross-cut the calc-silicate schists and coarse-grained greenschists along the south shore of Vierge Cove. The two types of veinlets often cross-cut each other implying a simultaneous temporal formation.

(c) Ore-host rock relationship

The ore samples were taken from ore piles adjacent to the

Dodd's Shaft and Payne's Shaft. Since the samples were taken from the top of the piles, they may represent the ore body at the depth of termination. Due to the snow cover thein situ ore was inaccessible and unfortunately, no samples were obtained. Consequently, there are no samples from the upper part of the ore body. However, mineralized porphyroclastic metavolcanics at Dodd's Shaft were sampled (JB-38A, JB-65A). Mineralogical or textural variation of the ore body may be revealed in the comparison of ore from the two shafts. Mineralized host rocks from the north shore of Three Mountain Harbour (JB-8, JB-12), the south shore of Vierge Cove (JB-74B) and along the Goose Cove Road (JB-14, JB-16A) will be included in the description of the ores.

The mineralized areas that have been mined can be correlated with porphyroclastic or banded metavolcanics and Fm anticlines. The cross-section C-D (Plate I) shows the ore body inclined to the north and following the north limb of a Fm fold. Ore from Dodd's Shaft has been stretched and orientated parallel to the Sm foliation while ore from Payne's Shaft appears to have undergone a lesser degree of deformation. This difference may be local and should not be interpreted as absolute. However, deformation of the ore does imply the ore emplacement pre-dates or is synchronous with the Fm event.

Ore from Dodd's Shaft (JB-30, JB-31) includes chalcopyrite (45-55%), pyrite (30-40%), pyrrhotite (5-10%) and minor sphalerite

(< 5%). Chalcopyrite is very fine-grained and occurs with fine-grained, disseminated pyrrhotite in thin, irregularly orientated bands or lenses (1-3mm. thick; 25-45%) that are intercalated with deformed porphyroclastic metavolcanics (55-75%). The existence of ore and host rocks as parallel alternating zones and the elongation of plagioclase-calcite fragments within the metavolcanics indicate deformation of the ore. Pyrite as blebs, lenses and veinlets (2mm.- 5cm. long; < 1mm.- 2mm. thick) parallel but also cross-cut the host rock metavolcanics and chalcopyrite (photo). Veinlets definitely indicate a secondary ore emplacement. Sphalerite is present as isolated patches of disseminated grains.

Samples from the ore pile adjacent to Payne's Shaft (JB-32, JB-33) are characterized by weakly to moderately deformed metavolcanic fragments (35-50%) within a matrix of pyrite (20-30%), chalcopyrite (15%), pyrrhotite (5-10%) and sphalerite (< 5%). Chalcopyrite is fine grained (< 1 mm.) and usually confined to the matrix but is rarely found within the metavolcanic fragments. Pyrite is coarse-grained (< 1mm.- 2mm.) and is found within the matrix and cross-cutting the metavolcanic fragments. There is a vague parallel orientation of the fragments but it is obviously less prominent than in the ores from Dodd's Shaft.

Banded metavolcanics at Dodd's Shaft contain disseminated, lenses and veinlets of pyrite and chalcopyrite. Pyrite is the

dominant sulphide. The veinlets are approximately 1 mm. thick and up to 1.5 cm. in length and parallel and cross-cut the foliation.

On the north shore of Three Mountain Harbour, there is a small mineralized post metamorphic shear zone in the porphyroclastic metavolcanics. The outcrop shows sulphide-poor boudins within a sulphide-rich matrix (photo). Sample JB-8 shows the contact between the two areas. The sulphide-poor metavolcanics have abundant deformed porphyroclasts and bands of altered plagioclase in a dark grey, dense matrix. The sulphide-rich metavolcanics are very fissile, medium green and contain few porphyroclasts. Pyrite and chalcopyrite exist as disseminated grains, lenses (3-7 mm. long; 0.5- 2 mm. thick) and veinlets (1-4mm. thick; irregular length) that parallel the foliation. Sample JB-12, taken from this area, exhibits the fissile texture of the brittly-deformed, mineralized metavolcanics which are distinct from the typical dense, mylonitic metavolcanics within the thesis area. The presence of pyrite in the boudins and the matrix and the elongation of pyrite parallel to the foliation (Sm) attests to the ore emplacement prior to or synchronous with the Fm foliation.

Along Goose Cove Road, pyrite and fine-grained chalcopyrite are associated with quartz veins cross-cutting the foliation of the massive metavolcanics. The calc-silicates on the south shore of Vierge Cove contain fine-grained pyrite and chalcopyrite in lenses and stringers that parallel the foliation and pyrite in epidote

stringers that cross-cut the foliation. The cross-cutting veinlets indicate a post-Fm emplacement while the pyrite and chalcopyrite lenses orientated parallel to the Fm foliation of the calc-silicates attest to a pre- or syn-Fm emplacement.

The field evidence would seem to indicate that mineralization is not restricted to the porphyroclastic metavolcanic unit, not confined to the hinges of Fm anticlines and emplacement was not a single epigenetic event post dating the Fm stage of deformation. It is suggested that ore formation was prior to or synchronous with the Fm event. However, additional evidence is required to confirm the mode of ore formation. Petrographic and geochemical studies included in the following chapters have been designed to investigate the 'syngenetic' (pre-Fm) and epigenetic (post-Fm) modes of ore emplacement.

CHAPTER 3 PETROGRAPHY

A petrographic study of the lithologic units defined within the thesis area and ore samples from Dodd's and Payne's Shafts was done to establish the variation of mineralogy, texture and metamorphic grade of the host rocks and to more clearly define the ore-host rock relationship. Appendix I is a compilation of the thin section descriptions and relative photographs.

(a) Host rocks

The metasediments which include semi-pelites and psammites are characterized by the mineral assemblage quartz-mica-sericite-plagioclase-(chlorite) and classified by the relative proportions of quartz and feldspar to mica and chlorite (Jamieson, 1979). The metamorphic grade ranges from greenschist to epidote-amphibolite.

In the garnetiferous semi-pelite (JB-3) on the south shore of Three Mountain Harbour, the garnets are either augen wrapped around by biotite or large crystals overprinting the foliation. The unit is distinguished by isoclinally folded and alternating mica-rich and quartz-rich bands. The metasediments are metamorphosed to epidote-amphibolite grade as characterized by the presence of epidote, biotite and garnet and absence of primary chlorite. As suggested by Jamieson (1979), the garnet and biotite probably form at the expense of chlorite at higher grades. The

higher grade of metamorphism and mylonitic texture indicates a high intensity of deformation.

The semi-pelites, west of Brimstone Ponds (JB-17) are distinguished by large, intensely deformed muscovites (15-20%) within a micaceous matrix of primary chlorite (10-15%) and sericite (20%). Small, rounded to subhedral garnets (5%) appear as inclusions in the muscovite or as isolated grains within the foliated matrix of alternating quartz and muscovite-rich layers. Opaques, present as inclusions, are folded and deformed with the muscovite.

The simple mineral assemblage quartz-mica-plagioclase, the predominance of quartz (50-55%) often present as lenses and veinlets and mylonitic texture are characteristic of the siliceous psammite (JB-81, JB-89) found west of Vierge Cove. The alignment of micaceous minerals and the segregation of quartz and mica minerals into bands defines a prominent foliation, that is commonly deformed into isoclinal folds. In the hinges, it is not unusual for the foliation to be highly contorted. The fine grain size and the segregation of the rock components onto laterally continuous bands allow the garnetiferous and siliceous metasediments to be termed mylonites.

The division between porphyroclastic and banded, greenschist facies, metavolcanics is difficult since the characteristic features of both units are often visible within one thin section.

Therefore, if the porphyroclasts were in excess of 5 to 10%, the sample was classified as a porphyroclastic metavolcanic.

The porphyroclastic metavolcanics are characterized by augen of plagioclase, generally replaced by sericite, epidote and calcite, in a fine-grained matrix of actinolitic hornblende or common hornblende, chlorite and feldspar. Sphene occurs as anhedral crystals within the foliation and euhedral crystals overprinting the foliation or within veinlets cross-cutting the foliation. Rare, subhedral plagioclase is present as relict phenocrysts. Commonly, the porphyroclasts are stretched and elongated in a parallel orientation that defines the S_m foliation. Thin sections often exhibit the deformation of S_m and formation of tight to isoclinal F_{m+1} folds. The foliation is highly contorted at Dodd's Shaft.

Progressive deformation of the porphyroclastic metavolcanics corresponds to elongation of the augen to lenses and eventually thin bands. The hornblende changes from rectangular crystals of actinolitic hornblende dispersed evenly throughout the matrix to compact and well-aligned aggregates of lensoid hornblende crystals. The latter texture is similar to banded metavolcanics.

The banded metavolcanics are distinguished by bands of plagioclase, calcite and sericite in a hornblende-epidote matrix. Common hornblende is predominant over actinolitic hornblende and primary chlorite is present in minor quantities. The banding

defines the Sm foliation which is rarely folded into isoclinal Fm+1 folds. The very fine grain size, the presence of porphyroclasts, compositional segregation and continuity of the banding are characteristic of mylonite.

The absence of porphyroclasts or banding in the greenschist has been used to classify massive metavolcanics. Actinolitic hornblende/hornblende and epidote are segregated to form compositional layers that define the Sm foliation. Sphene is present only in the samples from the base of Three Mountain Summit. Progressive deformation, parallels an decrease in grain size and increase in the percentage of epidote, sericite, secondary chlorite and calcite. The loss of primary chlorite is locally variable and indicates a change from greenschist to epidote-amphibolite grade.

Coarse actinolitic hornblende in an epidote-rich matrix is characteristic of the coarse-grained greenschist, located along the shore of Vierge Cove. Relict clinopyroxene porphyroclasts, partially replaced by actinolitic hornblende are present and believed to represent the relict original mineralogy and texture of a basic igneous rock. With increasing deformation, there is a change from a moderately to well-developed foliation (Sm) defined by the linear arrangement of hornblende augens in a finer-grained epidote-rich matrix to boudinage of hornblende and eventually to a mylonite consisting of hornblende-rich and epidote-rich bands. The

banding is locally crenulated and can be highly contorted.

The calc-silicate schists consist of alternating calcite-plagioclase-rich and epidote-rich bands. The bands define the Sm foliation which is locally contorted. The high percentage of calcium-bearing minerals and the low percentage of mafic components are considered indicative of a protolith, that may be a calcium-rich, fine-grained metasediment.

Opaques, which include sulphides and oxides, are present in all the lithologic units. They may include chalcopyrite or pyrite as inclusions in epidote or garnet, Ti-Fe-oxides in muscovite, pyrite or chalcopyrite parallel to or deformed with the Sm foliation, pyrite in veinlets cross-cutting the foliation or isolated, dispersed grains of chalcopyrite, pyrite, pyrrhotite and Fe- or Ti-oxides.

The metamorphic grade ranges from greenschist to epidote-amphibolite. The increase in grade is distinguished by the disappearance of chlorite and the change from actinolitic hornblende to common hornblende, as determined by Jamieson (1979). Petrological evidence indicates there is not a predictable progression of the grade that could result in the delineation of a boundary between the two grades. The variation appears to be local and may be spatially coincident with areas of high strain. The fluctuation of the grade probably indicates metamorphic conditions close to the greenschist- epidote-amphibolite facies boundary.

(b)Ore

Detailed descriptions of the ore samples, using polarized and reflected light, and accompanying photographs are given in Appendix I. Ore from both Dodd's and Payne's Shafts are included.

The sulphides and oxides, referred to as opaques in the previous section, include pyrite, chalcopyrite, pyrrhotite and sphalerite and magnetite and hematite. The sulphides have a variable habit and arrangement within the ore samples.

(1) Parallel zones of sulphides alternate with stretched porphyroclastic metavolcanic fragments and define a weak to moderate foliation (Sm).

(2) The sulphides may be a matrix within which undeformed fragments or isolated grains of silicates lie.

(3) Isolated grains of sulphides are evenly dispersed or rarely follow the main foliation (Sm) within the metavolcanic fragments.

(4) Coarse-grained sulphides exist as veinlets cross-cutting earlier structures.

The metavolcanic fragments are distinguished by augen of plagioclase and/or calcite, commonly stretched and deformed to lenses and bands in a matrix of or alternating with a band of actinolitic hornblende and chlorite. Epidote is present in the augen as an alteration product of plagioclase or as thin lenses within the matrix. Sphene are coarse grains that generally follow

the foliation (Sm) within the metavolcanic fragments.

The sulphide zones or matrix consist of intergrown, fragmented and irregularly shaped grains of pyrite (30-35%), chalcopyrite (25-45%), pyrrhotite (< 5-35%) and sphalerite (< 5-15%). However, the complete assemblage is very rarely seen and generally the matrix is composed of chalcopyrite-dominant or pyrrhotite-dominant patches with minor amounts of pyrite and sphalerite. Sphalerite generally exists as disseminated veins in all the ore samples. The isolated grains that are contained within and follow the banding of the metavolcanic fragments may be chalcopyrite or pyrite.

The coarse-grained veinlets that cross-cut all previous structures and imply a secondary stage of ore emplacement, are exclusively composed of pyrite.

Magnetite and hematite are secondary minerals rarely present as coarse grains overprinting the sulphide ore and silicate fragments.

CHAPTER 4 GEOCHEMISTRY

Major and trace element content were determined by atomic absorption spectrophotometry. The major elements expressed as oxides included FeO(total), MgO, MnO, TiO₂, Na₂O and K₂O. The trace elements included Cu, Zn, Co, Ni, Cr and V. The elements were chosen to indicate chemical trends related to syngenetic or epigenetic ore emplacement, sulphide mobility and alteration zoning.

The samples were selected on the basis of determining any trend in element concentration with respect to (1) the mined area of highest ore content (ie: Dodd's Shaft) and (2) the lithologic units. Twenty-two samples were analysed. Basically, the locations lie on concentric circles about the mine. In addition, three samples of ore and one of unmineralized metavolcanic host rock were taken at the mine. On two circles of varying radius, 5-20 meters and 200-600 meters, sets of six and twelve samples, respectively, were chosen. The concentric pattern was designed to test the initial theory of ore emplacement involving epigenetic replacement of the greenschist host rocks. A localized emplacement mechanism should reveal a pattern of decreasing ore concentration with distance from the deposit. In fact, this pattern could be indicative of any 'central' mode of ore emplacement and therefore the geochemical analyses will serve to test all means of ore formation with a

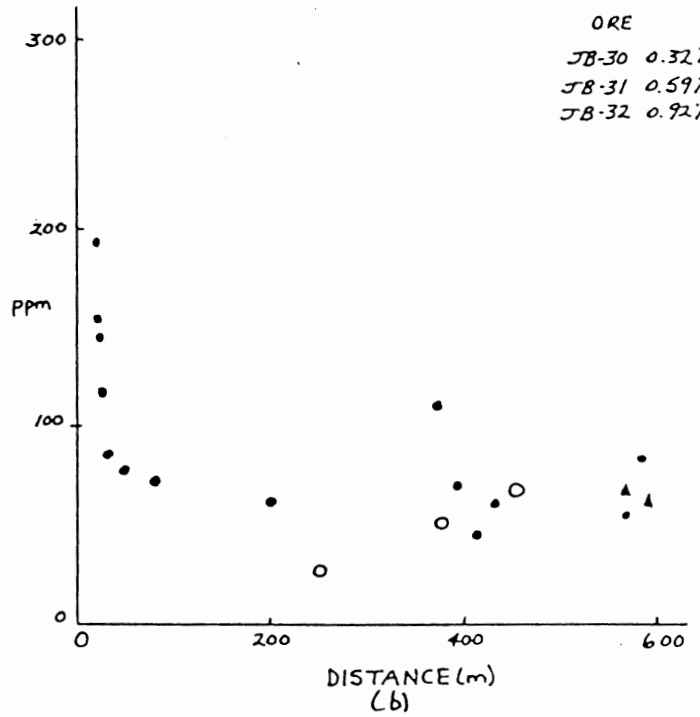
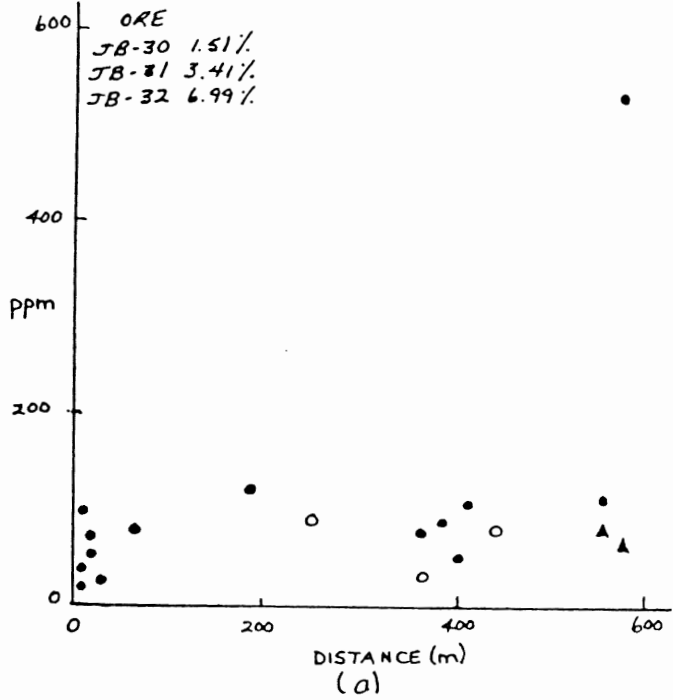
central source or mechanism of emplacement. The concentric pattern should also reveal alteration zoning if it exists.

All lithologic units were represented in the total sample set and consequently the analysis may determine whether a correlation between anomalous metal concentration and a particular lithologic unit exists. Other variables that may influence element distribution were not considered in this study, in the attempt to determine if there is a simple relationship between (1) metal concentration and distance from the mine or (2) metal concentration and lithology. The latter relationship may be modified by deformation and therefore suggests the metal concentration may be more properly interpreted with respect to the structural trends within the area.

The numerical values of the major and trace element analyses are listed in Appendix II. The results will be interpreted with respect to the models of ore emplacement. The epigenetic model is characterized by decreasing ore concentration from the deposit and plots of distance versus element concentrations should display the anticipated trend if it exists. Figures 4.1, 4.2 and 4.3 are graphs of distance, in meters, from the Dodd's Shaft versus weight percent of the oxide or ppm. of the trace element. Syngenetic emplacement is controlled by the lithology and structure. Consequently, element concentrations have been plotted on maps of the thesis area (Plates 2 and 3). This allows for the

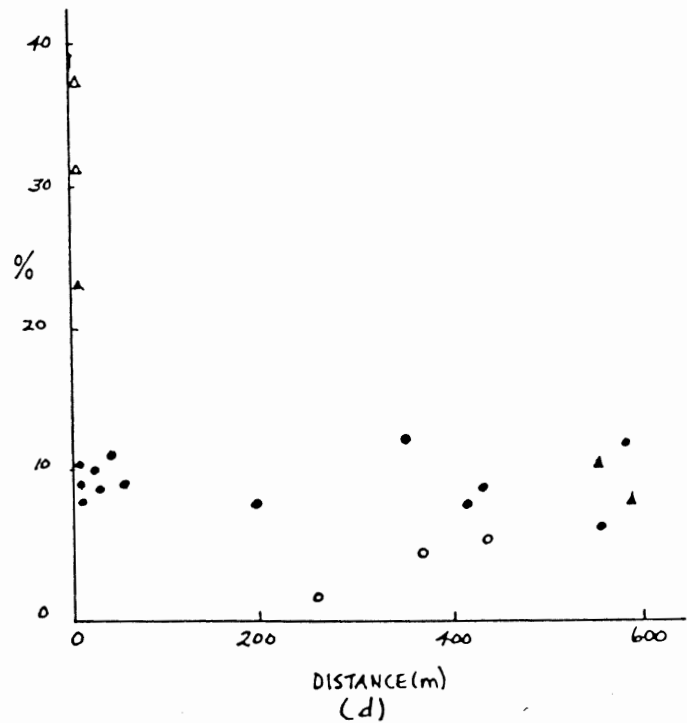
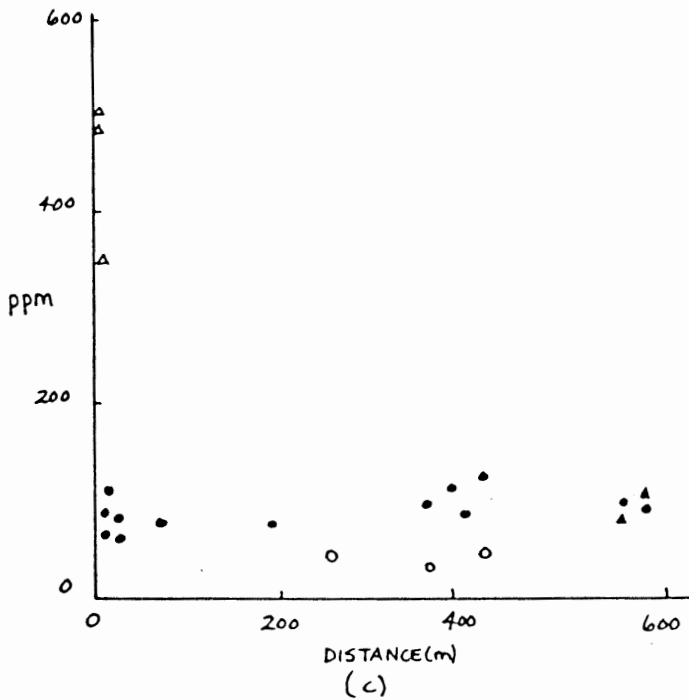
Cu

Zn



Co

FeO(T)



- FINE-GRAINED GREENSCHIST
- ▲ COARSE-GRAINED GREENSCHIST
- META SEDIMENTS
- ▲ ORE

Figure 4.1: Plots of distance from Dodd's Shaft versus weight percent of the oxide or ppm. for (a)Cu, (b)Zn, (c)Co and (d)FeO(T).

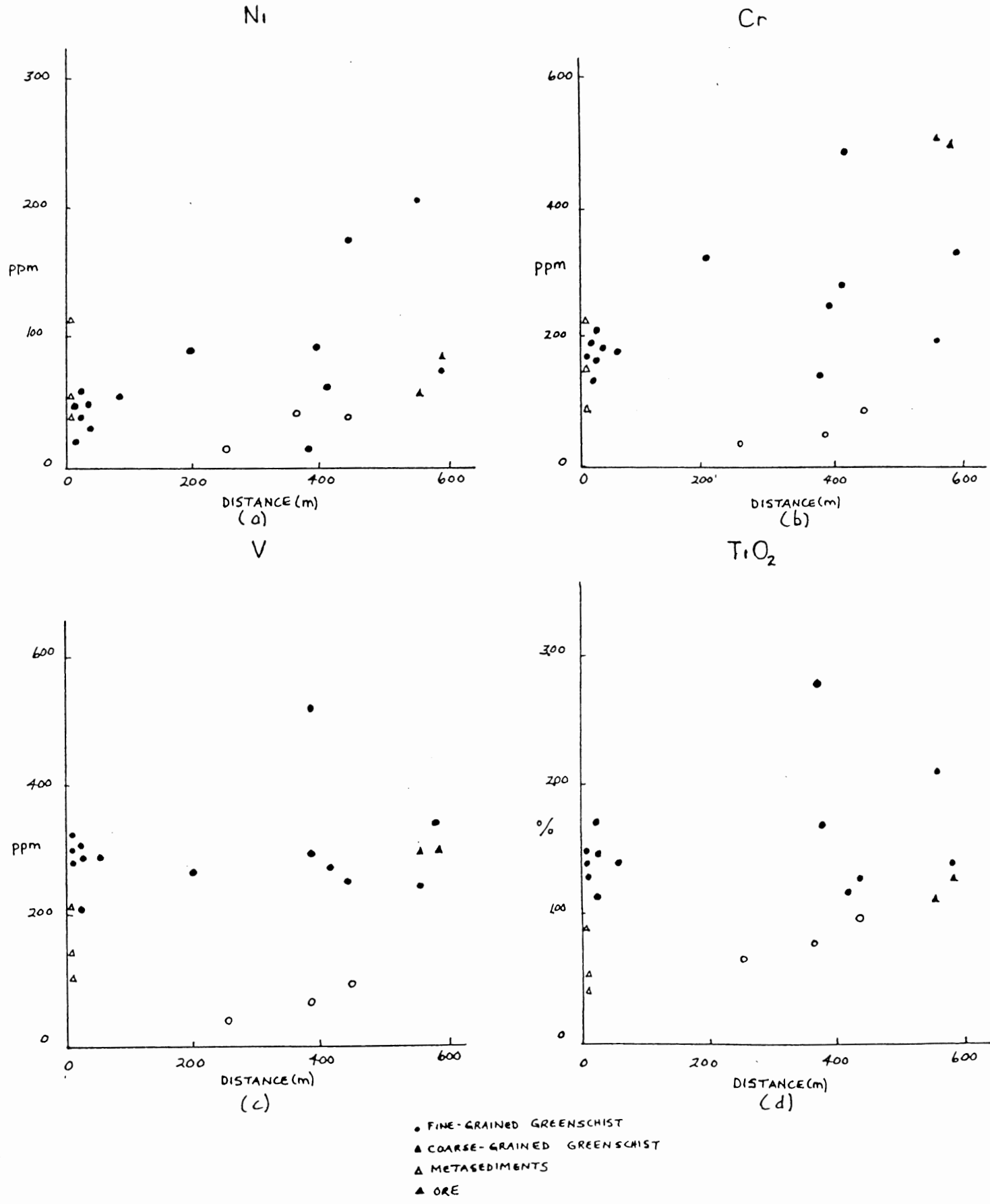


Figure 4.2: Plots of distance from Dodd's Shaft versus weight percent of the oxide or ppm. for (a)Ni, (b)Cr, (c)V and (d)TiO₂.

host rock metavolcanics is very significant. Since the element concentrations do not increase linearly or exponentially toward the mine, the possibility of a localized mechanism of emplacement seems unlikely. It would appear that the use of the hydrothermal replacement method to explain the occurrence of the ore deposit is not relevant.

Plate 2 shows a consistent correlation of highest Cu, Ni and Zn concentrations with the metavolcanic units, specifically the porphyroclastic metavolcanics.

Table 4.1 is a compilation of major and trace element concentrations of the greenschist metavolcanics of the Goose Cove Schist, the porphyroclastic pillow lavas of the Ireland Point Volcanics (Jamieson, 1979) and typical mid-ocean ridge, ocean-floor and ocean-island basalts.

Comparison of the greenschist metavolcanics and the undeformed equivalents (Ireland Point Volcanics) reveals the addition of TiO_2 , FeO , MnO , MgO , Na_2O , and V and depletion of K_2O , Cu , and Ni with respect to the former. The Cr concentration remains relatively constant. It is not possible to ascertain whether the concentration of Zn has varied since it is enriched and depleted with respect to unaltered and altered pillow lavas. The concentration changes are considered to be the effect of metamorphism and deformation. This implies a formation of the ore body by mobilization and reconcentration of the ore forming

TABLE 4.1: Major and trace element analyses of Goose Cove Schist metavolcanics, Ireland Point Volcanics pillow lavas and basalts from tectonic oceanic settings

Major or trace element	Greenschist Metavolcanics (from GCS)	Unaltered pillow lavas (from IPV) ¹	Altered pillow lavas (from IPV) ¹	Mid-ocean ridge basalt ²	Ocean-floor basalt ³	Ocean-island basalt ³
TiO ₂	1.43	0.68	0.75	1.43	1.43	3.12
Al ₂ O ₃	-	19.82	20.12	16.01	16.20	16.87
FeO _(T)	10.31	3.73 Fe ₂ O ₃ 2.52 FeO	3.54 Fe ₂ O ₃ 3.08 FeO	11.44	10.24	11.18
MnO	0.21	0.10	0.12	0.18	-	-
MgO	6.58	4.89	4.61	7.04	7.74	5.69
CaO	-	13.73	13.26	11.32	11.42	10.22
Na ₂ O	3.57	2.66	2.96	2.76	2.82	3.46
P ₂ O ₅	0.47	1.12	1.26	0.22	0.24	1.39
Cr	239	224	231	297	310	280
Ni	80	159	104	97	-	-
V	282	132	146	292	-	-
Zn	101	82	111	-	-	-
Cu	61	113	114	77	-	-

¹ Jamieson, 1979

² Engel *et. al.*, 1965

³ Pearce, 1975

TABLE 4.2: The Cu:Zn ratio of ore from Dodd's (JB-30, JB-31) and Payne's (JB-32) Shafts.

Sample #	Cu:Zn ratio
JB-30	2.56
JB-31	10.70
JB-32	7.60

elements (ie: Cu, Ni, Zn?).

However, the question remains whether the original pillow lavas had high anomalous concentrations of Cu, Ni and Zn due to syngenetic mineralization. Since the Ireland Point Volcanics are considered to be the protolith of the greenschist metavolcanics it is appropriate to compare the major and trace element concentrations of the Ireland Point Volcanics with typical basalts of the same paleoenvironment. Figure 4.4 shows the majority of the greenschist metavolcanics plots as ocean-floor basalts. Although Ti is expected to be immobile with greenschist metamorphism (Pearce, 1975) the metavolcanics show an enrichment of TiO_2 with respect to the Ireland Point Volcanics and therefore, the designation of the pillow lavas as ocean-floor basalts cannot be considered absolute. It is more likely that the metavolcanics plot near the boundary of the two basalt types.

The enrichment of Cu and Ni in the Ireland Point Volcanics with respect to the mid-ocean ridge basalts may be indicative of a syngenetic concentration that probably occurred by hydrothermal alteration of the primary basalts (Coleman, 1977; Mitchell and Garsen, 1977; Pearce and Gale, 1977). However, the comparison is not conclusive and since the paleoenvironment of the pillow basalts cannot be exactly determined, it is not possible to ascertain whether the Ireland Point Volcanics are enriched in Cu and Ni as a result of syngentic mineralization.

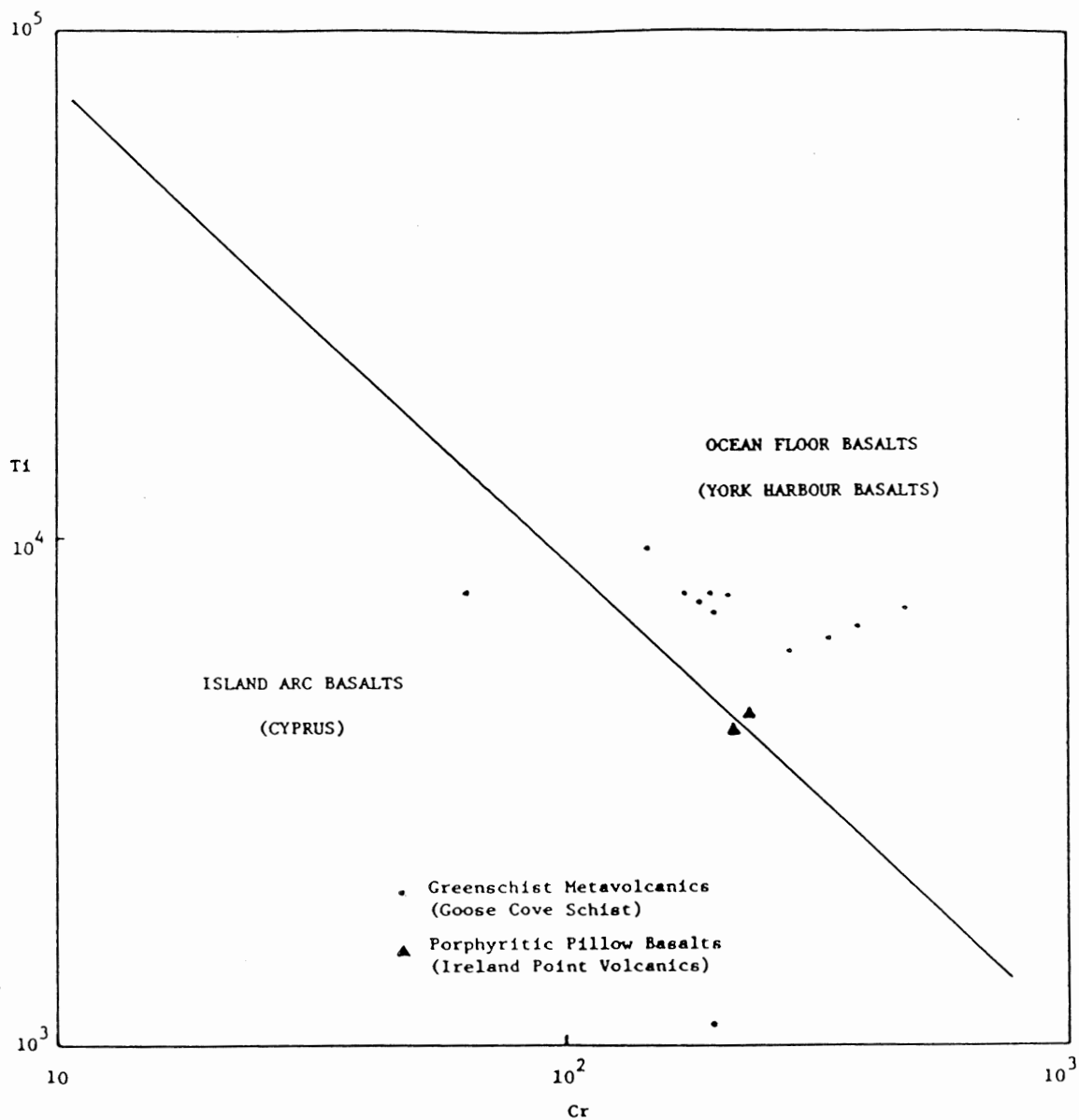


Fig. 4.4 Ti-Cr plot of greenschist metavolcanics (Goose Cove Schist) and porphyritic pillow basalt (Ireland Point Volcanics).

Regardless of the original basalt type, the data imply a mobilization and reconcentration of the ore-forming elements during metamorphism and deformation of the Ireland Point Volcanics with the resulting depletion of these elements in the host rock metavolcanics.

CHAPTER 5 MINERAL CHEMISTRY

(a) Microprobe analyses of sulphides and oxides

Opaque minerals in the ore and host rocks were analyzed by the electron microprobe. The main purpose was to delineate variation of the mineral chemistry if it exists. Each grain was tested for zoning by analyzing along a three-point traverse from the center to the rim of each grain. The minerals are present in different habits and arrangements and therefore it was necessary to test for variability with respect to the grain orientation. To test the chemical variation within each mineral type, at least three grains (if present) per slide were analyzed. The analysis was expected to reveal zoning of individual mineral types, differences of chemical composition within one mineral type and whether the difference could be related to a particular habit and deviation of the mineral chemistry from the ideal opaque minerals. A compilation of the representative analyses is listed in Appendix III. The data are arranged according to the mineral type and subdivided into lithologic categories. The data are mean values of analyses that differ by less than one mole percent with respect to the major elements. The number of grains included in the calculation of each average is given.

The opaque minerals include sulphides and oxides. The sulphides are pyrite, chalcopyrite, pyrrhotite and sphalerite and are

present in schist fragments within the ore matrix, in veinlets cross cutting the foliation, as isolated grains in the host rock, as inclusions, lamellae or replacement growths in other sulphides. The oxides include magnetite, hematite, ilmenite, goethite, rutile and a titanium-rich iron oxide which may be titanomagnetite. Except for titanium-rich oxides which exist as pre-tectonic grains within the muscovite of the pelitic metasediments, the oxides overprint the foliation (Sm). No relationship between the chemistry and the occurrence of individual sulphides or oxides within the host rock exists. Zoning does not exist in any mineral type. Some sulphide grains have rim overgrowths of iron oxide minerals but this is not primary and not considered to be zoning. Each mineral has a consistent composition irrespective of its occurrence and location within the host rocks.

Minor quantities of Zn, Cu, Ti, Co, Mn, V, Ca and Zn, Cu, Ti, Cr, V, Mn, Mg, Al are associated with the sulphides and oxides, respectively. These elements show no consistent variation with respect to zoning or grain orientation within the host rock. However, the presence of some elements can be correlated with a particular grain type. Substitution of Fe and Cu by Co, Ni, Zn and V occurs, respectively, in pyrite, pyrrhotite, chalcopyrite and magnetite. In sphalerite, Fe substitutes for Zn. The replacements are not unusual (Deer, Howie and Zussman, 1980). The minor elements may be present as impurities or in solid solution with

the major elements of the minerals. The presence of chalcopyrite blebs in sphalerite is particular to the ore from Payne's Shaft. Deer et.al. (1980) attribute this feature to exsolution on cooling from a higher temperature ZnS-CuFeS₂ solid solution. The chalcopyrite blebs, found only in ore from Payne's Shaft, infers a higher Cu concentration at this site. The correlation may be local and is therefore not conclusive. A more detailed study of the ores from each shaft should confirm any differences or similarities in mineral chemistry.

Titanomagnetite can also be explained as the addition of Ti to magnetite. The continuous relationship between magnetite, Fe₃O₄, and ulvospinel, Fe₂TiO₄ accounts for the formation of titanomagnetite. Only Ti-rich magnetite proven to contain the ulvospinel end member should be termed titanomagnetite and therefore the designation of the Ti-rich iron oxides as titanomagnetite should not be interpreted as absolute.

Since the formula of ilmenite may be expressed as (Fe, Mg, Mn)TiO₃, the high percentage of Mn is not uncommon.

The mineral chemistry of the sulphides and oxides of the green schists, metasediments and ore are graphically represented on Fe-Cu-Zn and Fe-Ti-O plots (Figures 5.1, 5.2 and 5.3). The ideal compositions of relative minerals are included on the plots.

Pyrite, pyrrhotite and chalcopyrite have very consistent chemical compositions comparable to the respective ideal minerals.

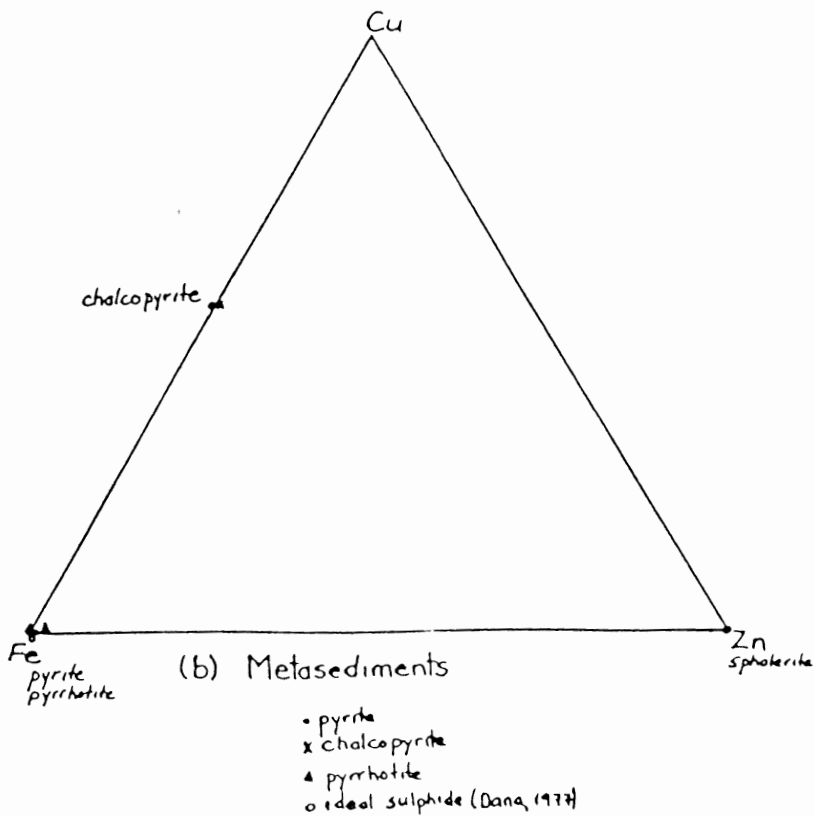
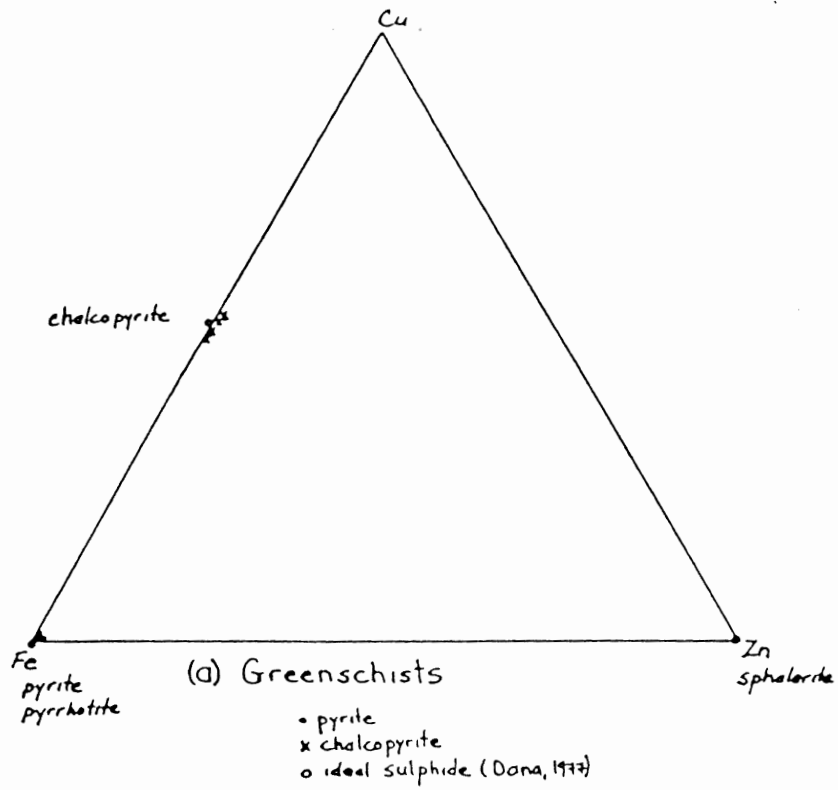


Figure 5.1: Fe-Cu-Zn plots of (a) greenschist and (b) metasediments

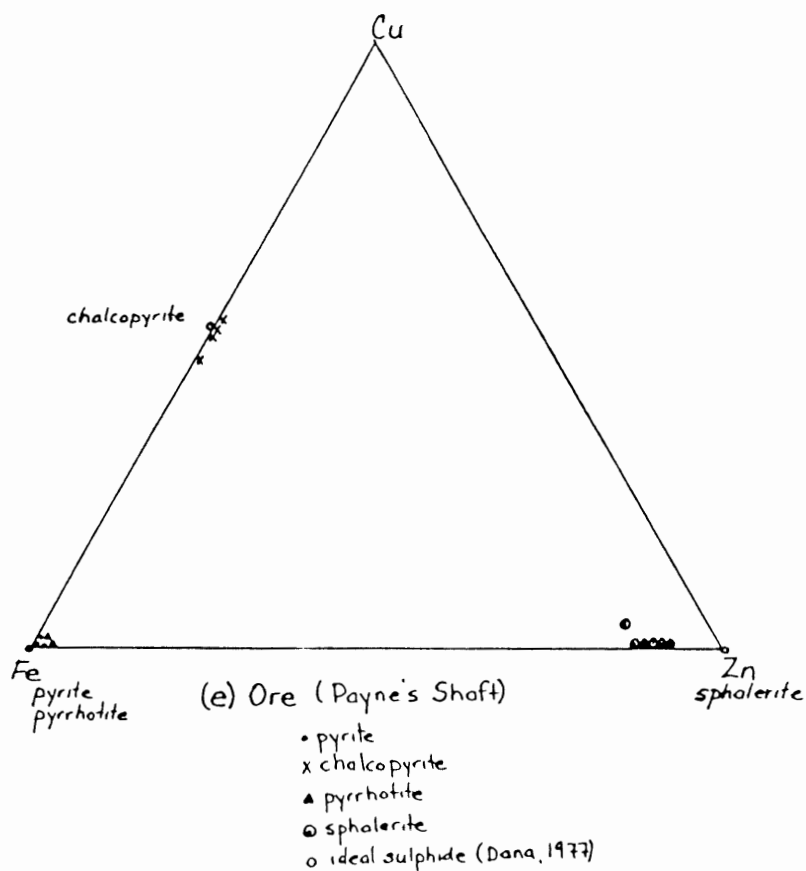
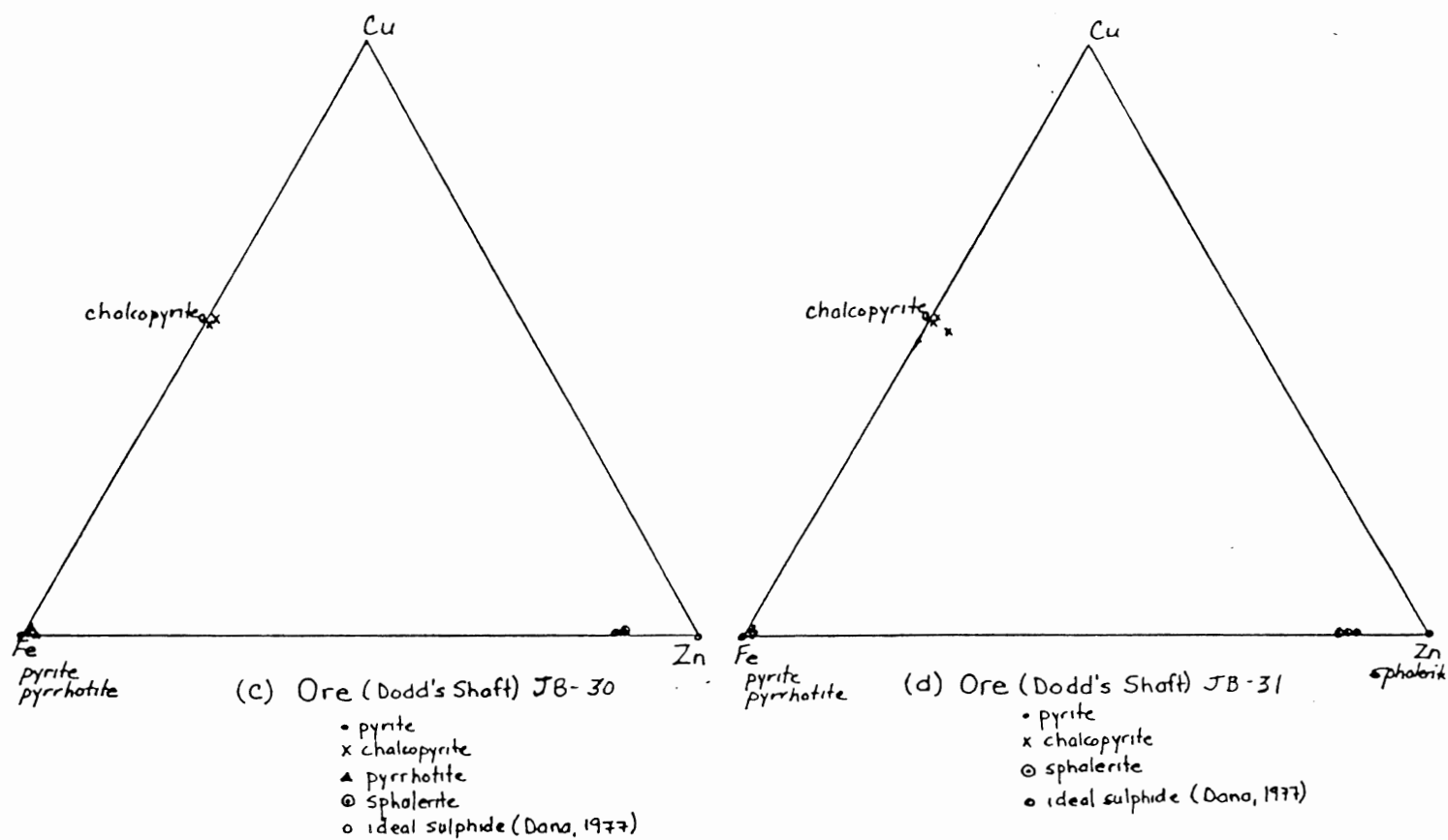
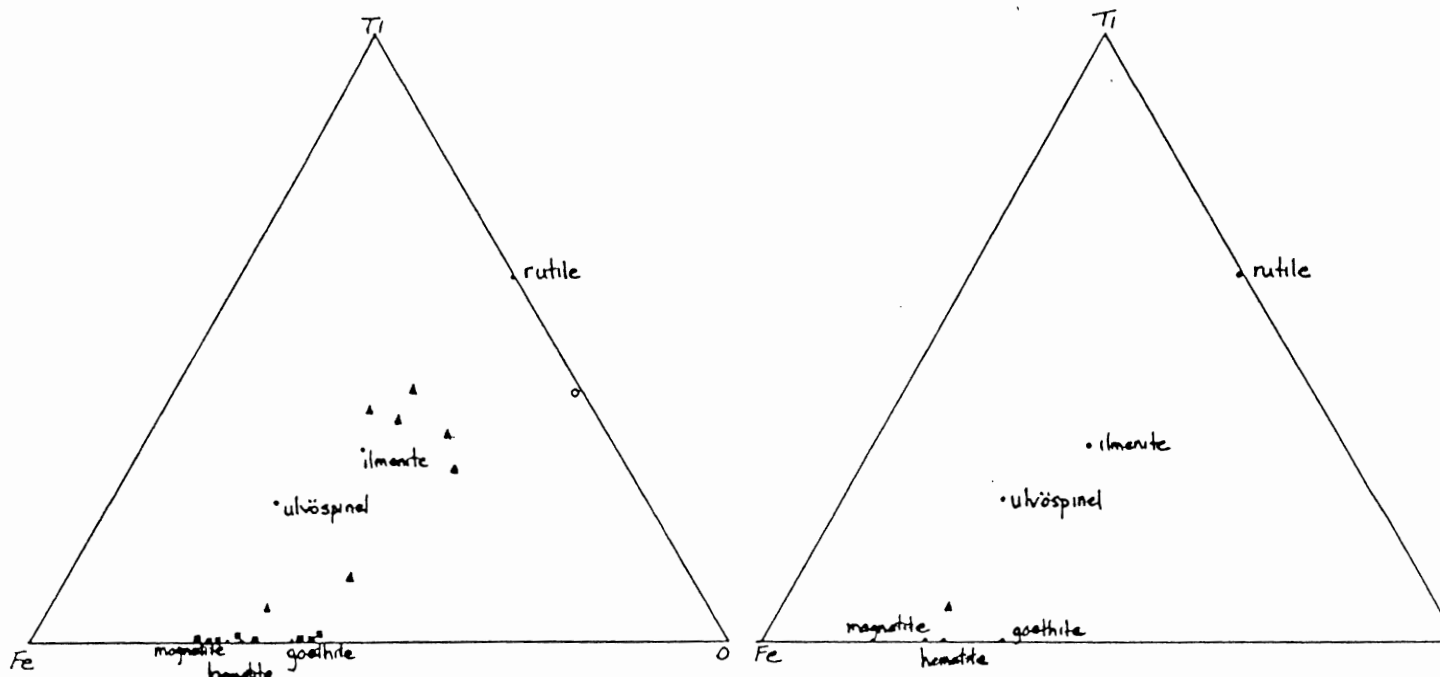
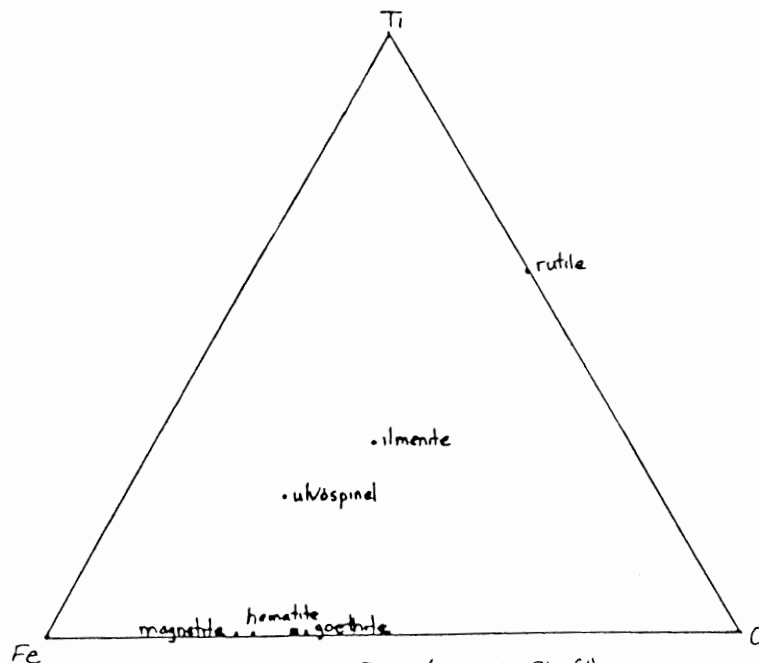


Figure 5.2: Fe-Cu-Zn plots of ore from Dodd's Shaft ((c) and (d)) and Payne's Shaft (e).



(a) Greenschists
 ■ Fe-oxide
 ○ Ti-oxide
 ▲ Ti-Fe-oxide
 • Ideal oxide (Dana, 1977)

(b) Metasediments
 ▲ Ti-Fe-oxide
 • Ideal oxide (Dana, 1977)



(c) Ore (Payne's Shaft)
 ■ Fe-oxide
 • Ideal oxide (Dana, 1977)

Figure 5.3: Fe-Ti-O plots of (a) greenschists (b) metasediments and (c) ore (from Payne's Shaft)

Sphalerite contains approximately 9-14% replacement Fe and as expected, shows a compositional variation of an increased Cu concentration in the ore from Payne's Shaft. Deviation of the chalcopyrite analysis of JB-31 from the ideal sulphide composition is attributed to alteration of the sample. The analysis shows a high percentage of elemental oxygen (9-10%) which probably is due to the presence of iron oxides at the rim of the chalcopyrite grain.

The oxide analyses of the greenschist show a clustering of points about ilmenite, goethite, hematite, and magnetite. The samples containing 5-10% Ti are Ti-rich iron oxides that could be titanomagnetite. The titanium oxide is probably altered rutile. The metasediments contain Ti-rich iron oxides interpreted to be titanomagnetite and the ore from Payne's Shaft has iron oxides which may be magnetite, hematite or the alteration product, goethite.

(b) Sphalerite geobarometry

The association of sphalerite with pyrite and pyrrhotite in the ore of the Goose Cove Deposit offers the opportunity to apply the sphalerite geobarometer. The coexistence of the ore minerals may be explained with respect to the Fe-Zn-S system. Figure 5.4 illustrates the phase relations in the system under isobaric conditions. Since the slope of A_0 is generally vertical over the

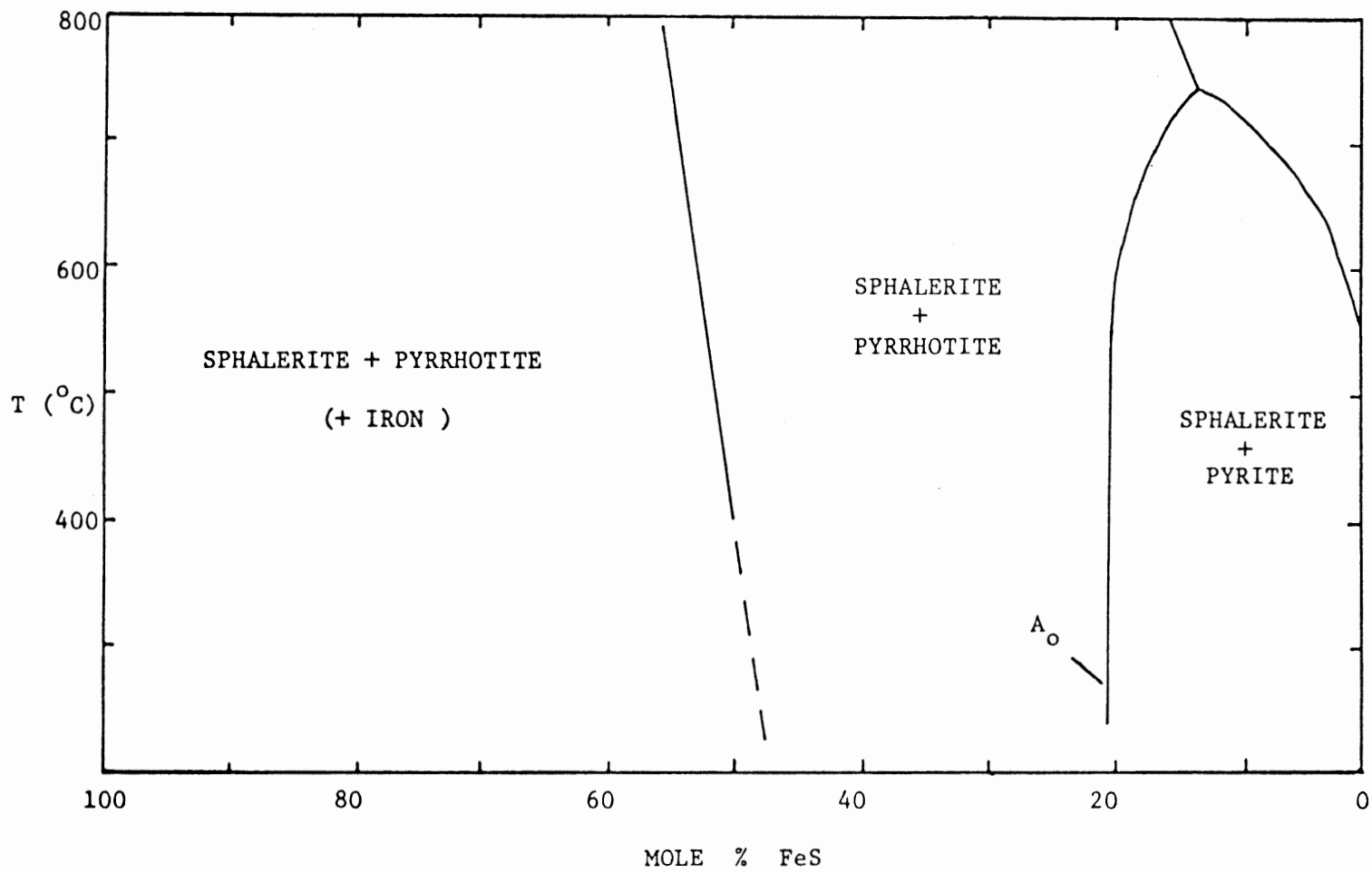


Fig. 5.4 Simplified phase relation diagram of the system Fe-Zn-S (after Barton and Skinner, 1979).

temperature range 100-600 degrees Celsius, the phase relations are constant and invariable. However a decrease in volume of FeS over the same temperature range is coincident with the structural change of sphalerite to pyrrhotite. Therefore the line, Ao, which is sensitive to pressure changes and simultaneously unaffected by temperature change provides a theoretical geobarometer.

Experimental work by Scott (1973,1976) and Scott and Hutchinson (1981) has resulted in the development of a formula (Eq.1) which expresses the pressure dependence of sphalerite in equilibrium with pyrite and pyrrhotite. Pressure is in kilobars and the mole % FeS refers to the amount in sphalerite.

$$P = 42.30 - 32.10 \log \text{mole \% FeS} \quad (\text{Eq.1})$$

Figure 5.5 shows the phase relations in the Fe-Zn-S system below 300 degrees Celsius, as outlined by Scott and Kissin (1973). It is a detailed study of the low temperature range of figure 5.4. Below 250 degrees Celsius, two primary phase fields do not exist. The line Ao is no longer a valid geobarometer for temperatures less than 250 degrees Celsius. An equilibrium pressure is only reliable if the temperature of equilibration is between 250 and 600 degrees Celsius. However, the temperature range is useful as it corresponds to many geological systems. It remains worthwhile to apply the sphalerite geobarometry to the ores.

Table 5.1 is a compilation of the sphalerite mineral chemistry and respective pressure values determined by Equation 1. The

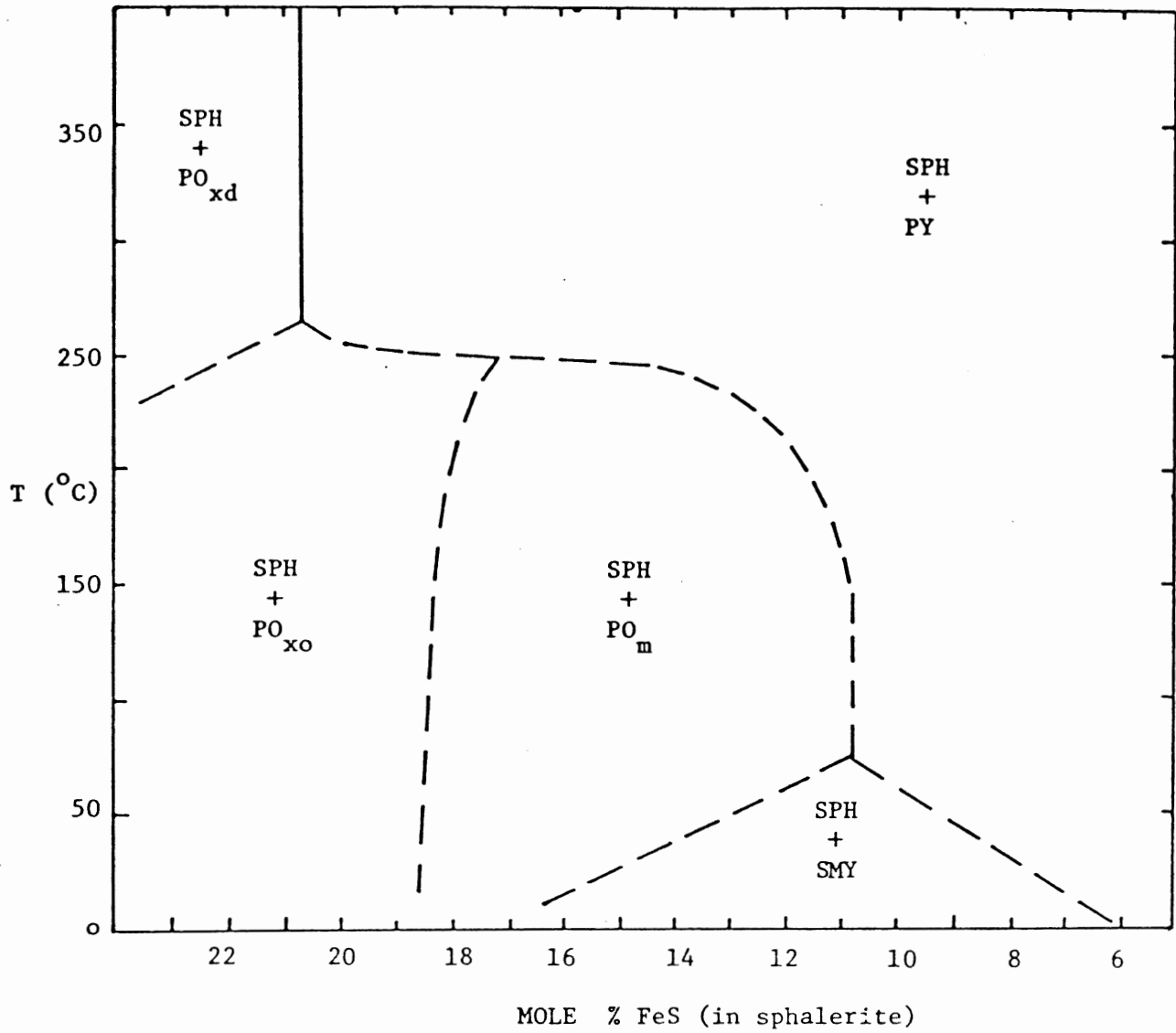


Fig. 5.5 Phase relations in the Fe-Zn-S system below 300 °C (after Scott and Kissin, 1973).

(Sph = sphalerite; Py = pyrite; Po = pyrrhotite; Smy = smythite; xd = hexagonal disordered; xo = hexagonal ordered; and m = monoclinic)

TABLE 5.1: SPHALERITE MINERAL CHEMISTRY AND RESPECTIVE PRESSURE VALUES

Slide #	Analysis (mole%)				Mole % FeS	Pressure (kb)
	Zn	Fe	S	Accessory Elements		
JB-30	60.28	7.02	31.13	+0.23 K; +0.84 Zn	11.05	8.81
JB-31	60.31	6.99	33.32	+0.09 Co; +0.04 Ti; +0.26 K ; +0.08 Mn; +0.06 Cu	11.00	8.87
JB-33	54.03	5.63	28.65	11.40 O; 0.07 Co; 0.18 K	8.86	11.89
	49.12	7.42	28.65	12.41 O; 0.20 K; 2.14 Cu	11.68	8.04
	59.97	6.77	32.92	+0.26 K; +0.07 Co; +0.05 Ti; +0.06 Mn; +0.40 Cu	10.66	9.31

calculated pressures range from 8.04 to 11.89 kilobars. This corresponds to a depth (approximately 10 kilometers) that is geologically unrealistic for the marginal marine pillow lavas. It is assumed there is error in the calculation of the pressure or one of the requirements necessary to ensure the successful application of the geobarometer has not been met. Since the calculated pressures are very similar to those determined by Bailey (1982) the former source of error seems unlikely. A recommendation made by Bailey to test the latter source of error was attempted.

In order that sphalerite geobarometry may be applied with success, particular requirements must be met. Sphalerite, pyrrhotite and pyrite must be present in the ore, the constituents must be present in sufficient quantities, the textures of the ore must indicate equilibrium among the ore constituents and finally the pyrrhotite crystal form must be hexagonal since the phase relations of the Fe-Zn-S system is dependent upon the existence of hexagonal or monoclinic pyrrhotite in the ore mineral assemblage (Fig. 5.5).

Magnetic separation and X-ray diffraction of the pyrrhotite was expected to discern the crystal structure. However, a series of separations of the magnetic minerals from a one kilogram, 200-mesh powder of the ore, using a large hand magnet, did not eliminate the gangue and the XRD pattern did not produce the clear

resolution required to distinguish between the two crystal forms of pyrrhotite. As an alternative, heavy liquid separation was attempted but the pyrrhotite did not separate and settled out with the gangue minerals.

Although the form of pyrrhotite could not be defined and its effect on the high pressure values remains uncertain, other possible sources of error were investigated. Repeated examinations of the ore thin sections confirmed the existence of all the required phases. However, it was noted that pyrrhotite and chalcopyrite, while ubiquitously associated with pyrite and sphalerite, were rarely present together. The mutual exclusiveness of the two minerals implies disequilibrium within the mineral assemblage, which interferes with the successful application of the sphalerite geobarometer.

In conclusion, the application of the sphalerite geobarometer to the ores of the Goose Cove deposit is not valid. Considering the small number of ore samples analysed, further work to positively ascertain the equilibrium conditions is suggested. In addition, a more exacting method of magnetic separation should be undertaken. Control of the quantity of magnetism in the magnetic separation should not only eliminate the gangue but also separate the pyrrhotite from the magnetite which is also present in the ore. An isolated sample of pyrrhotite will enable the determination of the crystal form by XRD analysis. The

recommendations should clarify the valid use of the sphalerite geobarometer in connection with the Goose Cove deposit.

CHAPTER 6 PETROGENESIS

Determination of the petrogenesis of the Goose Cove copper deposit involves the comparison of all field, petrographic and geochemical evidence. This chapter will discuss the results of previous chapters and what the implications are with respect to the paleoenvironment and mode of ore emplacement.

The field evidence indicates the ore was not emplaced by a single epigenetic event post-dating the Fm stage of deformation as suggested by Stephenson (1937). The ore is generally confined to the porphyroclastic metavolcanic unit and related to the Fm folding event. Deformation of the ore implies a pre- or syn-Fm ore emplacement. Veinlets that parallel and cross-cut the Sm foliation of the banded metavolcanics and calc-silicate schist are probably due to minor post-emplacement mobilization of the ore. Pyrite is relatively more mobile than chalcopyrite (Barnes, 1967) and it is not unusual for post-ore veinlets of pyrite to cross-cut the initial ore body.

Petrography of the ore and host rock lithologies reveals a predominant concentration of ore in the porphyroclastic metavolcanics. Minor amounts of sulphides are present in the other lithologic units but it is probably due to mobilization as a result of deformation. Inclusions of chalcopyrite and silicates (probably from the porphyroclastic metavolcanics) in pyrite,

pyrrhotite or chalcopyrite, the fragmented irregularly-shaped habit of the sulphide grains and the replacement of chalcopyrite by pyrite attests to the deformation of the original ore body.

The deposit may be termed a cupriferous pyrite ore body because of the high percentage of chalcopyrite and pyrite. This is characteristic of Cyprus-type deposits. However, the high concentration of pyrrhotite (<5%-35%) which may be related to the metamorphic conversion of primary pyrite to pyrrhotite (Grenne et al ,1979) may better define the ore body as a deformed Cyprus-type deposit. This interpretation implies a syngenetic mineralization of the primary pillow lavas followed by deformation and mobilization of the ore prior to or synchronous with the Fm folding event.

The major and trace element analyses reveal no correlation between element concentration and distance from the main ore body at Dodd's Shaft and consequently, do not support the epigenetic model of ore emplacement suggested by Stephenson, (1937). Comparison of the metavolcanic element concentrations with the undeformed porphyritic pillow lavas shows a depletion of Cu, Ni and possibly Zn in the former likely to be due to metamorphism and deformation of the primary pillow lavas.

The exact paleoenvironment cannot be determined since the metavolcanics plot on the boundary of ocean-floor and island-arc basalts. Comparison of the Cu, Ni and Zn concentrations in the

Ireland Point Volcanics with mid-ocean ridge basalts does show a slight enrichment that may be the result of syngenetic hydrothermal mineralization of the porphyritic pillow lavas. The high Cu:Zn ratios (table 4.2) are typical of Cyprus-type deposits (Grenne et al ,1979).

Microprobe analyses of the ore minerals produces a consistent chemical composition of all sulphides irrespective of the grain habit or arrangement and imply a single event of ore generation. Unfortunately, the mutual exclusion of pyrrhotite and chalcopyrite prevents the use of sphalerite geobarometry to determine the pressure conditions of the latest ore equilibration.

In summary, the evidence indicates the Goose Cove deposit was formed by the mobilization of Cu, Ni, + Zn during metamorphism of the porphyritic pillow lavas and reconcentration prior to or synchronous with the Fm folding event. The Cu, Ni + Zn may have had high anomalous concentrations in the primary pillow lavas.

The high percentage of chalcopyrite and pyrite in the ore, the Cu:Zn ratios over unity, the high percentage of pyrrhotite with respect to pyrite and the fragmented and deformed nature of the ore designate the ore body as a deformed "Cyprus-type" massive sulphide deposit. Since the ore is associated with host rock volcanics that are not part of the ophiolite but are marginal marine lavas which adhered to the base of the ophiolite during emplacement, the ore body cannot be considered a true Cyprus-type

massive sulphide deposit.

The ore controls are:

- (1) lithologic control - porphyroclastic metavolcanics with the related metasedimentary rocks
- (2) structural control - the Fm folding event (if pre-Fm, the ore is a planar body; if syn-Fm, the ore is concentrated in hinges of the Fm folds)
- (3) metamorphic control - greenschist facies of metamorphism
- (4) paleoenvironment control - tectonically unstable ocean setting (i.e., ocean basin, ocean-island, mid-ocean ridge)

CHAPTER 7 CONCLUSIONS

The purpose of the thesis was to incorporate the field relations, petrography and geochemistry of the Goose Cove copper deposit in an attempt to define the ore-host rock relationship and to develop an acceptable model, including paleoenvironment and mode of ore emplacement, for the formation of the deposit.

(1)The field evidence indicates an association of the ore with the porphyroclastic metavolcanics and the predominant, east-west trending foliation (Sm). Emplacement may be prior to or synchronous with the development of Fm folds.

(2)The petrographic evidence implies a cupriferous pyrite body that has been deformed subsequent to or simultaneous with the main foliation (Sm).

(3) The geochemistry evidence shows a depletion of Cu, Ni + Zn in the porphyroclastic metavolcanics with respect to the undeformed protolith (porphyritic pillow lavas of the Ireland Point Volcanics). Syngenetic mineralization of the primary pillow lavas cannot be ascertained.

(4)All the results support the emplacement of ore by mobilization of the ore-forming elements during metamorphism and deformation of the primary pillow lavas and re-concentration either prior to or synchronous with the Fm event.

(5)The paleoenvironment is a tectonically-active ocean setting.

(6) The Goose Cove deposit may be termed a deformed "Cyprus-type" massive sulphide deposit.

Recommendations for further study include:

- (1) REE and sulphur isotope analyses of the primary basalts to determine the exact paleoenvironment
- (2) detailed structural analysis to determine whether the ore was emplaced prior to or synchronous with the Fm event
- (3) geophysical surveys (magnetics, VLF, IP) to delineate the extent and size of the ore body
- (4) exploration for similar ore bodies in areas having the required ore controls (especially north of the thesis area)

APPENDIX I

MetasedimentsJB-3

Mineralogy: quartz (50-55%)
 biotite (15-20%)
 garnet (primary 5-10%)
 plagioclase (5%)
 epidote (5%)
 sericite (<5%)
 chlorite (retrograde 1%)
 alteration clays (smectite? 1%)
 opaques (1%)

Texture: alternating quartz-rich and garnet-epidote-rich
 compositional bands; well-foliated to mylon-
 itic; kink folds present but rare; coarse-
 grained quartz lenses and veinlets of strained
 quartz parallel and cross-cut foliation;
 opaques as inclusions in garnets

Notes: located on south side of Three Mountain Harbour;
 geochemical analysis Appendix II, # ; microprobe
 analysis Appendix III; photo 1

Metamorphic grade: greenschist

Name: Garnetiferous metasediment (mylonite)

JB-17

Mineralogy: quartz (30%)
 sericite (20%)
 muscovite (15-20%)
 chlorite (10-15%)
 garnet (5%)
 epidote (1-2%)
 plagioclase (An<10; albite; <1%)
 opaques (Ti-Fe-oxides; 5-10%)

Texture: alternating quartz-rich and muscovite-rich
 bands; well-foliated; isoclinal and box folds
 of layers; very fine-grained quartz in fold
 hinges; kink banding of opaque-bearing musco-
 vite; quartz lenses and blebs parallel to fol-
 iation

Notes: located on the north shore of Goose Cove, west
 of Goose Cove Road; geochemical analysis Appen-
 dix II, # ; microprobe analysis Appendix III;
 photo 2

Metamorphic grade: greenschist

Name: Semi-pelitic metasediment

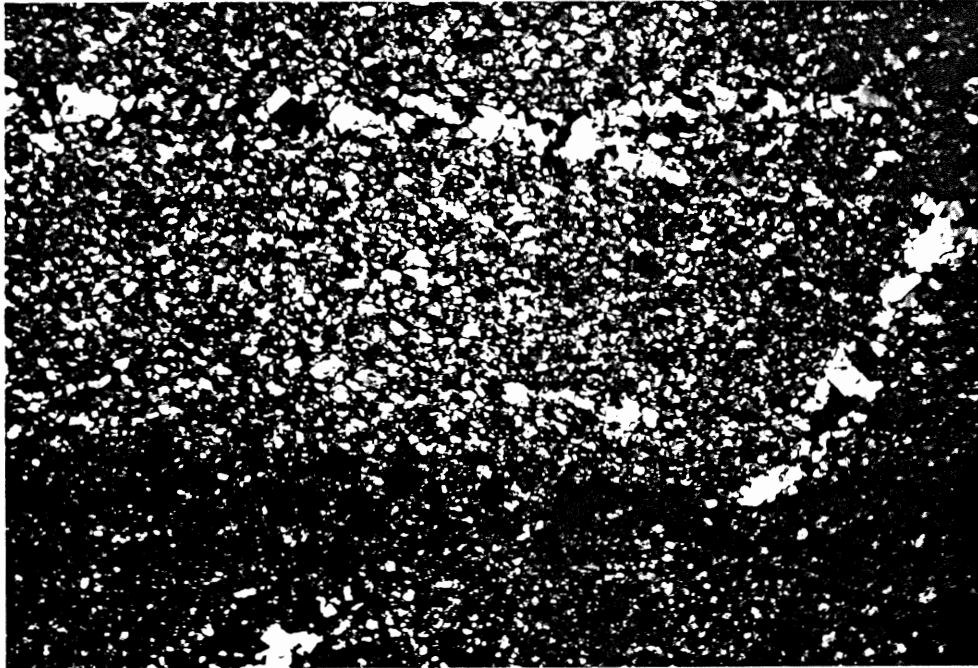


PHOTO 1: Alternating quartz-rich and garnet-epidote-rich bands with parallel and cross-cutting quartz lenses and veinlets in the garnetiferous semi-pelite. (160x)

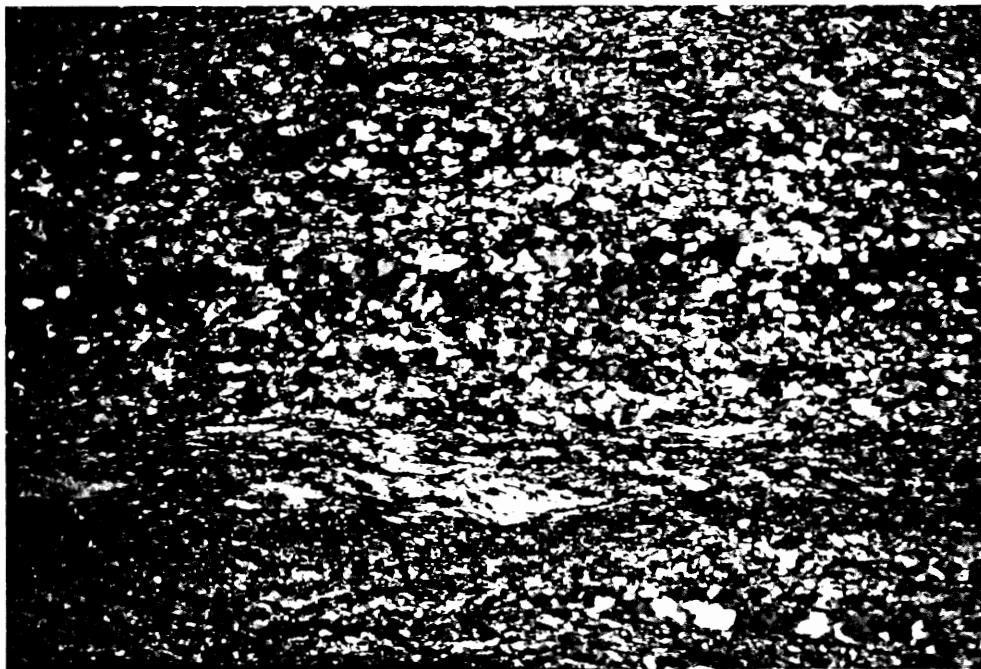


PHOTO 2: Alternating quartz-rich and muscovite-rich bands in the semi-pelite. (160x)

JB-81

Mineralogy: quartz (55-60%)
sericite (20%)
muscovite (10%)
garnet (10%)
chlorite (<5%)
clay (smectite? 1%)
opaques (<1%)

Texture: alternating mica-rich and quartz-rich bands;
well-foliated; isoclinal folds; kink banding
and folding of muscovite; preferred orienta-
tion of mica; complex folding in hinges of
isoclinal folds; sub-grain development of
quartz lenses and elongated patches

Notes: located on the northwest shore of Vierge Cove,
east of the fault; photos 3 & 4

Metamorphic grade: greenschist

Name: Semi-psammitic metasediment (mylonite)

JB-89

Mineralogy: quartz (50-55%)
sericite (primary 20%; secondary <1%)
muscovite (5-10%)
plagioclase (5%)
opaques (10%)

Texture: alternating quartz-rich and muscovite-opaque-
rich bands; well-foliated to mylonitic; au-
gens of plagioclase; muscovite in pressure
dows; preferred orientation of micas; quartz
lenses and veinlets parallel to foliation

Notes: located west of Vierge Cove at the base of Three
Mountain Summit; geochemical analysis Appendix
II; microprobe analysis Appendix III

Metamorphic grade: greenschist

Name: Siliceous metasediment (mylonite)

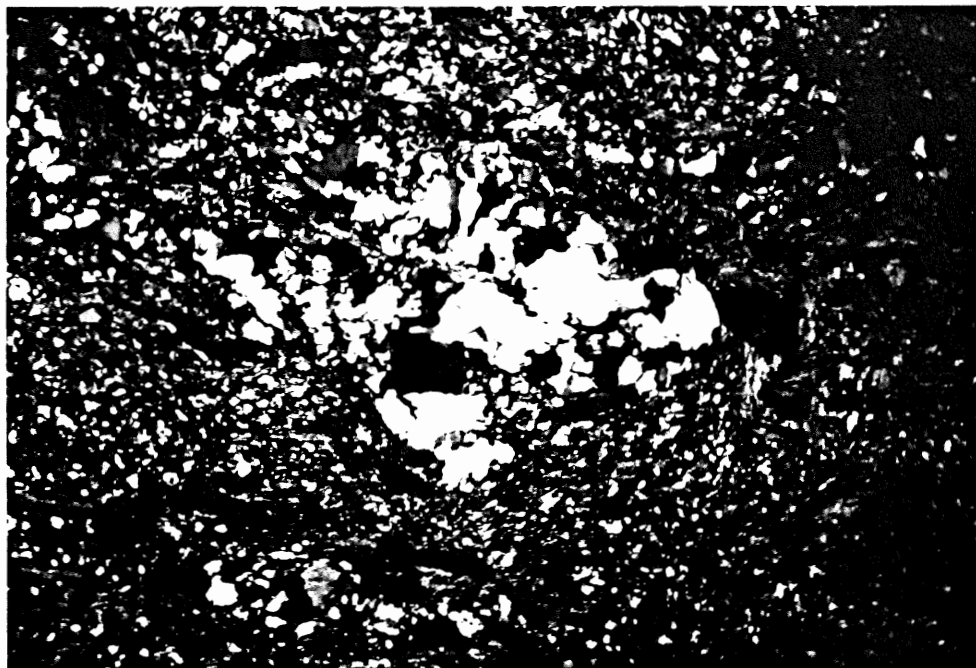


PHOTO 3: Isoclinally folded alternating mica-rich and quartz-rich bands in the siliceous psammite. (160x)

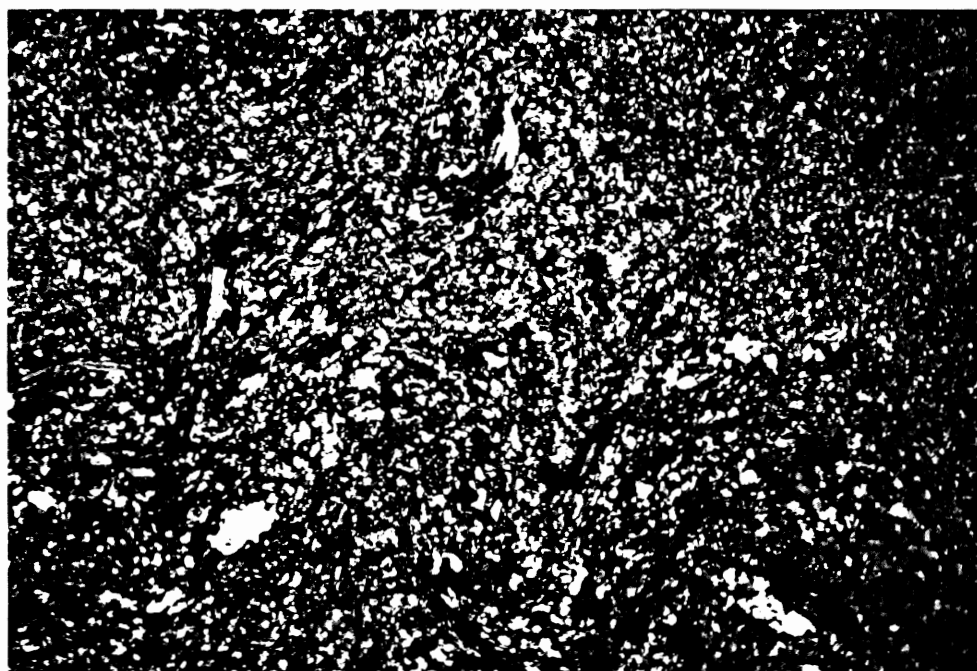


PHOTO 4: Extreme contortion of quartz-rich and muscovite-opaque-rich bands in the siliceous psammite. (160x)

Porphyroclastic Greenshist

JB-23 (JB-10, JB-6, JB-22, JB-23, JB-41B, JB-42, JB-47
JB-65 to JB-71)

Mineralogy: actinolitic hornblende (40-60%)
feldspar (5-20%)
epidote (5-15%)
chlorite (primary 1-5%; secondary 5-10%)
sericite (primary 2-10%)
+ sphene (1-2%)
+ calcite (1-10%)
opaques (1-2%)

Texture: moderately to well foliated; augens or boudinage of altered plagioclase in hornblende - epidote matrix; rare euhedral crystals of plagioclase as augens; augens altered to epidote, sericite or calcite; opaques common in matrix but also as inclusions in epidote; rare cross-cutting veinlets filled with plagioclase and kink folds disrupt the foliation; sphene as euhedral to subhedral grains in veinlets or cross cutting foliation or as brecciated grains parallel to foliation.

Notes: samples from the area surrounding Dodd's Shaft;
Norcat Point; north shore of Three Mountain
Harbour; photos 5 & 6 & 7

Metamorphic grade: greenschist

Name: porphyroclastic greenschist



PHOTO 5: Stretched and oval augens in the porphyroclastic metavolcanics. (160x)

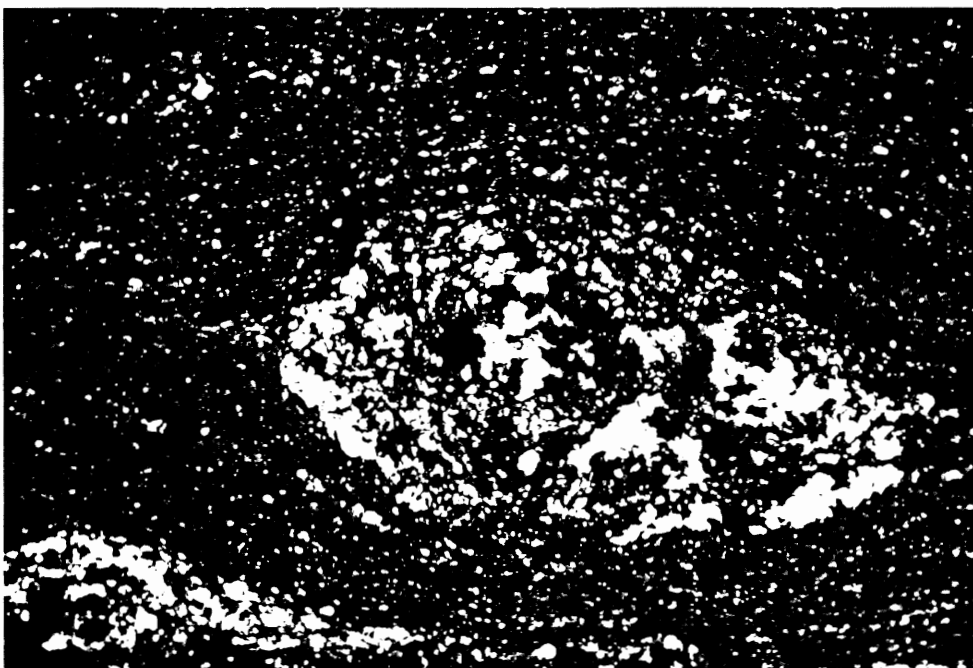


PHOTO 6: Alteration of relict plagioclase phenocrysts to sericite, calcite and epidote in the porphyroclastic metavolcanics. (200x)

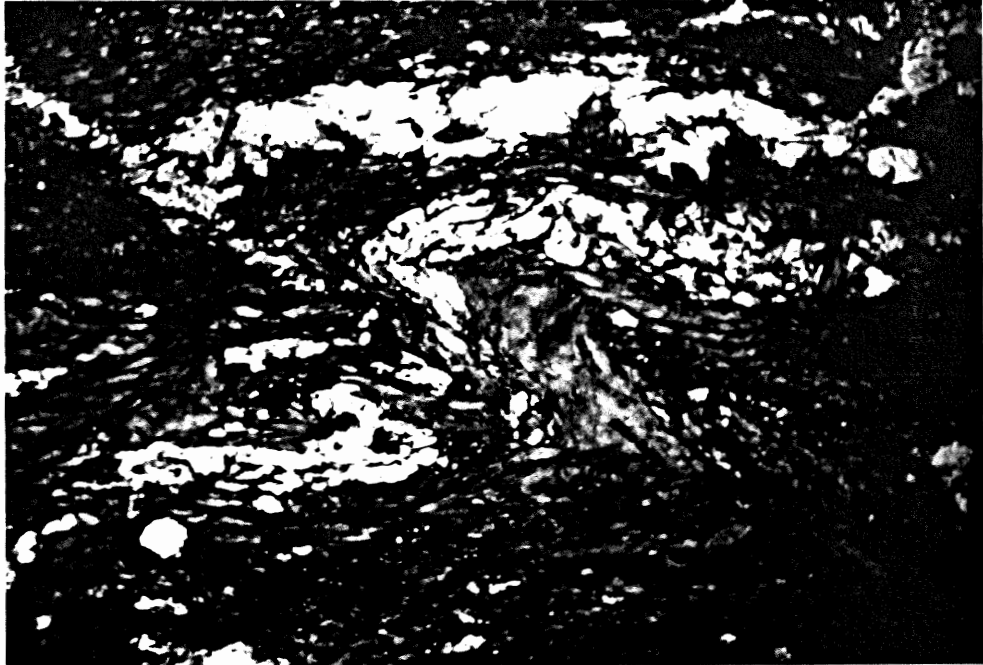


PHOTO 7: The elongation of porphyroclasts into lenses that are locally kink folded, within the porphyroclastic metavolcanics. (160x)

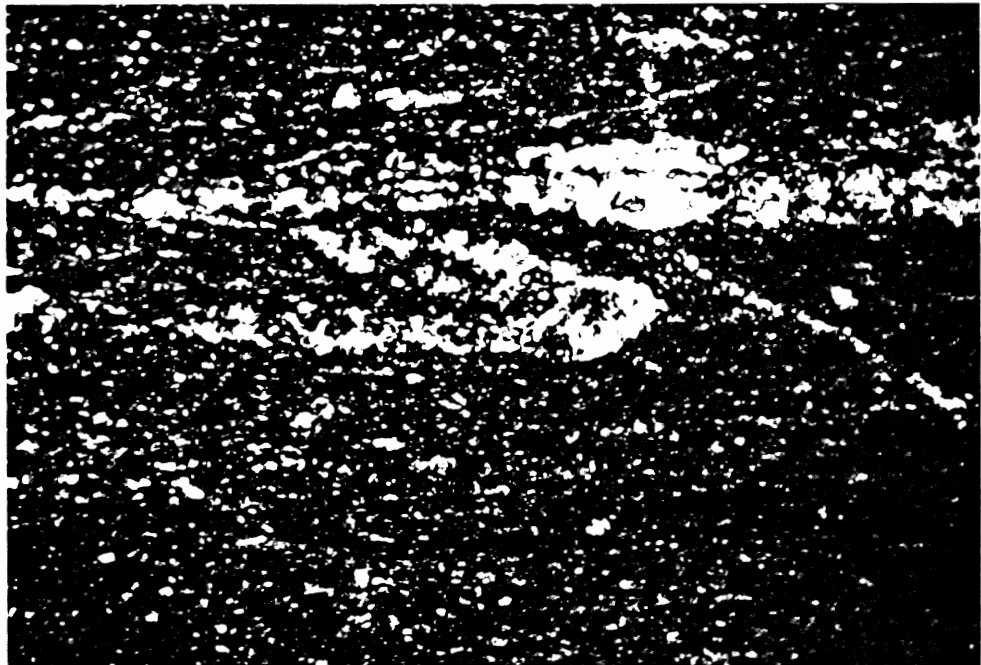


PHOTO 8: Isoclinal folds composed of sericite and calcite in the banded metavolcanics. (160x)

Banded Greenschist

JB-7 (JB-1, JB-2, JB-4, JB-5, JB-11, JB-18 to JB-20,
JB-22, JB-24, JB-34, JB-38A, JB-38B, JB-39,
JB-62-JB-64, JB-70, JB-72, JB-78, JB-79, JB-85,
JB-87)

Mineralogy: actinolitic hornblende/hornblende (50-70%)
epidote (10-20%)
calcite (5-10%)
chlorite (primary 1-2%; secondary 5-15%)
sericite (1-5%)
opaques (1-10%)

Texture: very strongly foliated to mylonitic; intercalated plagioclase-sericite (15-50%) with hornblende-epidote (50-85%); minor cross-cutting fractures filled with plagioclase or epidote; epidote commonly altered to fine-grained calcite; opaques as overgrowths (sphalerite) or within matrix; high percentage of opaques in JB-85 and JB-87

Notes: located along south shore of Three Mountain Harbour extending west to mine, Norcat Point, south shore of Vierge Cove and at the base of Three Mountain Summit; photo 8

Metamorphic grade: greenschist

Name: banded greenschist

Massive Greenschist

JB-14, JB-15, JB-16A, JB-16B, JB-86, JB-88

Mineralogy: actinolitic hornblende/hornblende (40-50%)
 epidote (20-50%)
 plagioclase (5-10%)
 chlorite (primary 1-2%; secondary 5-10%)
 sericite (secondary < 5%)
 calcite (< 1%)
 alteration clays (< 1%)
 + sphene (< 1%)
 + opaques (1-10%)
 sphalerite (< 1%)

Texture: moderately to well foliated; rare augens of plagioclase; cross-cutting veinlets of plagioclase and quartz; lenses and veinlets of coarse-grained epidote parallel to foliation; more intensely deformed samples have high percentage of epidote, sericite, chlorite and calcite; sphene present in samples at base of Three Mountain Summit; along Goose Cove Road, veinlets and lenses of opaques (sulphides) cross cut foliation (JB-16A); opaques tend to concentrate in bands parallel to foliation (JB-16B) or as disseminated grains (JB-16A)

Notes: located along Goose Cove Road and at the base of Three Mountain Summit; geochemical analyses
 Appendix II

Metamorphic grade: greenschist/epidote-amphibolite

Name: massive greenschist

Coarse-grained GreenschistJB-77

Mineralogy: hornblende (25-35%)
 epidote (45-55%)
 sericite (5%)
 clinopyroxene (1%)
 plagioclase (5%)
 chlorite (< 1%)
 opaques (< 1%)
 sphalerite (< 1%)

Texture: moderately to well foliated; coarse-grained augens and boudinage of hornblende in epidote-rich matrix; fracturing and rotation of hornblende is common; pressure shadows; opaques as inclusions in hornblende and within matrix

Notes: located on south shore of Vierge Cove; geochemical analysis Appendix II; microprobe analysis Appendix III; photos 9 & 10

Metamorphic grade: greenschist

Name: coarse-grained greenschist

JB-73

Mineralogy: actinolitic hornblende (20-30%)
 epidote (25%)
 chlorite (primary < 1%; secondary 20%)
 sericite (10-15%)
 plagioclase (5%)
 sphene (5%)
 calcite (5-10%)
 opaques (1-2%)

Texture: brittle deformation disrupts foliation; rotation and fracturing of hornblende augens; alteration is prominent; cross cutting, coarse-grained plagioclase veinlets have no preferred orientation

Notes: located on south shore of Vierge Cove

Metamorphic grade: greenschist

Name: coarse-grained greenschist

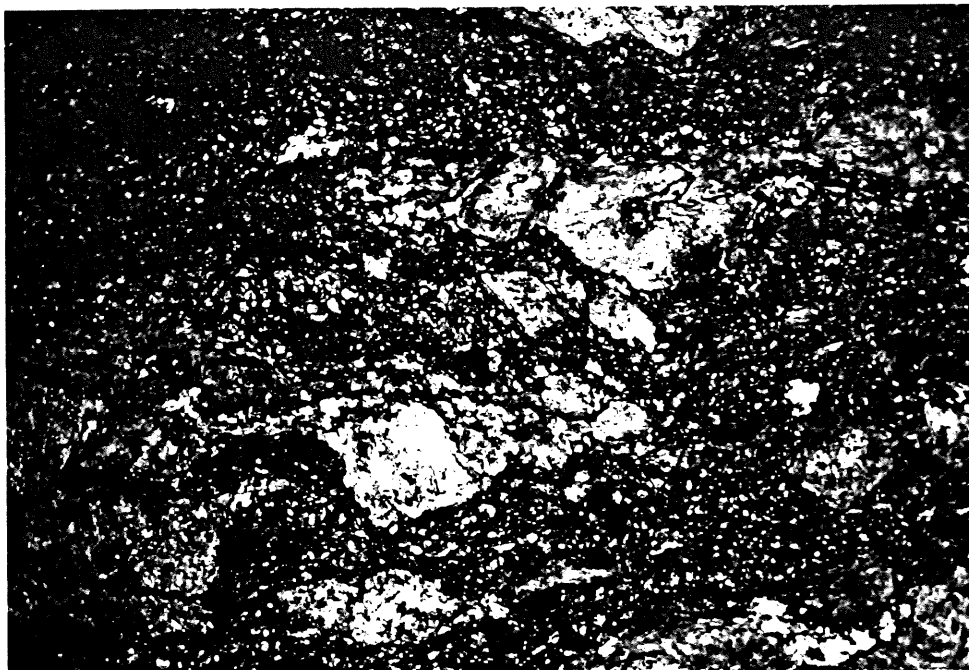


PHOTO 9: Moderately folded coarse-grained greenschist.
(160x)

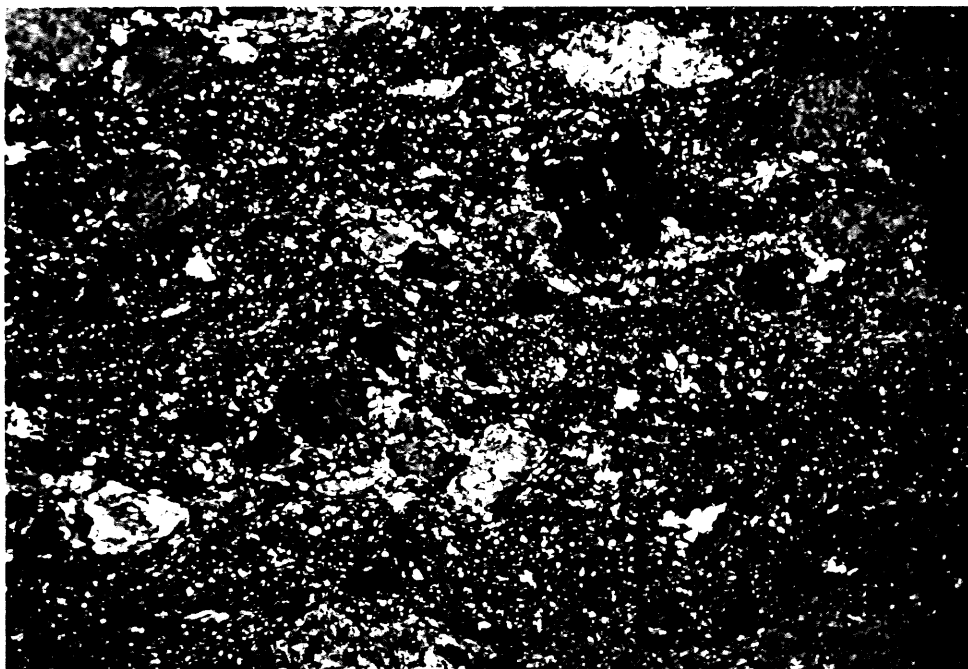


PHOTO 10: Same as above but under crossed-nicols. (160x)

JB-84

Mineralogy: epidote(45%)
actinolitic hornblende (35%)
chlorite (secondary 5%)
plagioclase (2-5%)
sericite (< 5%)
opaques (1-2%)
sphalerite (< 1%)

Texture: very strongly foliated; hornblende augens arranged as boudinage within a finer-grained epidote-rich matrix; kink folds and local contortions of foliation; cross-cutting fractures filled with sericite, plagioclase and epidote parallel and cross cut foliation; opaques as inclusions

Notes: located on the north shore of Vierge Cove; geochemical analysis Appendix II; photo

Metamorphic grade: greenschist/epidote-emphibolite

Name: coarse-grained greenschist

JB-83

Mineralogy: epidote (40-50%)
actinolitic hornblende (35-40%)
chlorite (5-10%)
plagioclase (1-2%)
sericite (1-2%)
opaques (1%)

Texture: very strongly foliated to mylonitic; alternating hornblende and epidote-rich bands; elongated or augen hornblende; crenulations and contortion of bands common; fractures cross cutting foliation; opaques parallel to foliation

Notes: located on the north shore of Vierge Cove; photo

Metamorphic grade: greenschist

Name: coarse-grained greenschist

Calc-silicate Schist

JB-80

Mineralogy: calcite (45%)
 epidote (15-25%)
 plagioclase (10-15%)
 chlorite (5-10%)
 sericite (1-2%)
 opaques (5%)

Texture: calcite-plagioclase-rich and epidote-rich bands; moderately to well-foliated; augens of plagioclase altered to calcite and sericite; preferred orientation of chlorite; local highly contorted foliation; coarse-grained calcite and epidote in veinlets cross-cutting foliation; opaques as inclusions in epidote, brecciated and generally parallel to foliation

Notes: located on the south shore of Vierge Cove; geochemical analysis Appendix II, # ; microprobe analysis Appendix III

Metamorphic grade: greenschist

Name: Calc-silicate schist (metamorphosed limy shale)

JB-74B

Mineralogy: sericite (primary 20-25%)
 plagioclase (15-20%)
 epidote (10-15%)
 chlorite (20%)
 calcite (5%)
 biotite (primary 1-2%)
 sphene (2%)
 clays (smectite? 1%)
 opaques (5-10%)

Texture: interbanded calc-silicate schist and greenschist; well-foliated; isoclinal folds of calc-silicate schist; cross-cutting veinlets of epidote, sphene, plagioclase and calcite; fractures cross-cutting foliation; opaques parallel and cross-cut foliation

Notes: located on the south shore of Vierge Cove

Metamorphic grade: greenschist

Name: Intercalated calc-silicate schist and greenschist

OreJB-30Plane-polarized Light

Mineralogy: actinolitic hornblende (30-35%)

sericite (10-15%)

plagioclase (5%)

chlorite (5%)

calcite (1%)

sphene (< 1%)

iddingsite (?) (< 1%)

opaques (40-45%)

sphalerite (2-3%)

Texture: oval to elongated fragments of banded or porphyroclastic greenschist deformed and rotated in a matrix of opaques (ore); rare isoclinal folds in schist fragments; veinlets of opaques cross cut fragments and matrix; veinlets of plagioclase, altered to sericite, cross cut banding in fragments

two distinct forms of ore:

(1) disseminated grains within greenschist fragments; concentrated in bands parallel to foliation or as isolated grains

(2) later, large grains in veinlets parallel and cross cutting foliation

Notes: Dodd's Shaft; geochemical analysis Appendix II; microprobe analysis Appendix III; photos 11 & 12

Metamorphic grade: greenschist

Reflected Light

Mineralogy: pyrite (15-20%)

pyrrhotite (10-20%)

chalcopyrite (10-15%)

sphalerite (5%)

hematite (< 1%)

silicate gangue (40-50%)

Texture: chalcopyrite + pyrrhotite + sphalerite occurs as intergrown, fragmented irregularly-shaped forms; patches of chalcopyrite dominant and pyrrhotite dominant assemblages; pyrite as larger grains confined to veinlets; rare large pyrrhotite intergrown with pyrite; hematite present as overgrowths; minor silicate inclusions in chalcopyrite and pyrite

Notes: photos 13 & 14

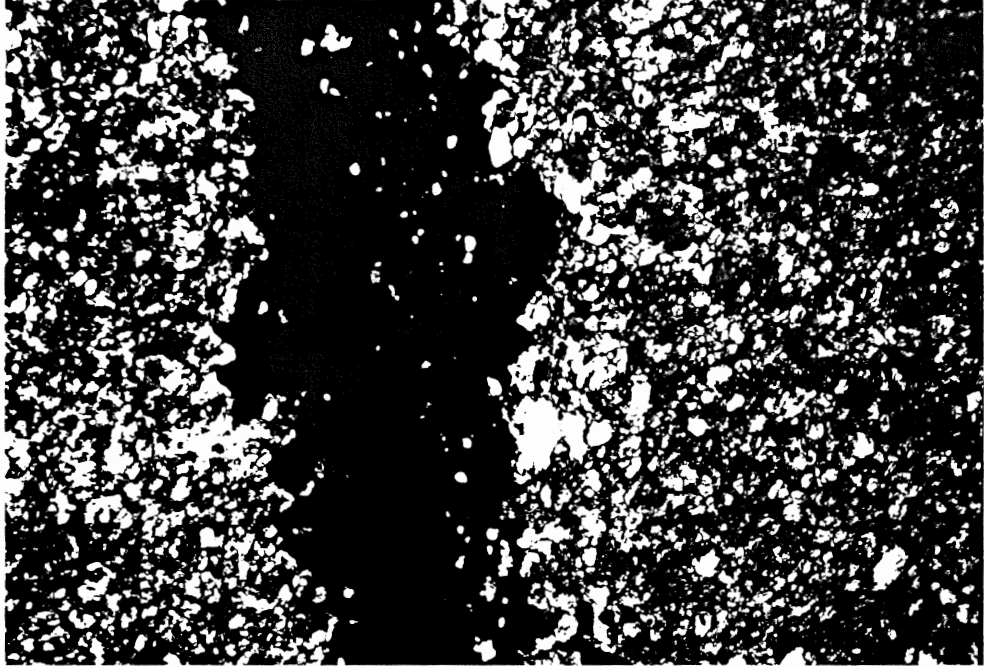


PHOTO 11: Cross-cutting sulphide veinlet in hornblende-epidote-calcite-rich metavolcanics. (160x)

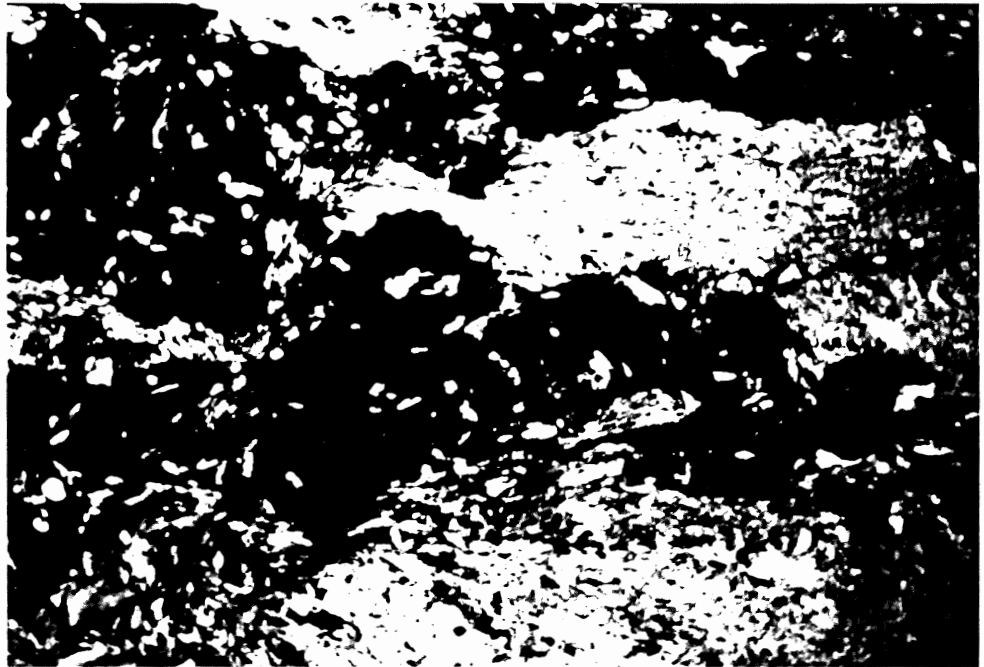


PHOTO 12: Fragments of metavolcanics within the sulphide matrix. (160x)

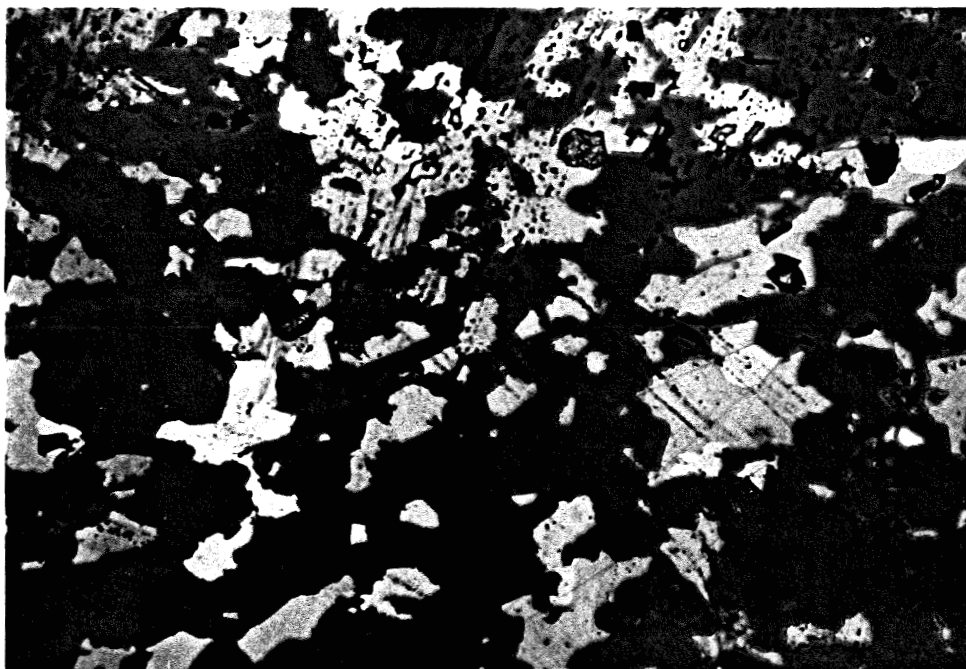


PHOTO 13: Fragmented and irregularly-shaped chalcopyrite and pyrrhotite in a matrix of silicate gangue. (reflected light 160x)

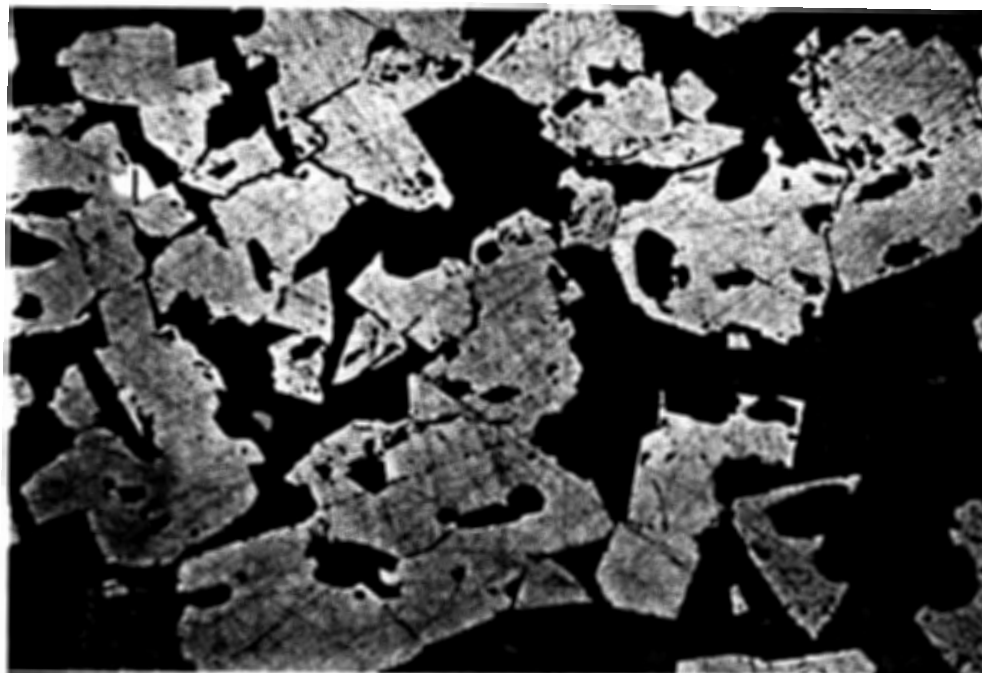


PHOTO 14: Coarse-grained pyrite as a veinlet within the sulphide ore. (reflected light 160x)

JB-31Plane-polarized Light

Mineralogy: actinolitic hornblende (40-50%)
chlorite (5-10%)
sericite (5-10%)
plagioclase (5%)
iddingsite (?) (5%)
calcite (< 5%)
opagues (25-30%)

Texture: vague banding of hornblende-opaque-rich and plagioclase-rich layers disrupted by late post-ore deformation and veinlets of coarse-grained opaques; rare augens of altered plagioclase; ore also present as disseminated grains

Notes: Dodd's Shaft; geochemical analysis Appendix II; microprobe analysis Appendix III; photo 15

Metamorphic grade: greenschist

Reflected Light

Mineralogy: chalcopyrite (10-15%)
pyrrhotite (5-10%)
pyrite (10%)
iron oxides (1-2%)
sphalerite (< 1%)
silicate gangue (55-65%)

Texture: chalcopyrite + pyrite + pyrrhotite assemblage of intergrown fragmented grains; rare occurrence of pyrite + pyrrhotite; rare isolated sphalerite grains; pyrite also present as larger grains in veinlets; chalcopyrite and silicate inclusions in pyrite; isolated grains of iron oxides

Notes: photo 16

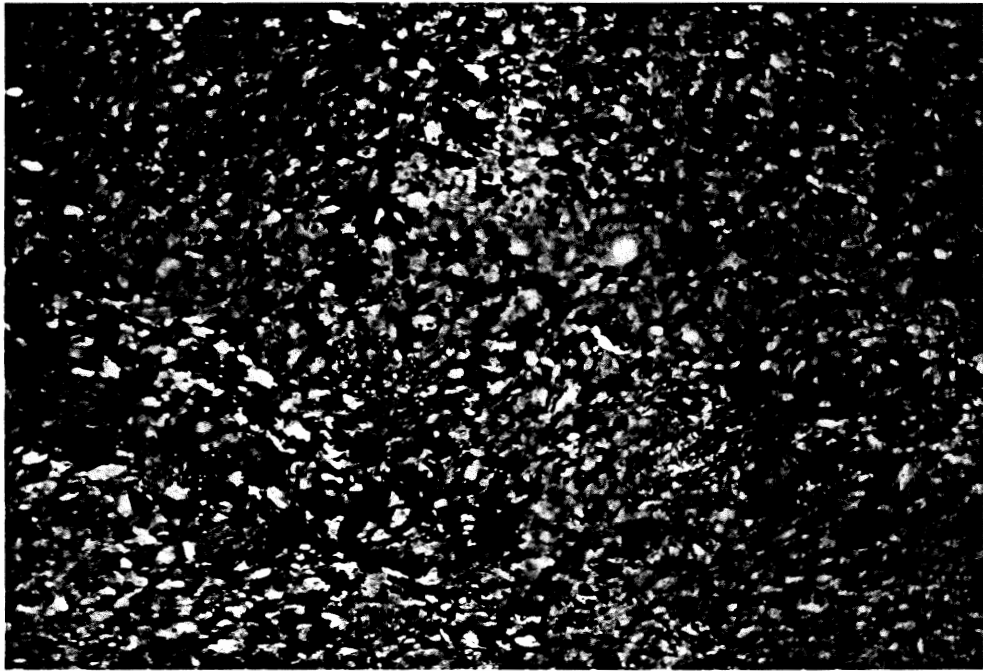


PHOTO 15: Intergrowth of sulphide and silicate grains.
(160x)

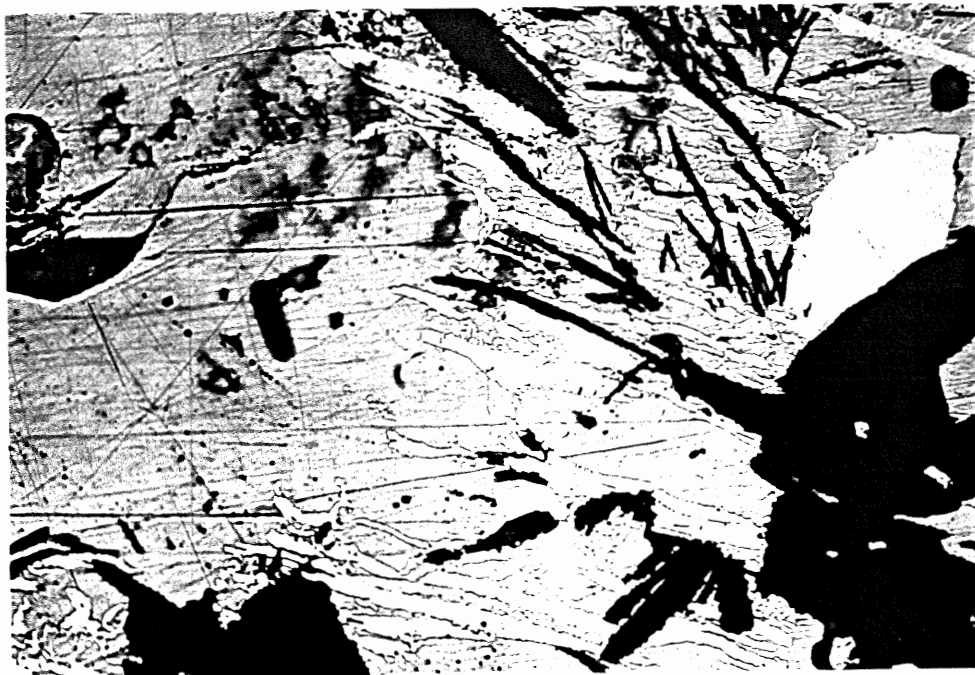


PHOTO 16: Replacement of pyrite by chalcopyrite in the ore from Payne's Shaft. (reflected light 250x)



PHOTO 17: Exsolution blebs of chalcopyrite in sphalerite. (reflected light 250x)

JB-32Plane-polarized Light

Mineralogy: actinolitic hornblende (20-25%)
chlorite (primary 1-2%; secondary 10-15%)
epidote (5-10%)
sphene (< 1%)
iddingsite (?) (< 5%)
opaques (50-55%)
sphalerite (1-2%)

Texture: greenschist fragments in opaque matrix; sphene
within fragments and parallel to foliation

Notes: Payne's Shaft; geochemical analysis Appendix II;
microprobe analysis Appendix III

Metamorphic grade: greenschist

JB-50Plane-polarized Light

Mineralogy: actinolitic hornblende (25-30%)
chlorite (secondary 5-10%)
plagioclase (1%)
sericite (< 1%)
calcite (< 1%)
opaques (40-45%)
sphalerite (2-3%)

Texture: distinguished by unaltered plagioclase in
greenschist fragments; deformation is less
intense

Notes: Dodd's Shaft

Metamorphic grade: epidote-amphibolite

APPENDIX II

Atomic Absorption Spectrophotometry Analysis

Major Element

Sample	FeO(total)		MgO		MnO2	
	(1:200 dilution)		(1:1000 dilution)		(1:100 dilution)	
	abs/conc	calc(%)	abs/conc	calc(%)	abs/conc	calc(%)
smp.bk.	7	-	9	-	3	-
std.bk.	5	-	6	-	-*	-
std.#1	34	-	48	-	63	-
std.#2	62	-	89	-	120	-
std.#3	89	-	130	-	178	-
std.#4	118	-	170	-	-**	-
std.#5	143	-	214	-	-	-
#82	57	5.1	44	1.41	9	0.12
#23	115	10.8	187	7.40	12	0.19
#31	251	24.5	177	7.10	21	0.38
#28	111	10.5	167	6.65	13	0.21
#45B	104	9.8	173	6.93	12	0.20
#65A	112	10.4	186	7.35	12	0.20
#30	317	31.1	178	7.06	17	0.30
#48	110	10.4	179	7.17	12	0.20
#7	112	10.3	179	6.97	17	0.28
#79	128	12.2	85	3.39	14	0.23
#76	133	12.7	135	5.39	13	0.22
#32	388	37.8	91	3.60	11	0.16
#84	105	9.9	207	8.37	12	0.19
#15	106	9.9	111	4.38	12	0.18
#16B	140	13.4	151	6.08	14	0.23
#56	108	10.1	184	7.35	14	0.23
#89	24	1.7	16	0.64	9	0.13
#77	95	8.9	215	8.62	11	0.17
#3	75	6.9	59	2.35	24	0.44
#5	92	8.5	201	7.96	11	0.16
#10	95	8.8	155	6.13	11	0.16
#68	72	6.6	227	9.00	12	0.19
BCR-1	138	13.3	95	3.81	13	0.21
BM	98	9.2	197	2.94	11	0.17
G-2	32	2.6	23	0.95	6	0.09
TB	73	6.6	51	2.08	7	0.09
NIM-N	95	8.9	196	1.94	13	0.21

* no standard blank was run for MnO2

* only three standards were run for MN02

Sample	Na2O (1:200 dilution)		K2O (1:100 dilution)		TiO2	
	abs/conc	calc(%)	abs/conc	calc(%)	abs/conc	calc(%)
smp.bk.	2	-	2	-	26	-
std.bk.	34	-	3	-	21	-
std.#1	63	-	32	-	220	-
std.#2	94	-	59	-	381	-
std.#3	122	-	86	-	552	-
std.#4	159	-	123	-	708	-
std.#5	186	-	141	-	-*	-
#82	130	2.31	181	3.09	1687	0.80
#23	193	3.42	32	0.51	3457	1.64
#31	154	2.73	54	0.92	1992	0.94
#28	202	3.61	29	0.47	2783	1.32
#45B	186	3.31	17	0.25	2569	1.22
#65A	204	3.59	24	0.38	2796	1.32
#30	106	1.86	30	0.48	1373	0.65
#48	197	3.51	31	0.51	2736	1.29
#7	207	3.60	40	0.65	2760	1.30
#79	253	4.53	34	0.55	3265	1.54
#76	263	4.71	30	0.48	3872	1.83
#32	46	0.78	9	0.13	974	0.46
#84	146	2.61	24	0.37	2686	1.27
#15	248	4.39	56	0.94	2568	1.21
#16B	186	3.32	24	0.38	44960	2.75
#56	199	3.54	29	0.46	7812	1.30
#89	106	1.82	188	3.20	3573	0.60
#77	145	2.58	34	0.55	7614	1.27
#3	181	3.21	145	2.45	6115	1.02
#5	160	2.82	17	0.25	6397	1.07
#10	172	3.04	36	0.58	6906	1.15
#68	147	2.61	15	0.22	6828	1.14
BCR-1	210	3.76	98	1.66	-**	-
BM	281	5.05	15	0.22	2972	1.14
G-2	249	4.47	252	4.32	1306	0.62
TB	99	1.75	230	3.95	2404	1.14
NIM-N	166	2.97	19	0.29	538	0.25

* only four standards were run for TiO2

** the concentration of BCR-1 was beyond the detection limits

Atomic Absorption Spectrophotometry Analysis
Trace Elements

Sample	Cu		Zn		Cr		Co	
	abs/conc	calc*	abs/conc	calc	abs/conc	calc	abs/conc	calc
smp.bk.	6	-	11	-	6	-	9	-
td.bk.	45	-	18	-	9	-	25	-
.25ppm.	69	-	59	-	19	-	52	-
0.50ppm.	90	-	97	-	28	-	73	-
1.00ppm.	135	-	174	-	44	-	125	-
2.00ppm.	224	-	325	-	76	-	213	-
3.00ppm.	312	-	457	-	109	-	312	-
#82	25	21	118	64	25	57	58	51
23	30	26	143	83	56	145	96	89
#31	-**	-	-	-	58	152	349	352
#28	55	54	327	201	78	210	109	104
45B	46	45	146	86	74	197	92	86
65A	36	32	242	145	75	197	90	83
#30	-	-	-	-	81	216	494	502
#48	94	98	202	121	71	189	98	93
7	83	83	142	81	68	177	95	87
#79	70	71	136	80	107	292	118	113
#76	491	541	171	102	71	190	101	96
32	-	-	-	-	35	84	521	525
#84	75	77	128	75	183	511	85	80
#15	31	27	122	70	173	476	109	130
16B	65	65	181	108	63	167	106	101
56	34	31	240	145	62	163	97	91
#89	71	72	53	23	18	38	68	62
#77	56	56	111	64	184	513	103	98
3	79	80	122	70	33	80	70	63
#5	118	123	120	69	125	341	95	89
#10	91	94	108	62	98	265	90	84
68	97	101	116	67	123	336	98	93
-CR-1	26	22	222	135	12	21	69	63
BM	-***	-	204	123	57	149	78	72
-2	-	-	146	86	11	17	36	28
B	-	-	164	98	44	126	52	45
NIM-N	-	-	114	66	19	41	92	87

corrected concentrations are in ppm.

* ore samples #31, #30 and #32 were over the detection limits-refer to following table for results.

** rock standards BM, G-2, TB and NIM-N were not run for Cu analysis

Trace Elements(dilution 1:100)

Sample	Cu		Zn	
	abs/conc	calc.(%)	abs/conc	calc.(%)
mp.bk.	10	-	21	-
std.bk.	43	-	17	-
0.25ppm.	66	-	53	-
.50ppm.	84	-	88	-
1.00ppm.	128	-	163	-
2.00ppm.	213	-	287	-
3.00ppm.	301	-	419	-
#31	167	3.41	67	0.32
#30	139	1.51	106	0.59
#32	613	6.99	155	0.92

Trace Elements(bracketing technique)

sample#	std.bk.	smp.bk.	Nickel		sample	calc.(ppm)
			1st. std.*	2nd.std.		
82	0	0	21	32	28	10
23	0	0	55	76	59	43
31	0	0	55	76	66	48
28	0	0	55	76	66	49
45B	0	0	55	76	66	49
55A	0	0	55	76	67	49
30	0	0	76	127	115	104
48	0	0	32	55	52	37
7	0	0	55	76	73	53
19	0	0	76	127	104	91
76	0	0	76	127	94	79
32	0	0	54	76	76	56
34	0	0	76	127	85	68
15	0	0	76	127	172	175
16B	0	0	54	76	75	56
56	0	0	54	76	75	56
39	0	0	21	32	25	9
77	0	0	76	127	96	82
3	0	0	55	76	61	44
5	0	0	76	127	99	85
10	0	0	76	127	88	71
68	0	0	76	127	209	222

* 6ppm.std= 21

13ppm.std= 32

40ppm.std= 55
57ppm.std= 76
120ppm.std=127

Vanadium

sample#	std.bk.	abs/conc		2nd.std.	sample	calc.(ppm)
		smp.bk.	1st.std.			
82	45	45	67	87	74	67
23	9	9	99	145	151	211
31	16	16	66	114	125	222
28	27	27	125	174	166	283
45B	28	28	126	166	158	275
65A	35	35	131	180	171	276
30	11	11	118	165	106	174
48	20	20	110	150	155	312
7	9	9	110	158	155	284
79	10	10	117	170	149	259
76	14	14	122	163	178	336
32	19	19	68	118	80	123
84	19	19	121	167	161	288
15	19	19	118	175	135	228
16B	5	5	104	140	202	514
56	1	1	107	158	142	270
89	8	8	22	32	27	37
77	5	5	94	153	146	288
3	6	6	36	57	62	109
5	10	10	113	161	130	232
10	11	11	112	156	129	240
68	8	8	109	163	130	231
CR-1	13	13	112	147	230	477
BM	10	10	117	159	121	212
G-2	12	12	116	38	30	36
TB	11	11	24	68	72	108
IM-N	17	17	40	176	133	233

Atomic Absorption Spectrophotometry Analysis
Weight of Samples and Rock Standards

Sample Number	Weight(gms.)
#82	1.0027
#23	1.0167
#31	1.0062
#28	1.0035
#45B	1.0046
#65A	1.0167
#30	1.0081
#48	1.0049
#7	1.0295
#79	1.0038
#76	1.0034
#32	1.0174
#84	0.9977
#15	1.0140
#16B	1.0021
#56	1.0064
#89	1.0046
#77	1.0013
#3	1.0099
#5	1.0128
#SG	1.0110
#68	1.0049
BCR-1	1.0005
BM	1.0000
G-2	1.0000
TB	1.0000
NIM-N	1.0000

Rock Standards*

Element	BCR-1	BM	G-2	TB	NIM-N
Cu(ppm)	19	45	11	50	11
Zn(ppm)	120	105	85	95	62
Co(ppm)	27	34	6	13	60
Cr(ppm)	16	125	9	80	34
Ni(ppm)	13	57	6	40	120
V(ppm)	410	180	34	105	210
FeO(total-%)	13.52	9.68	2.67	6.92	8.91
MgO(%)	3.49	7.46	0.77	1.94	7.48
MnO(%)	0.19	0.14	0.04	0.05	0.18
K ₂ O(%)	1.68	0.20	4.52	3.85	0.25
Na ₂ O(%)	3.29	4.64	4.06	1.31	2.46
TiO ₂ (%)	2.22	1.14	0.50	0.93	0.20

* the rock standard values were obtained from the GSC report on rock standards(1977)

Calculations to Determine Element Concentration

Example: Cu

- Step #1: Average the three runs for blanks and standards.
- Step #2: Subtract standard blank(avg) from the standards.
- Step #3: Normalize the standard values on the basis of 1 ppm.
- Step #4: Find a representative value for the 1 ppm standard by averaging.
- Step #5: Calculate the F factor where $F = 100/R_{std}$.
- Step #6: Subtract the sample blank(avg) from all the samples.
- Step #7: Calculate the element concentration using the formula

$$[\text{element}]_{\text{ppm}} = \frac{R_{\text{sample}} \times F}{\text{sample weight (gms.)}}$$

Adjustments to the above method are necessary for diluted samples and for the major elements. The variations are given as follows.

Diluted samples:

- Step #7a: Calculation of the element concentration requires a multiplication factor that represents the dilution.
(ie: samples diluted by 1:200 must be multiplied by 200)

Major elements:

- Step #7a: Major elements must be multiplied by a conversion factor that changes the element value to an oxide value.
(ie: conversion from Ti to TiO₂ requires a multiplication factor of 1.66806)

Since the elements, Ni and V, require a bracketing technique to adjust for background fluctuation, the concentration was determined using a computer program whereby values were obtained directly from the output. The equation below gave the final concentration.

$$[\text{element}]_{\text{ppm}} = \frac{\text{computer value} \times 100}{\text{weight of sample (gms.)}}$$

APPENDIX III

Microprobe Analysis

pyrite

Smp. #	# grains	Analysis (mole %)				Grain Orientation
		Fe	S	Minor elements		
JB-30	8	46.69	53.77	0.05 Ti; 0.16 Zn		within schist fragments in ore
JB-31	13	46.18	53.36	+1.57 O; +0.38 Co; +0.06 Ti; +0.13 Zn		within schist fragments, cross-cutting foliation and as lamellae in ore
JB-33	7	46.48	53.36	+1.85 O; +0.44 Co; +0.06 Ti; +0.18 Zn		within schist fragments and cross-cutting foliation in ore
B-62	3	46.23	53.79	0.04 Zn		isolated grains in metavolcanics
JB-63	4	45.55	53.07	+1.00 O; +0.91 Co; +0.07 Ti; 0.17 Zn; +0.08 Mn		isolated grains in the metavolcanics
JB-20	5	45.99	53.14	+0.15 Ti; +0.16 Zn		"
B-3	3	46.30	53.66	+0.07 Ti; 0.17 Zn		"

Chalcopyrite

mp. #	# grains	Analysis (mole %)				Grain Orientation	
		Cu	Fe	S	Minor elements		
JB-30	7	34.48	30.69	34.78	-	cross-cutting foliation and isolated grains in ore	
JB-31	3	33.85	29.94	33.99	+2.100; 0.05Ti	replacement texture with py intergrowths with sphalerite replacement texture with py	
		33.02	28.84	34.30	+1.690; 2.26Zn		
		34.90	30.81	30.81	+0.05Ti		
JB-33	3	33.63	30.72	34.81	+0.07V	cross-cutting foliation in ore	
		1	35.33	31.02	35.38	-	inclusion in py on ore
		4	29.02	32.36	29.17	9.400	replacement texture in ore
		1	30.95	27.38	30.58	10.950	within schist fragment in ore
		1	33.43	30.49	34.99	1.040	replacement texture in ore
JB-38A	2	32.61	32.10	34.57	-	isolated grains in metavolcanics	
JB-63	2	32.77	30.33	34.69	-	"	
JB-5	2	32.53	29.77	34.27	+0.10Ti; 0.06Mn	isolated grains in metaseds.	
JB-3	4	33.93	30.53	35.11	-	"	
JB-76	3	35.05	30.54	35.25	-	isolated grains in metavolcanics	
JB-77	2	29.77	31.59	26.77	7.400; 0.14Zn; 0.31Ca	isolated grains in coarse-grained greenschist	

Sphalerite

Smp. #	# grains	Analysis (mole%)			Grain Orientation
		Fe	S	Minor elements	
JB-30	3	60.67	38.61	1.100; 0.04Ti; 0.15Zn; 0.06Mn; 0.07Ca	cross-cutting foliation in ore
	4	61.05	40.01	+0.06Ti; +0.15Zn; +0.05Ni; +0.06Mn; +0.07Ca	"
JB-33	2	59.13	39.32	+2.420; +0.08Ti; +0.11Zn; +0.04Mn	"
	5	63.93	35.75	+0.08Ti	"
JB-3	1	58.39	37.36	2.980; 0.09Ti; 0.70Zn; 0.09Ni; 0.05Mn; 0.97Ca	"
	3	61.01	38.83	+0.05Ti; 0.10Zn; +0.07Ni; +0.04Mn	"

Iron oxides

Smp. #	# grains	Analysis (mole%)			Grain Orientation
		Fe	O	Minor elements	
JB-33	2	63.93	35.75	0.05V	post-tectonic growths
JB-62	4	61.07	38.70	0.06Mn; 0.14Mg	"
	2	68.73	31.02	0.18Mg	"
JB-79	2	62.58	37.10	0.11Mn;	"
	3	74.86	23.92	0.35V; 0.06Ti; 0.07Mn; 0.32Al; 0.22Mg	"
JB-76	2	74.04	25.27	0.36V; +0.05Mn; +0.10Cr	"
JB-82	2	73.66	24.99	0.31V; +0.07Mn; +2.05Zr	"
JB-89	5	74.82	25.50	0.30V; +0.11Ti; +0.08Mn	"

Tantalum oxides

Smp. #	# grains	Analysis (mole%)				Grain Orientation
		Fe	Ti	O	Minor elements	
JB-63	2	36.36	30.75	27.62	4.72Mn; 0.12Ca	post-tectonic growths
	2	22.66	38.84	31.05	4.23Mn; 1.41Ca	"
JB-20	4	58.86	0.42	39.74	0.07Cr	"
	2	63.95	5.62	29.70	0.78Cr	"
JB-76	3	24.92	27.42	45.03	1.84Mn	"
	2	1.31	41.05	56.93	-	"
	3	48.93	10.89	39.85	0.35Mn; 0.04Cr	"
JB-79	3	70.61	0.84	29.25	-	"
	2	74.89	0.41	23.28	0.52Ca	"
	3	29.02	37.20	34.05	4.13Mn; 2.77Ca	"
JB-89	2	23.60	27.50	50.02	4.61Mn; 0.37Ca	"
	1	1.76	57.05	42.03	1.39Ca	"
	1	0.58	63.10	37.11	-	"
	2	71.84	1.49	28.80	0.40Ca	"

	2	32.43	31.44	30.05	6.69Mn;0.05Zn	"
	2	63.25	9.96	29.85	0.59Mn	"
JB-17	3	67.34	5.69	26.05	+0.05Mn;+0.40Zn	"

APPENDIX IV

Sample #	Lithologic Unit
82	siliceous psammite
23	porphyroclastic metavolcanic
31	ore
28	porphyroclastic metavolcanic
45B	porphyroclastic metavolcanic
65A	porphyroclastic metavolcanic
30	ore
48	porphyroclastic metavolcanic
7	porphyroclastic metavolcanic
79	banded metavolcanic
76	porphyroclastic metavolcanic
32	ore
84	coarse-grained greenschist
15	massive metavolcanic
16B	massive metavolcanic
56	porphyroclastic metavolcanic
89	siliceous metasediment
77	coarse-grained greenschist
3	garnetiferous semi-pelite
5	banded metavolcanic
10	porphyroclastic metavolcanic
68	porphyroclastic metavolcanic
33	ore
62	porphyroclastic metavolcanic
63	porphyroclastic metavolcanic
20	porphyroclastic metavolcanic
38A	porphyroclastic metavolcanic

REFERENCES

- Bailey, D. Mineralogy of Ore Samples From The Goose Cove Massive Sulphide Deposit, Northwestern Newfoundland. Unpub. report. Dalhousie University (1982) 39 pp.
- Barton, P.B., Jr. and Skinner, B.J. Sulphide mineral solubilities. Geochemistry of hydrothermal ore deposits. John Wiley and Sons, New York, New York (1979) pp. 278-403.
- Barnes, H.L. Geochemistry of Hydrothermal Ore Deposits. Holt, Rinehart & Winston. New York (1967).
- Billings, M.P. Structural Geology. Prentice-Hall Inc. (1972) 606 pp.
- Coleman, R.G. Ophiolites. Springer-Verlag. New York (1977) 229 pp.
- Constantinou, G. and Govett, G.J.S. Geology, Geochemistry & Genesis of Cyprus Sulphide Deposits. Econ. Geo. v. 68 (1973) pp. 843-858.
- Cooper, J.R. Geology and Mineral Deposits of the Hare Bay Area. Nfld. Dept. Nat. Res., Geol. Sect. Bull. No. 9 (1937)
- Dean, P.L. The Volcanic Stratigraphy and the Metallogeny of Notre Dame Bay, Nfld. Memorial University of Newfoundland, Geology Report 7 (1978) pp. 80-82.
- Deer, W.A., Howie, R.A. and Zussman, J. An Introduction to the Rock-Forming Minerals. Longman (1980) 528 pp.
- Dewey, J.F. and Bird, J.M. Origin and Emplacement of the Ophiolite Suite: Appalachian Ophiolites in Newfoundland. J. Geophys. Res., v. 76 (1971) pp. 3179-3206.
- Douglas, G.V., Williams, D. and Rove, O.N. Copper Deposits of Newfoundland. Geo. Surv. Nfld. Bull. No. 20 (1940) 176 pp.
- Duke, N.A. and Hutchinson, R.W. Geological Relationships Between Massive Sulphide Bodies and Ophiolitic Volcanic Rocks Near York Harbour, Nfld. Can. J. Earth. Sci., v. 11 (1)(1974) pp. 53-69.
- Engel, A.E.J., Engel, C.J. and Havens, R.G. Chemical Characteristics of Oceanic Basalts and The Upper Mantle. Geol. Soc. Amer. Bull. v. 76 (1)(1965) pp. 719-734.
- Evans, A.M. An Introduction to Ore Geology. Elsevier. New York (1980) 231 pp.

Grenne, T. Grammeltvedt, G. and Vokes, F.M. Cyprus-Type Sulphide Deposits in the Western Trondheim District, Central Norwegian Caledonides. In: Ophiolites. Proc. Int. Ophiolite Symp. Cyprus (1979) pp. 727-743.

Hawkins, J.W. Petrology of Back-Arc Basins and Island Arcs: Their Possible Role in the Origin of Ophiolites. In: Ophiolites. Proc. Int. Ophiolite Symp. Cyprus (1979) pp. 244-254.

Haworth, R.T., LeFort, J.P. and Millar, H.G. Geophysical evidence from an east-dipping Appalachian subduction zone beneath Newfoundland. *Geology*, v.6., no.9 (1978) pp.522-526.

Hobbs, B.E., Means, W.D. and Williams, P.F. An Outline of Structural Geology. John Wiley & Sons. New York (1976) 570 pp.

Hughes, C.J. Igneous Petrology. Elsevier. New York (1982) 551 pp.

Hurlbert, C.S. and Klein, C. Manual of Mineralogy (After James D. Dana). John Wiley & Sons. New York (1977) 532 pp.

Jamieson, R.A. A Suite of Alkali Basalts and Gabbros Associated With the Hare Bay Allochthon of Western Nfld. *Can. J. Earth Sci.* v. 14 (1977) pp. 346-356.

Jamieson, R.A. The St. Anthony Complex, Northwestern Nfld.: A Petrological Study of the Relationship Between a Peridotite Sheet and its Dynamothermal Aureole. Unpub. Ph.D. Thesis (1979).

Jamieson, R.A. Formation of Metamorphic Aureoles Beneath Ophiolites—Evidence from The St. Anthony Complex, Nfld. *Geology* v. 8 (1980) pp. 150-154.

Jamieson, R.A. and Strong, D.F. A Metasomatic Mylonite Zone Within the Ophiolite Aureole, St. Anthony Complex, Nfld. *Am. J. Sci.* v. 281 (1) (1981) pp. 264-281.

Lynas, C.M.T. and Calon, T.J. Northwestward directed thrusting related to closing of the Iapetus Ocean in the Hare Bay Allochthon, Newfoundland. *Geol. Soc. Am., Abst. Programs*, v.12, no.2 (1980) pp.71.

McDonald, J.A. Metamorphism and Its Effect on Sulphide Assemblages. *Min. Deposita*, v. 2 (1967) pp. 200-220.

Mitchell, A.H.G. and Garson, M.S. Mineral Deposits and Global Tectonic Settings. Academic Press (1981) 405 pp.

Newhouse, W.H. and Flaherty, G.F. The Texture and Origin of Some Banded or Schistose Sulphide Ores. *Econ. Geo. Laboratory*.

Pearce, J.A. Basalt Geochemistry Used to Investigate Past Tectonic Environments on Cyprus. *Tectonophysics*, v. 25 (1975) pp. 41-67.

Pearce, J.A. and Cann, J.R. Tectonic Setting of Basic Volcanic Rocks Determined Using Trace Element Analyses. *Earth Plan. Sci. Let.*, v. 19 (1973) pp. 290-300.

Pearce, J.A. and Gale, G.H. Identification of Ore Deposition Environment from Trace Element Geochemistry of Associated Igneous Host Rocks. In: *Volcanic Processes in Ore Genesis*. The Geological Soc. of London, (1976) pp. 14-24.

Ragan, D.M. *Structural Geology-An Introduction to Geometrical Techniques*. John Wiley & Sons (1973) 208 pp.

Schwartz, G.M. Classification and Definition of Textures and Mineral Structures in Ores. *Econ. Geol.*, v. 46 (1951) pp. 578-591.
Scott, S.D. Experimental calibration of the sphalerite geobarometer. *Econ. Geol.*, v. 68 (1973) pp. 466-474.

Scott, S.D. Application of the sphalerite geobarometer to regionally metamorphosed terrains. *Amer. Mineral.*, v. 61 (1976) pp. 661-670.

Scott, S.D. and Hutchinson, M.N. Sphalerite geobarometry in the Cu-Fe-Zn-S system. *Economic Geology*, V. 76 (1981) pp. 143-153.

Scott, S.D. and Kissin, S.A. Sphalerite composition in the Zn-Fe-S system below 300°C. *Economic Geology*, v. 68, (1972) pp. 475-479.

Stephenson, K. *Geology and Mineralogy of the Goose Cove Copper Deposits, northwestern Nfld. Mt. Union College* (1937) 30 pp.

Strong, D.F., Dickson, W.L., O'Driscoll, C.F. Geochemical evidence for an east dipping Appalachian subduction zone in Newfoundland. *Nature*, v. 248, no. 5443 (1974) pp. 37-39.

Talkington, R. An usual occurrence of gabbro veins in a west Newfoundland ophiolite, White Hills Peridotite, St. Anthony Complex. *Geol. Assoc. Can.-Min. Assoc. Can. Joint Annual Meeting Program Abstract*, v. 4 (1979) pp. 82.

Talkington, R.W. and Jamieson, R.A. The geology of the St. Anthony Complex, northwestern Nfld. In: *Memorial University of Nfld. Report no. 8* (1980)

Tarney, J., Saunders, A.P., Matthey, D.P., Wood, D.A. and Marsh, N.G. Geochemical aspects of back-arc spreading in the Scotia Sea and western Pacific. *Phil. Trans. R. Soc. London.*, v. A300 (1981) pp. 263-285.

Tullis, J., Snoke, Arthur W., and Todd, Victoria R. Penrose Conference Report; significance and petrogenesis of mylonitic rocks. *Geology*, v. 10, no. 5 (1982) pp. 227-230.

Williams, H. Mafic-ultramafic complexes in West Nfld. Appalachians and the evidence for their transport: A review and interim report. In: A Nfld Decade. *geol. Assoc. Can. Proc.*, v. 24, no. 1 (1971) pp. 9-25.

Williams, Harold. Bay of Islands map area, Newfoundland. *Can. Geol. Surv. Pap.*, no. 72-34 (1973).

Williams, H. Structural Succession Nomenclature and Interpretation of Transported Rocks in Western Newfoundland. *Can. J. Earth Sci.*, v. 12 (3) (1975) pp. 1875-1894.

Williams, H. and Smyth, W.R. The Hare Bay Allochthon, Northern Newfoundland. *Geol. Surv. Can. Pap.* 74-1 (1974) pp. 3-6.

Williams, H., Smyth, W.R. and Stevens, R.K. Hare Bay Allochthon, Northern Newfoundland. *Geol. Surv. Can. Pap.* 73-1 (1980) 231 pp.

Williams, Harold and Stevens, R.K. Taconic orogent and the development of the ancient continental margin of eastern North America in Newfoundland. *Geoscience Canada*, v. 1, no. 2 (1974) pp. 31-33.

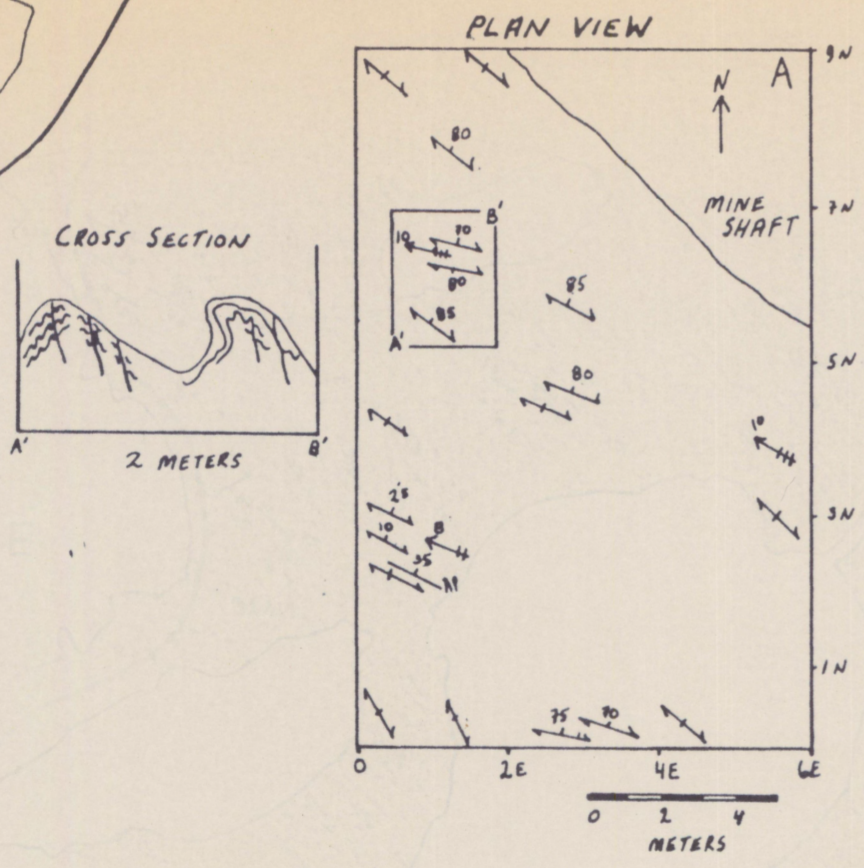
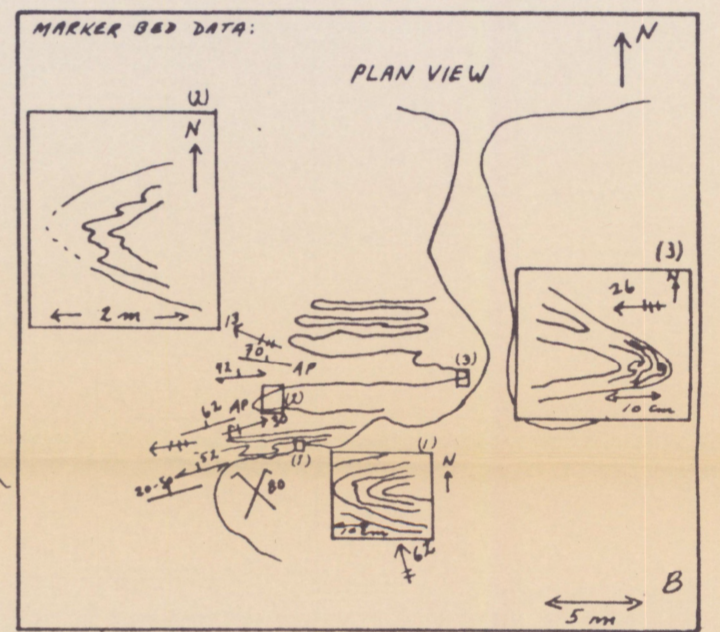
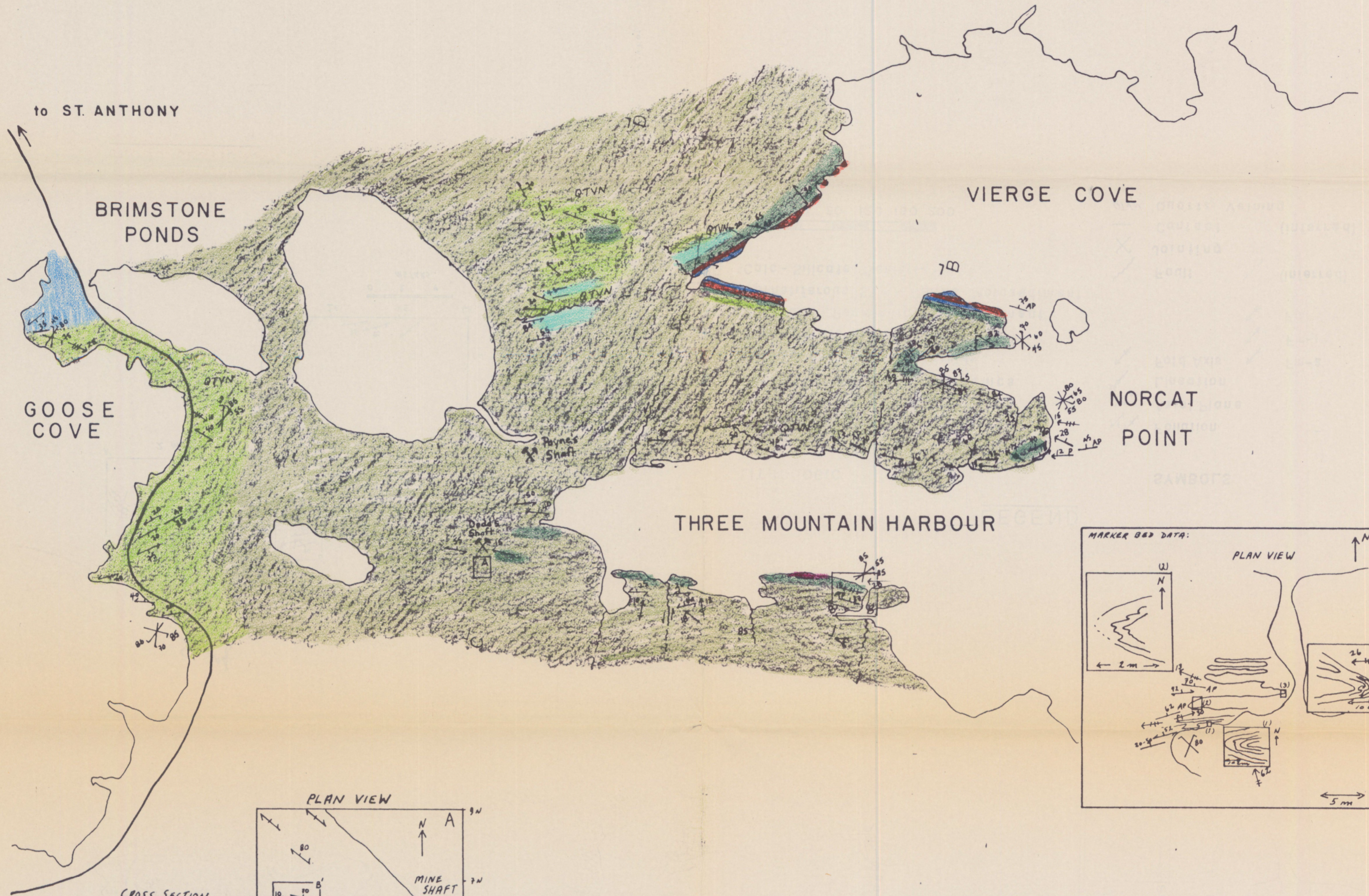
Verwoerd, W.J. Mineralization in metamorphic terrains. *Cong. Geol. Soc. Africa. "Geokongres 75"*. (1975) pp. 41-51.

Vokes, F.M. A Review of the Metamorphism of Sulphide Deposits. *Earth-Science Reviews*, v. 5 (1969) pp. 99-143.

PLATE I GEOLOGY

N

THREE MOUNTAIN SUMMIT



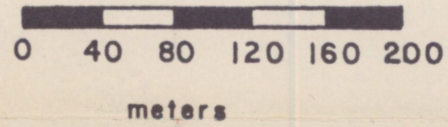
LEGEND

LITHOLOGIC UNITS

- Porphyroclastic Metavolcanics
- Massive Metavolcanics
- Banded (Mylonitic) Metavolcanics
- Coarse-grained Greenschist
- Semi-Pelitic Metasediment
- Siliceous Psammitic Metasediment
- Garnetiferous Semi-Pelitic Metasediment
- Calc-Silicate Schist

SYMBOLS

- Foliation
- Axial Plane
- Lination
- Fold Axis
- Fault
- Jointing
- Contact
- Quartz Veining
- Fm-2
- Fm-1
- Fm
- (inferred)
- (inferred)



CROSS SECTIONS

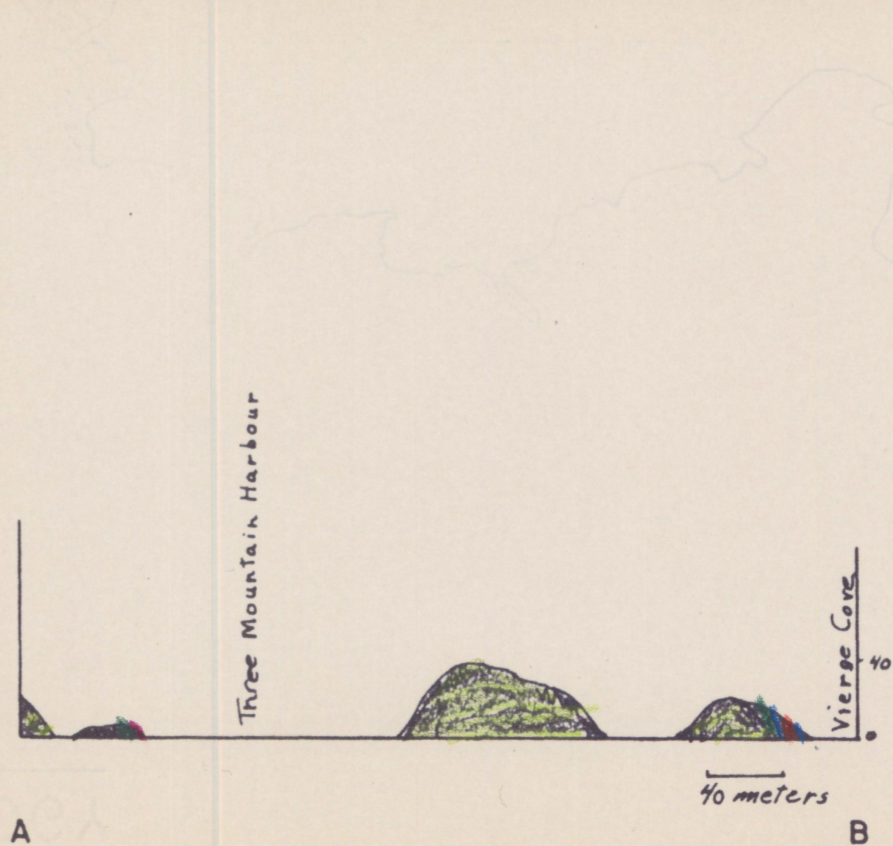
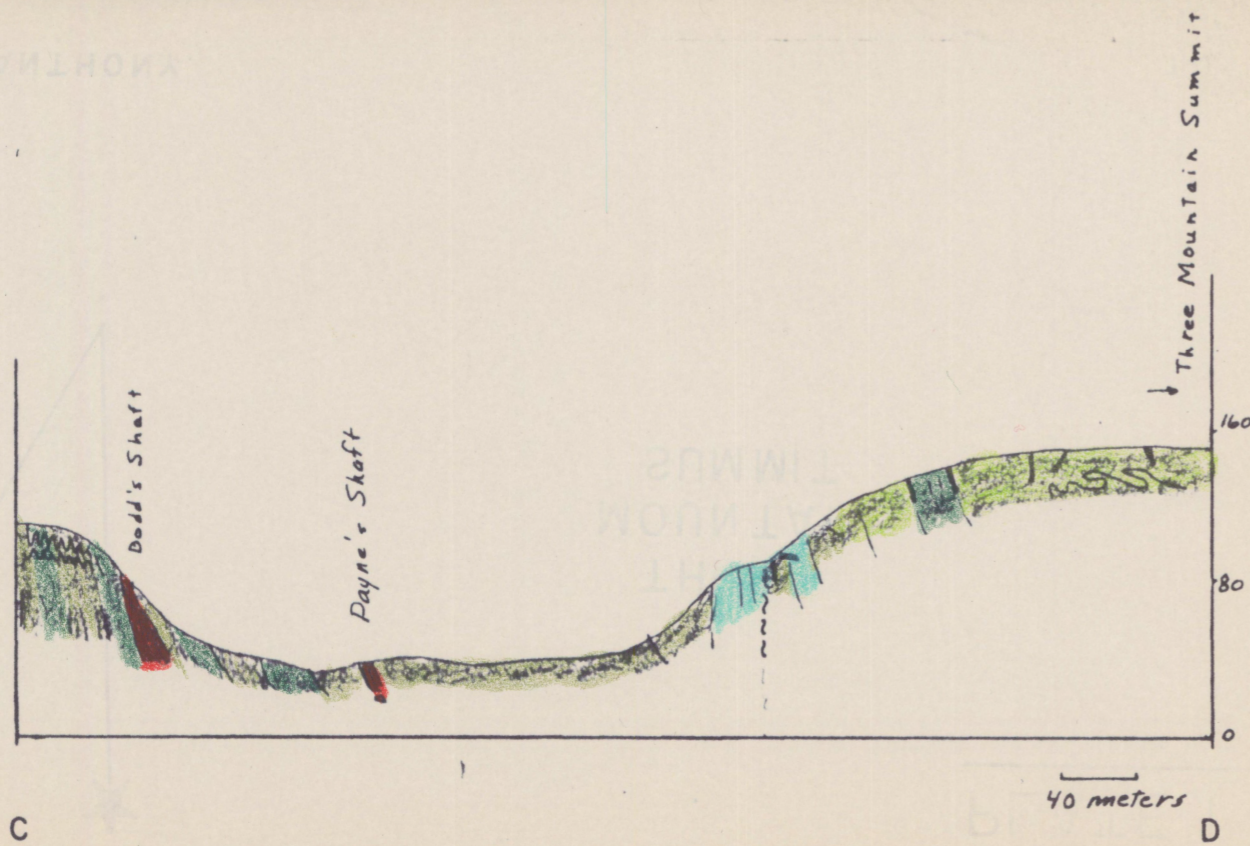
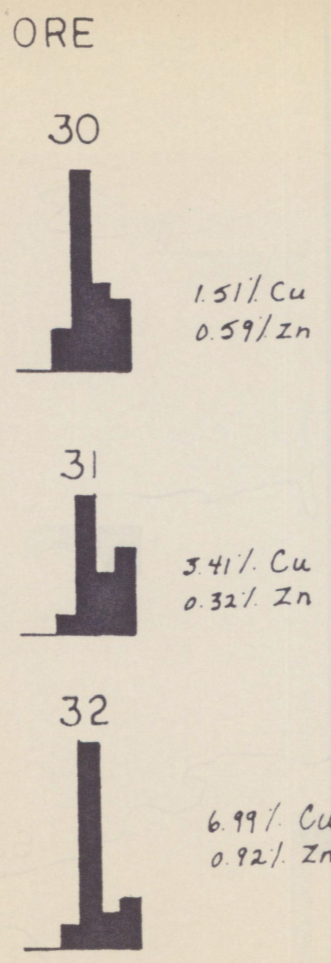
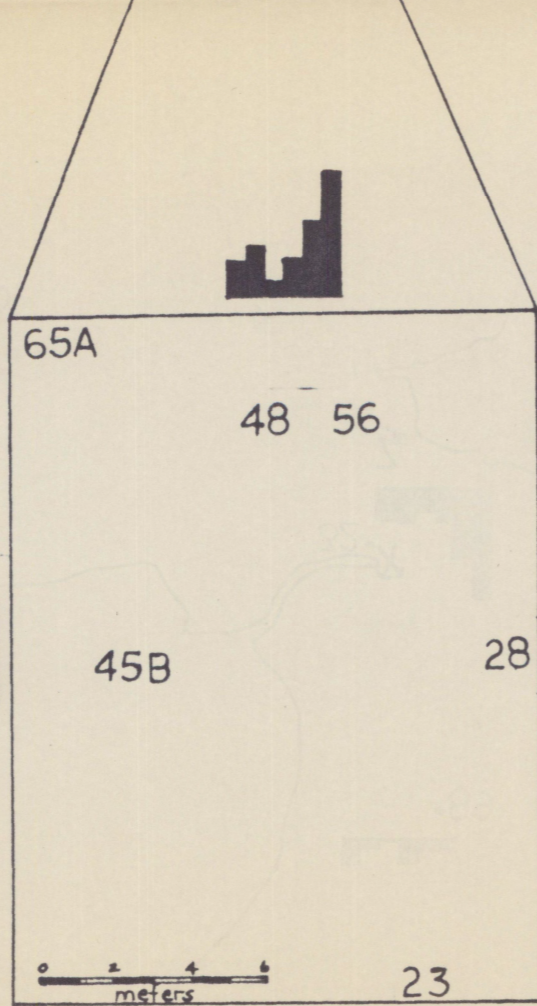
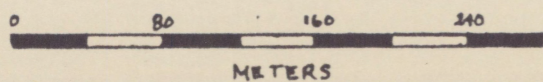
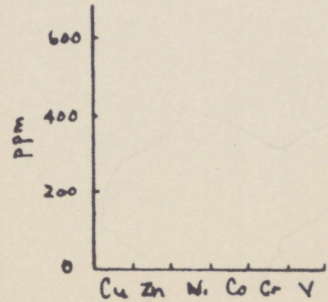
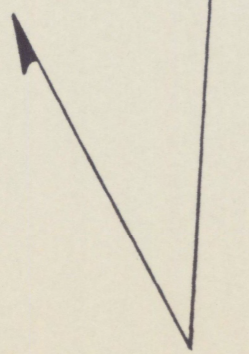


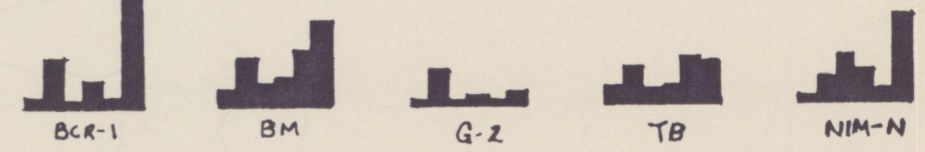
PLATE 2 GEOCHEMISTRY

Cu-Zn-Ni-Co-Cr-V

N



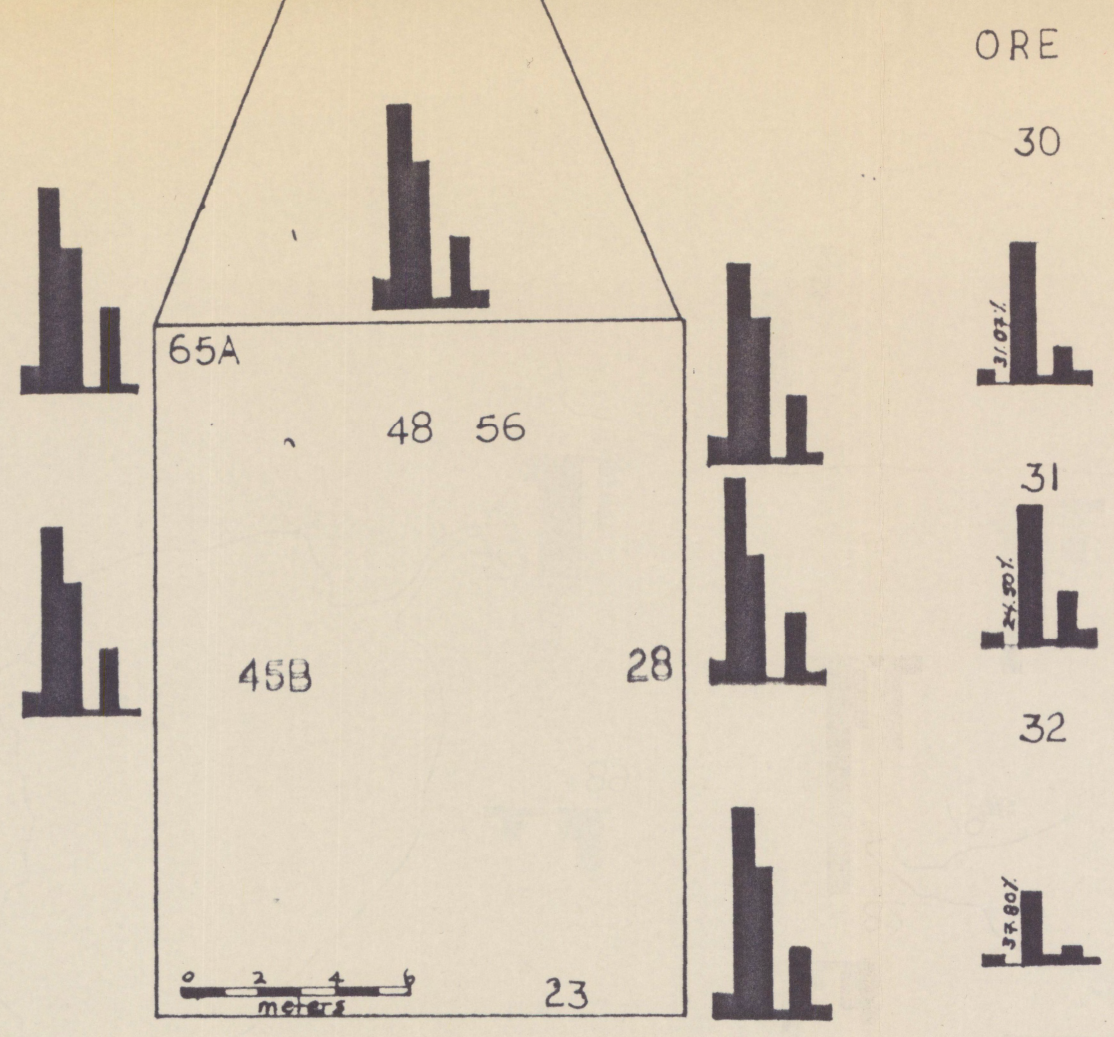
STANDARDS



N

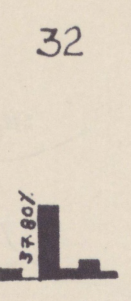
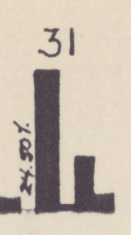
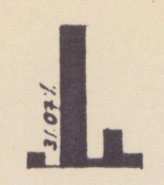
PLATE 3 GEOCHEMISTRY

TiO₂ - FeO_(T) - MgO - MnO - Na₂O - K₂O



ORE

30



STANDARDS

